DEVELOPMENT OF UTILITY SCALE BUOYANT ENERGY STORAGE TECHNOLOGY

A THESIS SUBMITTED TO THE GRADUATE DIVISION OF THE UNIVERSITY OF HAWAI‘I AT MĀNOA IN PARTIAL FULFILLMENT OF THE REQUIREMENTS FOR THE DEGREE OF

MASTER OF SCIENCE

IN

MECHANICAL ENGINEERING

MAY 2012

By

Tyler B. Thornbrue

Thesis Committee:

Reza Ghorbani, Chairperson
Brian Bingham
Peter Berkelman

To my wife,

Leah Dianne Keene Thornbrue,

for patiently waiting for me to get home for dinner at a decent hour, for the 10 minute house cleanings that significantly destress my existence, and for doing an amazing job taking care of Mya and Daniel while I work.
I appreciate you for so many more reasons than this, but probably shouldn't get into them in my thesis!

Acknowledgments

This project and all the peripheral work around it would not have been possible were it not for the help of many amazing people. The following list is an attempt to name some of those directly involved, and by no means is exhaustive. I apologize ahead of time to those I should have listed.

1. My advisor, Reza Ghorbani, for all the brainstorming sessions, advice, laughter, and for taking that initial risk on me back in January 2010.

2. My colleague and friend, Volker Schwarzer, for the indispensable advice on and proofreading of my papers, and for making the REDLab a fun place to do work.

3. My colleague, Randall Sparks, for brainstorming with me and helping to refine and assess the economic and technical feasibility of buoyant energy storage technology.

4. My colleague, Iman Nasseri, for working with me to develop a cost comparison analysis of energy storage technologies.

5. My colleague, Victor Kis, for drafting early renditions of buoyant energy storage technology and creating animations that were extremely useful in communicating functionality.

6. My colleague, Nate Calio, for designing, drafting, and building the prototype testbed and assisting in experiments.

7. My family in Virginia, the Keenes, for their generous support of us and my quest for a better career.

8. The Renewable Energy and Island Sustainability (REIS) program at UHM, and the supporting funds from the Department of Energy's Workforce Training Initiative

Abstract

Power intermittency is a growing concern as variable renewable power producers increase their penetration on utility grids. With a majority of US states adopting renewable portfolio standards, mitigation strategies such as energy storage are receiving renewed attention.

This thesis presents the developmental progress of a novel method of energy storage referred to as buoyant energy storage technology (BEST). Various concepts are presented, and benefits highlighted before demonstrating a basic system's performance through dynamic modeling. A control methodology is then designed and implemented to improve the performance and functionality of the same model. Further expansion to a dual buoy model and control methodology follows to enhance the system through a regenerative braking power transfer technique. A proof of concept is then demonstrated and options for scaled up testing discussed. Finally, a cost comparison analysis is presented that juxtaposes BEST with pumped hydroelectric and battery energy storage technologies.

Table of Contents

List of Tables

List of Figures

Chapter 1

Introduction

1.1 The Renewable Resource Challenge

With rising concerns over the repercussions of continued dependence on fossil fuels, the world has begun a shift in its energy paradigm. Renewable energy sources are being developed in lieu of conventional power plants where resources are available and economics make sense, and Hawaii provides a unique microcosm of the larger transformation taking place. Due to its isolation, the State currently imports nearly 90% of its energy in the form of fossil fuels [1], and has the highest consumer electricity rate in the Nation [2]. It is also home to an abundance and variety of renewable energy resources such as wind, solar thermal, photovoltaic, biomass, biofuels, biogas, geothermal, hydroelectric, ocean wave, and ocean thermal energy conversion [3].

Though there are no renewable portfolio standards (RPS) or Feed-In-Tariffs (FIT) at the Federal level, 29 states have adopted their own RPS's and 8 have adopted renewable portfolio goals (which are non-binding) as of June 2011 [4]. Hawaii's RPS is the most aggressive and far-reaching in the Nation. Enacted through the Hawaii Clean Energy Initiative (HCEI), 40% of generated electricity will come from renewable resources by 2030 [5], and progress is already being made [6]. Other aggressive RPS adopters include California with its goal of 33% by 2020, Colorado with 30% by 2020, and New York with 29% by 2015 [4].

1.2 Intermittency

For this growth to continue to such high levels, a limiting factor identified by the Department of Energy must be mitigated: intermittency [7].

Wind and Solar, the most commercialized and widely applicable renewable energy resources, are inherently variable, making accurate and consistent forecasting difficult [8]. As a result of meteorological events, their outputs can change unexpectedly and drastically in relatively short periods of time. Figure 1.1 demonstrates sudden drastic changes in solar and wind output over a 24 hour period.

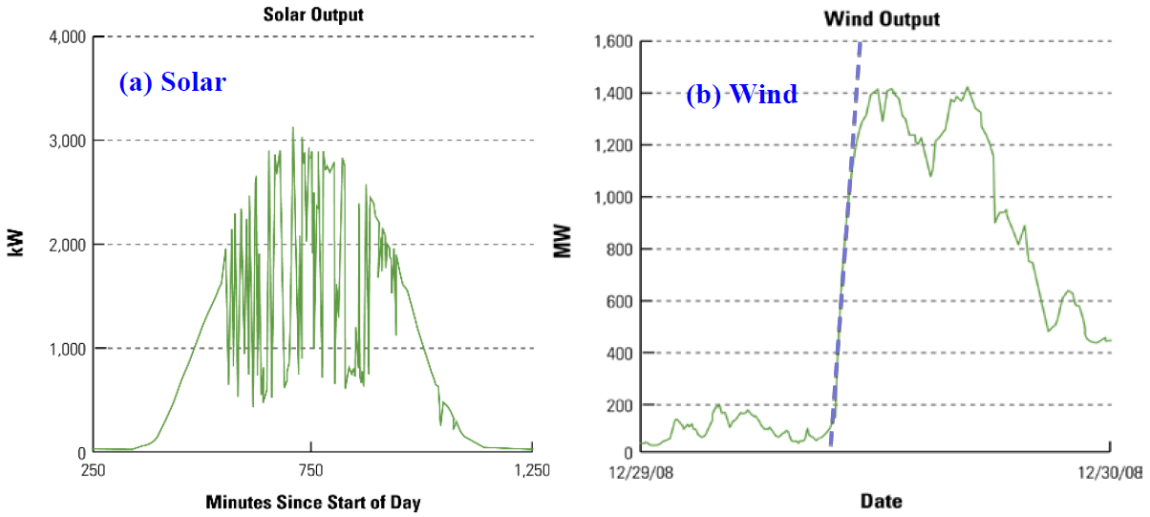

Figure 1.1. This DoE sourced graph from the ARPA-E GRIDS Funding Opportunity Announcement in 2010 [7] illustrates rapid changes in output for (a) Solar and (b) Wind generation units from the Bonneville Power Administration.

Due to the just-in-time nature of grid operation, a constant balancing act of supply and demand must be maintained. Sudden changes on the supply side, introduced by these renewable resources, can pose significant risks to economic and efficient operations. These include grid destabilization, frequent power curtailments, and a limit to renewable energy penetration [7][8][9].

The current methodology for supply and demand management is to have firm generation capabilities available, known as spinning reserves [7][8]. "Spinning reserves are essentially extra (generators) that are on-line but unloaded and that can respond within 10 minutes to compensate for generation or transmission outages [10]." Under normal circumstances, this method is effective, but a challenge known as ramping arises when high levels of renewables are introduced. Typical electric generators cannot change outputs as fast as large quantities of renewable resources making frequency regulation difficult, inefficient, and taxing on equipment [11]. The result is a destabilized grid with higher costs of operation [9]. Additionally, the fast-responding generation units, known as peaking units, that are used as spinning reserves tend to be carbon intensive and are highly expensive

to operate relative to base load units [7]. Figure 1.2 demonstrates the use of peaking units to mitigate a hypothetically high percentage of renewable energy on the island of Oahu.

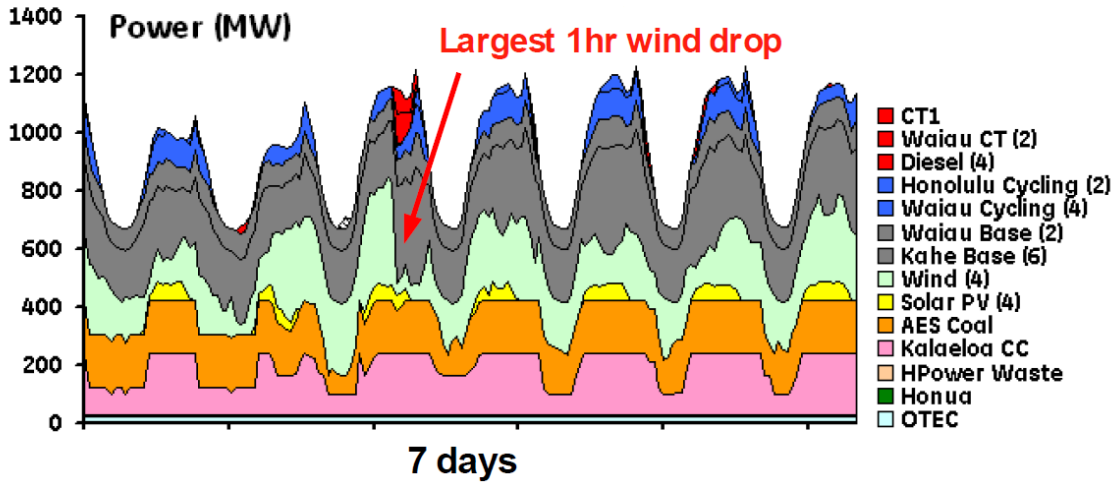

Figure 1.2. This graph, from the Oahu Wind Integration Study [12], shows the dispatch of various generation units during an example week of operation for a hypothetical high renewable energy penetration scenario. CT1, Waiau CT, and Diesel units (red) denote highly expensive peaking units that maintain grid stability during significant wind events.

During times of low demand, another method of load balancing must be employed. It's not as simple as just powering down generators. Electrical generating units have minimum capacity thresholds, that cannot be breached without requiring a costly and time intensive restart [13]. Additionally, "excessive on-and-off cycling can be a problem for combustion generators, leading to damage and faster deterioration. It is also inefficient, causing them to burn more fuel than necessary [13]." When all base-load units are minimized and supply still exceeds demand, the best option is to curtail renewable resources, effectively wasting usable electrical energy. This situation, illustrated in Fig. 1.3, results in higher costs of electricity, making it more difficult to foster renewable resource development [13].

1.3 The Role of Energy Storage

If the renewable energy penetration is to be increased, a solution to the challenge of intermittency is needed. One that carries with it many benefits is utility scale energy storage (USES) [9]. USES systems can improve power quality through voltage and frequency regulation, manage peak loads with off-peak energy, enable energy arbitrage, defer infrastructure upgrades, and provide

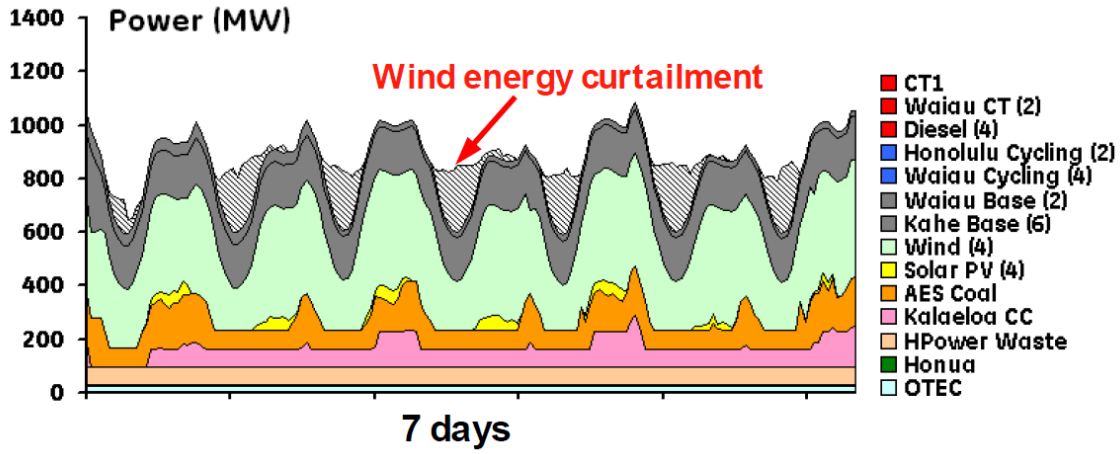

Figure 1.3. This graph, from the Oahu Wind Integration Study [12], shows the curtailment of renewable resources during an example week of operation for a high renewable energy penetration scenario.

ramping capability supporting economic integration of renewable sources of energy [7][10][15][16]. This equates to USES being an enabling technology useful for meeting RPS and reliability needs [17]. A report by Sandia National Laboratories [18] expands on these benefits and includes many others along with their respective category. A summary of these benefits is shown in Table 1.1.

As the United States transitions to higher penetrations of renewable energy, increasing the efficiency and operational capabilities of power grids has become an important goal as well. The grid of the future, touted the smart grid, uses digital technology to improve reliability, security, and efficiency (both economic and energy) of the electric system from large generation, through the delivery systems to electricity consumers, and a growing number of distributed-generation and storage resources [19].

One of the seven key principals of the smart grid is its ability to accommodate all generation and storage options [20]. Since renewable energy is often a distributed energy resource, its geographic diversity coupled with its intermittency makes it difficult to accommodate in the legacy grid. Through accommodating energy storage options, these issues are mitigated and synergistic benefits generated. These include improvements in reliability, security, economics, efficiency, and environmental impacts [21].

USES systems have the ability to provide the ancillary services required by grid operators. Depending on the type of storage technology, this can include frequency regulation (response times on the order of seconds, low energy requirements), spinning reserve (response times on the order of

Category	Benefits
Electric Supply	Electric Energy Time-Shift Electric Supply Capacity
Grid Operations	Load Following Area Regulation Electric Supply Reserve Capacity Transmission Support Voltage Support
Grid Infrastructure	Transmission Congestion Relief Transmission and Distribution Upgrade Deferral Substation Onsite Power
End-User	Time-of-Use Energy Cost Management Demand Charge Management Electric Service Reliability Electric Service Power Quality
Renewables Integration	Renewable Energy Time-Shift Renewable Generation Capactity Firming Wind Generation Grid Integration

Table 1.1. A table from Sandia National Laboratories showing the benefits of energy storage and their respective categorization

seconds, higher energy capacity), and/or load shifting (response times on the order of minutes with massive amounts of energy capacity) [10].

1.4 The Market for Utility Scale Energy Storage

Due to the increase in renewable energy usage, the need for smart grid adoption, and requirements for high power quality, USES technologies are projected to grow both domestically and internationally in the coming years. Coupled with changing regulations such as the Federal Energy Regulatory Commission's Order Number 755 which implements a pay-for-performance rate schedule for USES technologies based on response times [22], the market is poised for explosive growth.

Several market research organizations have been following the expanding energy storage market with varying predictions. In March 2010, Lux Research released a report predicting the world's USES market to grow from $460 million in 2010 to $1.4 billion in 2015 [23].

In June 2011, BCC Research predicted that global sales of USES technology will grow at a 36.6% compound annual growth rate (CAGR) over the next five years, from $3.9 billion in 2010 to $18.5 billion in 2015. When broken down by region, BCC claims sales will grow fastest in North America, increasing at a CAGR of 86.2% from $272 million in 2010 to $6.1 billion in 2015, USES sales in Europe will grow at a 41% CAGR from nearly $1 billion in 2010 to $5.3 billion in 2015, and sales in Asia/Australia will grow at a 21.7% CAGR from $2.7 billion in 2010, to nearly $7.2 billion in 2015 [24].

Pike Research released another report in November 2011 that is predicting a 100-fold global energy storage capacity increase by 2021. This equates to just over $122 billion in investments over a ten year period. [25]

To address these projected growth trends, Lux Research hosted a webinar entitled "Grid Storage: Connecting the Dots in a Fragmented Market" in December 2011. Rather than developing a one-size fits all system, a "sniper approach" was stated as the best approach, meaning to target individual utility needs and to design a custom fit solution for that need. Additionally, the most important attribute of a USES system is its lifetime. In terms of a cost comparison analysis, as presented in Chapter 6, this proves to be true. Interestingly, efficiency differences between systems by only several points does not make a significant difference in terms of net present value [26].

Also interesting is the notion that pumped hydroelectric and compressed air energy storage systems are not direct competitors to battery storage systems, rather they are complements to each other. They serve different needs as discussed below, and have vastly different scales [26]. It does seem that a hybrid system with the ability to scale and the fast response characteristics of batteries would be a welcome addition to the market.

Finally, if advances in smart grid technology develop and effective demand response programs are established, the need for energy storage could decrease. By curbing electricity use at peak times and incentivizing more usage at off-peak times, similar results can be had as with implementing energy storage. Demand response is a direct competitor to energy storage. It is much cheaper and offers an order of magnitude larger return on investment [26].

1.5 Commercialized Energy Storage Technologies

Not all energy storage technologies are created equal. They can come in a variety of sizes and configurations, and can range from applications in cell phones, to automobiles, to the grid. One way to classify USES technologies is through their application for power or energy.

Power applications require high power output, usually for relatively short periods of time (seconds to minutes). Storage used for power applications usually has the capacity to store fairly modest amounts of energy per unit of rated power output. Notable storage technologies that are especially well-suited to power applications include batteries, capacitors, SMES, and flywheels [18]. Typical functions of power applications include frequency regulation, short duration spinning reserve, and voltage support, as well as backing up power for localized uninterruptable power supplies.

Energy applications are uses of storage requiring relatively large amounts of energy, often for discharge durations of many minutes to hours. Thus, storage used for energy applications must have a much larger energy storage reservoir than storage used for power applications. Storage technologies that are best suited to energy applications include compressed air energy storage, pumped hydroelectric energy storage, thermal energy storage, and most electrochemical energy storage types [18]. Typical functions of energy applications include acting as spinning reserves and load shifting, thus aiding with renewable energy integration.

Each technology has its own distinct advantages and disadvantages that determine its value for certain applications. The following subsections will describe commercialized energy storage technologies, and elaborate on their capabilities and weaknesses.

1.5.1 Pumped Hydroelectric Energy Storage

Pumped Hydroelectric Energy Storage (PHES) is a time tested and efficient solution that currently serves 99% of the U.S.' large scale energy storage needs [7]. Energy is stored and generated by moving water via large turbines between massive reservoirs with an elevation differential. Round trip efficiencies range from 70% to 80% and are dependent on plant size, penstock diameter, type of turbines used, elevation differential, and the rate of storage and discharge. To be cost effective, projects are typically large scale (on the order of hundreds of megawatts and gigawatt-hours), are therefore capitally intensive, and are limited to geographically favorable locations which can be extremely difficult to source and permit [16],[27].

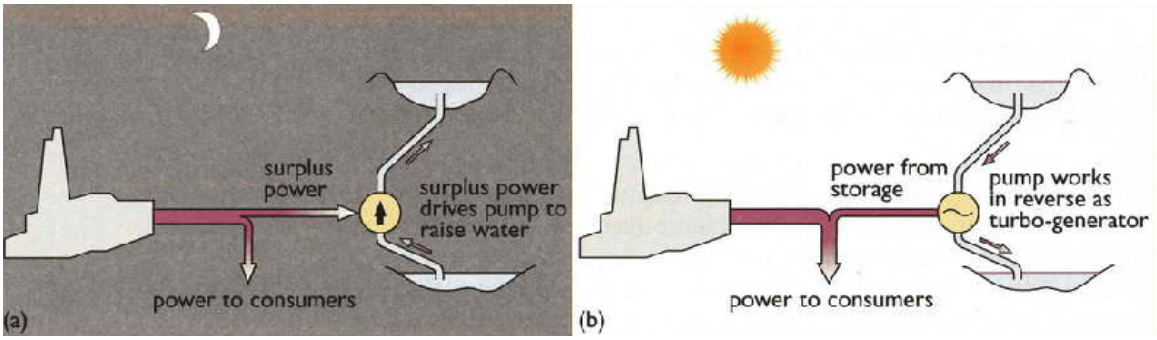

Figure 1.4. Pumped hydroelectric energy storage system operation. (a) at time of low demand, storing energy (b) at time of high demand, discharging energy. [28]

PHES is appropriate for load-leveling because it can be constructed with large capacities and discharged over long periods of time (4 to 10 hours) [29]. It also has response times on the order of minutes, making it suitable as a spinning reserve, and boasts a long projected life-span [17].

There is currently a limited installed base (on the order of kilowatts) of PHES on the Big Island of Hawaii that piggy-backs on existing Department of Water Supply infrastructure. Several major studies have been conducted to explore the feasibility of 160MW for 8 hours of storage on Oahu, 30MW for 6 hours of storage on the Big Island, and 30MW for 6 hours of storage on Maui, but costs ranged between $2400 and $3400 per kW [17].

1.5.2 Compressed Air Energy Storage

Compressed Air Energy Storage (CAES) is a large scale means of energy storage that compresses air into large underground reservoirs. When electricity is needed, the pressurized air is used to drastically boost the efficiency of a gas turbine electric generator. A diagram of operation is shown in Fig. 1.5. Its energy storage roundtrip efficiency (wire to wire) accounts for thermal and electrical inputs, and is roughly 85% [16].

Currently there are only two CAES plants in operation, one in Germany and one in Alabama. More have recently began construction due to higher natural gas prices and the increase in wind energy capacity [29]. Sizes range from 20 to 350 MW [16], and larger plants are estimated to cost near $550 per kW [29]. Like PHES, CAES has response times on the order of minutes which, when coupled with its scale, makes its use appropriate for load-leveling [29].

Since CAES requires fuel, it is considered a hybrid storage and generation plant [16]. In Hawaii, traditional natural gas could be replaced with biofuels, but a suitable geologic feature still must be located and permitted to maintain good economics. Additionally, public opposition is

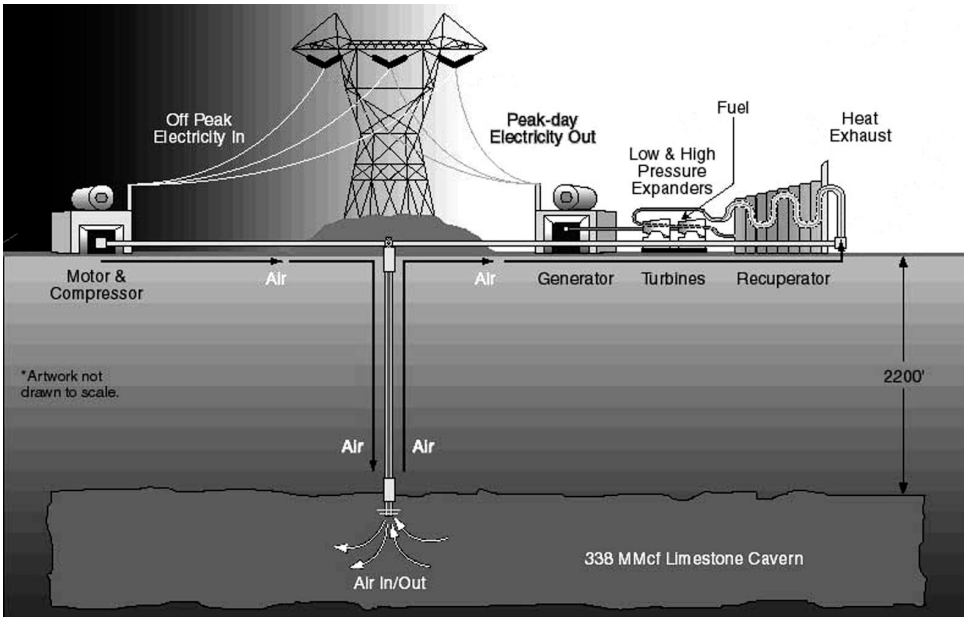

Figure 1.5. The basic operation of a compressed air energy storage system. Off peak electricity is used to drive a compressor that pressurizes air in a sealed underground cavern. When needed, the pressurized air is then used to boost the efficiency of a combustion driven generator [30].

a major concern due to the potential for environmental damage and the loss of land use for other activities [17].

1.5.3 Electrochemical Energy Storage

Perhaps the most well known of energy storage technologies is batteries, also known as electrochemical energy storage (EES). EES stores energy through the conversion of electrical energy to chemical energy, and discharges energy through the conversion of chemical energy to electrical energy. This occurs through electrochemical reactions between the cell's cathode and anode. Cells are connected together in series or in parallel to achieve a required power and energy configuration. For grid scale applications, this can range from kilowatts to megawatts, and minutes to hours of storage [31].

EES options for the grid are increasing in their adoption rate due to their desirable characteristics such as rapid response times (on the order of milliseconds), flexibility, portability, and high energy density [16]. Existing installations of batteries added up to roughly 370MW globally in 2010, and are predicted to grow to a US$4.1 Billion market by 2018 [7], [33].

Figure 1.6. Xtreme Power's DPR^{TM}, a modular advanced lead-acid battery storage system [32]

EES systems typically serve power applications such as frequency regulation and spinning reserves, and have already proven their functionality for renewable energy integration [34]. An aggregation of large numbers of dispersed battery systems in smart-grid designs could even achieve near large-scale energy storage levels enabling load shifting capabilities like CAES and PHES [29], [35].

With many different chemical and physical configurations, the attributes of EES systems can vary widely, and subsequently so can their performance. As the aim of this section is merely to introduce EES systems as a point of reference, a table of useful comparison metrics from LUX Research [23] is presented in Table 1.2 for several commercialized options. In general, high costs and life cycle limitations are detriments to these technologies [36].

1.5.4 Flywheel Energy Storage

Flywheels are growing in popularity in grid scale and smaller scale power applications. Proven with third party testing, field trials, and commercially deployed units, flywheels can be used for low voltage ride-through and backup power (UPS) at the local level, as well as power quality, frequency regulation, and short term spinning reserve applications at the grid level [29], [37], [38].

Energy is stored by using electricity to drive a motor that accelerates a spinning mass. The mass is typically suspended in a vacuum sealed chamber on magnetic bearings to minimize losses and increase speed. The energy stored is proportional to the square of angular velocity, which can reach speeds as high as 50,000 rpm [39]. To retrieve stored energy from the flywheel, the process is reversed with the motor acting as a generator powered by the braking of the rotating disc [35].

Storage Technology	**Benefits**	**Drawbacks**	**Efficiency** (AC - AC)	**Cycle Life**	**Costs** $/kW; $kWh
Molten salt	Good energy density, high efficiency	Expensive, moderate cycle life, reactive liquid sodium in use	89%	4500 at 90% DoD	2250 to 3000 375 to 500
Lithium-ion	Excellent power and good energy density, good cycle life	Expensive, safety concerns	85% to 90%	5000 to 7000 at 90% DoD	350 to 450 1400 to 1800
Advanced lead-acid	Good power density, existing mfg base, potential modest cost	Short cycle life, low energy density	80% to 85%	1500 to 2000 at 90% DoD	275 to 350 1100 to 1400
Flow batteries	Good cycle life, power and energy decoupled, low energy cost	Moderate efficiency, large size, high complexity	70% to 75%	11,000 at 100% DoD 90% DoD	1800 to 4750 300 to 792

Table 1.2. A table from LUX Research comparing key attributes of several leading technologies in utility scale electrochemical energy storage

The overall efficiency (energy out/energy in) of the total system including electronics, bearings, and flywheel rotor drag is roughly 85% round trip [40]. Other advantages are their high power density, fast response times (on the order of seconds), minimal maintenance requirements, and 20 year lifespan (hundreds of thousands of cycles) [40][36].

Beacon Power opened their first 20MW flywheel energy storage plant in Stephentown, New York in 2011. The plant, which is the largest advanced energy storage facility currently operating in North America, utilizes two hundred high-speed Beacon flywheels, each rated at 100kW, to provide fast-response frequency regulation services to the New York electricity grid [42]. This is the largest demonstration of the technology to date and proves its usefulness for grid scale applications. Figure 1.7 provides an aerial view of the facility to illustrate the system's scale.

Ultimately, flywheels are difficult to scale up in terms of energy capacity. Typical projects are aimed at providing full power for 15 minutes [40], meaning Beacon's 20MW plant in New York holds 5MWh of energy. Without significant up-sizing, this means load shifting and spinning reserve applications are not possible, though small wind farms may benefit from ramp rate reduction capabilities.

Figure 1.7. Beacon Power's 20MW flywheel energy storage facility in Stephantown, NY [41]

1.5.5 Thermal Energy Storage

Energy can be stored in a material utilizing either its sensible or latent thermal properties. Sensible heat can be utilized to store energy simply by adding heat to a material, and extracting this heat later when needed. The amount of energy stored (E_s) is dependent on the change in temperature of the material and can be defined using

$$E_s = m \int_{T_1}^{T_2} C_p \, dT, \tag{1.5.1}$$

where m is the mass, C_p is the specific heat, and $T_2 - T_1$ represents the temperature swing [43]. Solar hot water systems are an example of sensible heat storage.

Latent heat can be utilized to isothermally store energy through the phase transition of a material. A congruent material maintains the same chemical composition throughout the change in phase, and is reversable. The amount of energy stored as latent heat (E_l) can be defined using

$$E_l = m \, \lambda, \tag{1.5.2}$$

where λ is the latent heat of fusion of the material [43].

As defined in the closed system energy balance equation,

$$Q - W = (U_2 - U_1) + (KE_2 - KE_1) + (PE_2 - PE_1), \tag{1.5.3}$$

where Q is heat energy, W is work, U is internal energy, KE is kinetic energy, and PE is potential energy. In the case of thermal energy storage, it can be assumed that effects from KE and PE are negligible, leaving only internal energy responsible for the storage of both heat energy and available work. Not all internal energy can be converted to produce work, however. This is where losses occur in the form of heat energy escaping to the surrounding environment, both during storage and conversion. Some losses can be mitigated through insulation, but some are unavoidable.

A good example of thermal energy storage is the use of solar energy to heat a storage material, followed by conversion to electricity through a turbine generator. Concentrating solar collectors or heliostats can be used to focus a large area of solar radiation onto a smaller point on a thermally conductive material. In the case of heliostats, large arrays of mirrors collectively focus sunlight onto a central point where temperatures reach up to 2000K [43]. This heat energy can be transfered into a reservoir of storage material such as molten salt to increase its internal energy. Typically a storage material is selected that maintains a liquid state throughout the designed temperature range, rendering it transportable via pipes between processes. When generation of electricity is desired, the heat from the storage material is transferred to another working fluid, causing it to expand as it vaporizes which then drives a turbine coupled to a generator [44]. It is possible with methods such as underground insulated tanks to achieve thermal equilibrium efficiencies of up to 90% [45].

An example of the above system is the Gemasolar CSP electrical plant (formerly named Solar Tres) found in Spain. With 19.9MW peak power output, the plant gathers sun using 2,650 heliostats over 185 hectares and focuses them on a 140m high solar power tower. The thermal energy storage system uses 6,250 metric tons of molten nitrate salt to allow for 600MWh of total storage, which enables an annual capacity factor of 63% to be reached and 110GWh of electricity to be produced annually [46]. An aerial picture of this plant is shown in Fig. 1.8.

1.6 Thesis Motivation

Though the merits of energy storage are sound, costs have proven to be the key limiting factor to its widespread adoption [7]. Xtreme Power's DPR battery storage module (advanced lead-acid) is a commercialized example of a high cost energy storage solution at $1250 per kWh [23].

Figure 1.8. The Gemasolar CSP plant which utilizes thermal energy storage to increase availability of electricity production [47]

As a point of reference, the Department of Energy Advanced Research Projects Agency - Energy (ARPA-E) solicited proposals in 2010 for new transformative concepts in energy storage with a cost target of $100/kWh [7]. A comparison of existing technologies in terms of power and energy costs, response capabilities, and capacities from this funding opportunity announcement (FOA) is seen in Fig. 1.9. As of April 3, 2012, another FOA was released from ARPA-E, again targeting similar cost and performance goals [48].

From Fig. 1.9, it can be seen that incumbent technologies such as PHES and CAES already meet this cost goal. However, as discussed previously, both are limited to suitable geographies and geologies. Above ground CAES shows promise, though has shown limited development thus far. These technologies are represented by large circles in the figure which means they can respond in minutes. The small circles represent technologies with fast response times, the most cost effective being conventional Lead-Acid batteries. Note the diagonal capacity lines that separate these technologies from the slower responding PHES and CAES technologies. A key gap in the state of the art is therefore identified that falls between quick responding, low capacity systems and slow responding, large capacity systems.

The motivation behind the development of buoyant energy storage technology is to approach the cost target of $100/kWh with fast response times, a competitive round trip efficiency, and the ability to scale to capacities greater than existing battery systems.

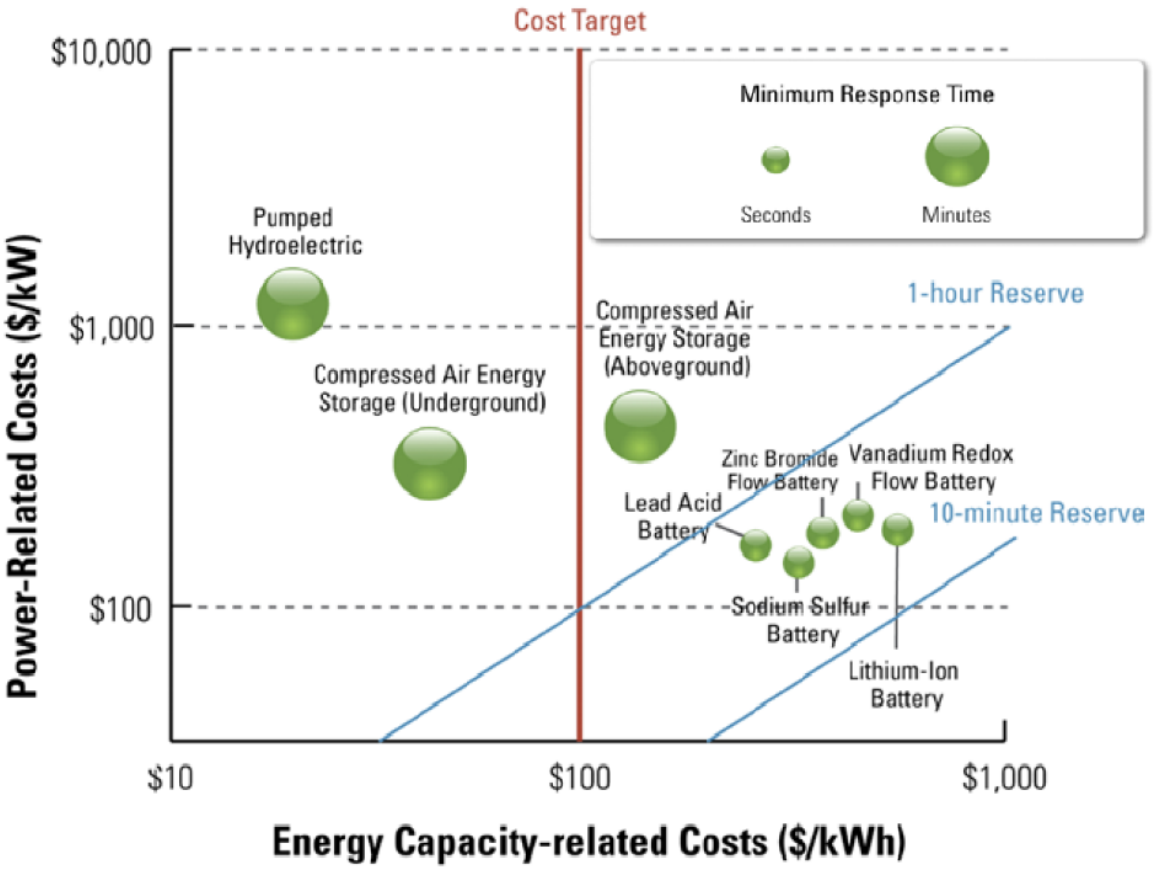

Figure 1.9. This DoE sourced graph from the Advanced Research Projects Agency-Energy (ARPA-E) Grid-Scale Rampable Intermittent Dispatchable Storage (GRIDS) Funding Opportunity Announcement in 2010 [7] compares the capital costs of energy storage technologies per unit power and per unit energy. It also illustrates inherent differences in technology capacities and response capabilites.

Chapter 2

The Novel Idea of Buoyant Energy Storage Technology

In light of the above motivation, the novel idea of buoyant energy storage technology (BEST) was conceived of by Assistant Professor Reza Ghorbani in 2009.

2.1 How it Works

The principle is simple. Intermittent electricity powers a motor connected to a cable that pulls a large pressure proof buoy to depth. During descent, kinetic energy is converted to potential energy due to the force of buoyancy. When demand warrants, the buoy is allowed to ascend, this time driving the motor, which puts firm and predictable electricity back into the grid. Fig. 2.1 shows the principle in its simplest embodiment.

2.2 Theorized Benefits

Benefits are numerous and have been theorized to include the following relative to existing energy storage technologies.

2.2.1 New Locations for Energy Storage

PHES and CAES, some of the largest energy storage technologies, require a specific geographic or geologic feature to make them feasible which limits their cost effective application. BEST enables the use of lakes and oceans as a medium to store energy, thus opening up a range of applications. Considering that population densities are consistently high near bodies of water and in coastal regions, this is a substantial benefit.

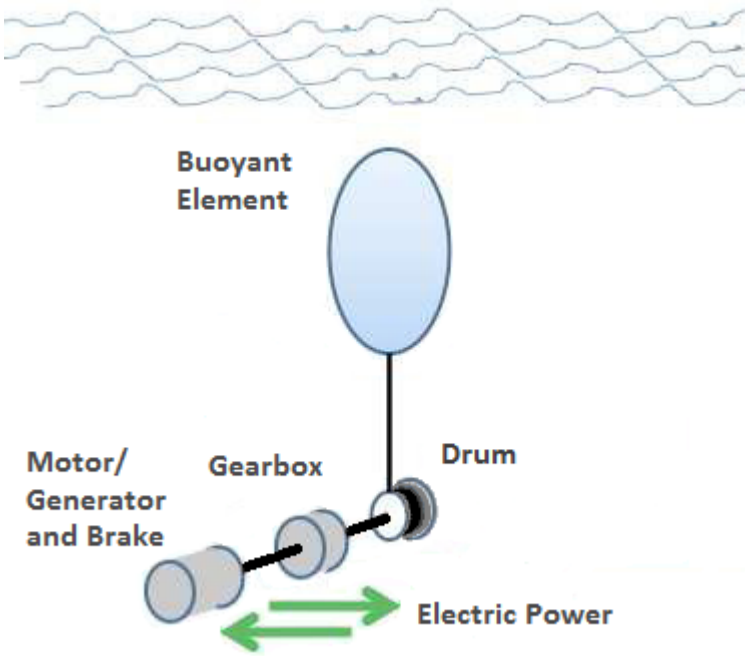

Figure 2.1. A simple embodiment of BEST

2.2.2 Minimal Land Use

Inherent in the use of BEST is its requirement for aquatic space, but also its small requirement for land. The only foreseeable land use is from the on-shore undersea transmission cable termination point, above ground transmission lines (if necessary), and grid tie in.

2.2.3 Competitive Efficiency

Initial napkin based estimates predicted a competitive efficiency for BEST based on highly efficient motors, slow speeds, and low friction losses. These estimates are quantified through numerical modeling in Chapter 4.

2.2.4 Modular and Scalable by Design

With its power output based on a few easily modifiable parameters such as number of buoys, buoy volume, and motor size, BEST is easily scalable to specific applications ranging from kilowatts to megawatts. Both power and energy can be adjusted through stacking BEST modules for parallel or series operation, respectively. The potential to adjust many of the system's design

parameters also allows for precise design targets to be hit, while allowing flexibility in the design optimization process.

2.2.5 Applications in Multiple Ancillary Service Markets

Leveraging the modularity and scalability of BEST, systems can be custom tailored to multiple concurrent applications as well. Higher power needs can be addressed by implementing many parallel buoys that provide a short burst of power; this same system can then also provide low power for long periods by cascading buoy movements. This could enable a single system to cover multiple ancillary services from frequency regulation through spinning reserves and load shifting.

2.2.6 Known State of Charge

Whereas many battery technologies rely on inaccurate estimates of state of charge (SOC) that change with time due to degradation and parasitic losses, BEST can give a precise measurement of the SOC using the buoyant element's position. Grid operators then know exactly what capabilities their storage system has at a given moment.

2.2.7 Stable State of Charge

Batteries are known to slowly lose energy over time due to internal parasitic losses [49]. PHES can suffer similar effects due to seepage and evaporation [45], and CAES can leak slowly out of imperfectly sealed underground reservoirs. BEST avoids this problem through mechanically braking the buoyant element at any position, locking it in place. Since energy stored is proportional to depth, it loses no energy over time. This gives BEST the ability to store energy for virtually unlimited durations.

2.2.8 Minimal Degradation Losses

Unlike many battery technologies, cycle rate and depth of discharge do not negatively affect BEST performance. At the end of its lifespan, it can still store the same amount of energy and produce the same amount of power as it did during its first day of operation.

2.2.9 Long Projected Lifespan

Initial projections estimate BEST's lifespan to be near 40 years. This number could be shorter depending on the many unknowns of the marine environment as well as the design of moving

components and the maintenance plan employed. This is comparable to PHES and very long relative to many batteries which require replacement after a limited number of cycles.

2.2.10 Low Predicted Environmental Impact

The impact of BEST is predicted to be low due to the low velocities of the buoyant elements (< 0.2 m/s), and the minimal amount of moving components exposed to water. The motor can be housed in a sealed chamber, the load-bearing cable is similar to marine anchoring systems, and the undersea transmission cable is similar to other installations found around the world. Locating in non-protected or sensitive areas is key to maintaining a low impact.

2.2.11 Synergistic Relationship With Offshore Renewables

When coupled with offshore wind or wave energy systems, BEST can enable higher capacity factors through load shifting and ramp rate reductions. This could be accomplished either through electrical interconnection, or direct mechanical coupling.

2.2.12 Competitive Cost

As elucidated in Chapter 6, BEST is competitive, in terms of lifetime costs, with other commercial technologies. This analysis is based on a number of estimates, assumptions, and potential oversights, but nonetheless indicates excellent potential to overcome energy storage's cost hurdle.

2.3 Scope of Research

To further the concept, more detailed analysis is required to support the theorized benefits listed above. Research performed includes four key phases, each with their own chapter, which were aimed to encompass as much of the front-end of product development as possible. Chapter 3 presents design ideation, common component options, and a method to calculate scale. This is followed by Chapter 4 which defines and combines various subsystems and component choices into a single dynamic model. This is then instantiated in Simulink® to investigate the system's performance in terms of response times and efficiency. Subsequently, a control system is designed and tested for a single buoy system followed by a dual buoy system, both of which improve the operating characteristics of the device. Chapter 5 presents a proof of concept experiment and results at a

miniature scale followed by a brief discussion of two scaled up test options. To estimate how BEST compares economically with other technologies, Chapter 6 presents a cost comparison analysis between BEST, PHES, and batteries. Finally, Chapter 7 summarizes key results and draws conclusions about BEST's performance and where it fits in the market for energy storage. The thesis concludes with future work and funding opportunities.

Chapter 3

Design Ideation and Selection

With the simple idea being that forcing a buoy underwater creates potential energy, much like lifting a weight up in the air, many design variations were immediately realized. The marine environment has a reputation for destroying man-made equipment; therefore, the qualitative goal was to maintain simplicity while at the same time minimizing costs and maximizing efficiency, scalability, and lifespan. Other considerations include manufacturability, the method of deployment, and maintenance requirements. Toward this end, numerous ideas were spawned and subsequently categorized into five types as presented below with their corresponding advantages and disadvantages. Components common to multiple types are then presented with their design options. Finally, a method of calculating scale, based on several known parameters, is presented.

3.1 Simplest Embodiment

Aimed at keeping system complexity minimized, the concept shown in Fig. 2.1 and also Fig. 3.1.a was conceived and became known as the simplest embodiment. A motor is positioned on a counterweight on the sea floor and transmits bi-directional power flow via an undersea transmission cable. The motor is connected to a gear box, which reduces the shaft's angular velocity and multiplies the torque delivered to a cable drum. The cable then connects to a large buoyant element that can be raised and lowered as desired to produce and consume electrical energy respectively. The system is held stationary by a mechanical brake connected to the drum.

Advantages of this design are its minimal use of moving parts, and simple deployment; the entire assembly can be lifted from a barge and lowered to its eventual permanent resting place on the sea floor.

Disadvantages to this design include the complicated maintenance requirements from critical components such as the motor, gearbox, and drum being located at extreme depth. With depths of 1 kilometer being considered, this is a serious issue.

One solution is to house all critical components inside the buoyant element. The volume and structure of the buoyant element would need substantial increases, but maintenance is then simplified by surfacing the system.

Another solution is to leave the deployment cable in place with a small underwater buoy maintaining its position near the surface. This cable could be retrieved and used to lift the entire assembly back to the surface for maintenance. Avoiding damage to the undersea cable could still remain problematic.

A final, more extreme solution is a counterweight separation strategy where remotely activated solenoids would be used to disconnect the undersea cable and the mounts on the counterweight. The buoyant element would then rise quickly to the surface pulling with it the entire assembly which could then be retrieved. Simple reinstallation could be more cost effective than a complicated deep sea maintenance operation.

3.2 Inverse Concept

An obvious variation on this concept is to avoid the use of buoyancy and the marine environment by simply raising and lowering a weight. The problem with this is mainly of structural concern; a kilometer tall structure under compression would encounter problems with bending, twisting, and forces from wind that could destroy it. Unless integrated into an existing building or structure with extra load bearing capabilities and its working height reduced, such a tall structure is impractical.

The ocean based variation on this idea is to use a weight suspended from a large floating platform shown in Fig. 3.1.b. The motor/generator, gearbox, and power electronics are housed on the floating platform, which could be a retired barge, thus eliminating the need for a support structure entirely. Advantages include the simplicity of the design, likely lower costs due to the reuse of an unwanted barge, and ease of maintenance since critical components out of the water. Disadvantages include public opposition due to a visible system within sight of the shoreline, connecting a permanent undersea cable to a dynamic vessel, and power limitations due to the buoyancy of the barge and the weight being required to exert a smaller downward force.

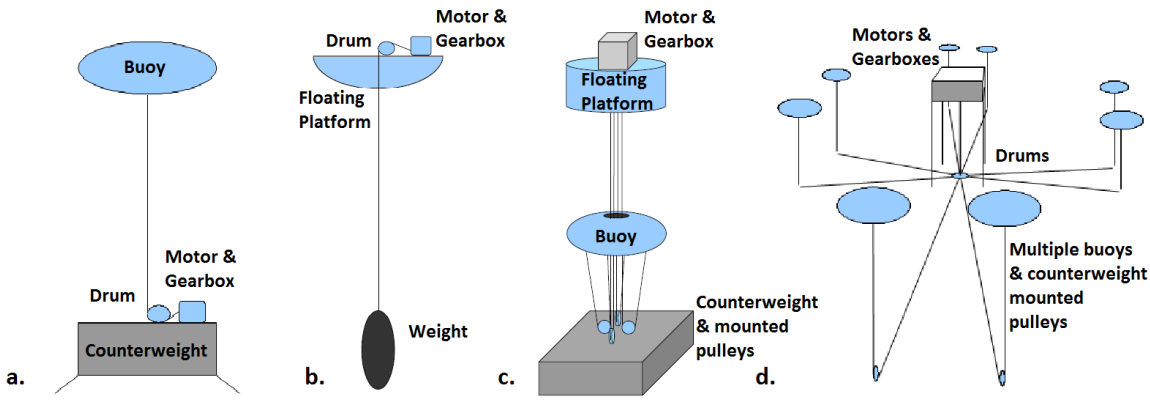

Figure 3.1. Four variations on BEST design

The land based variation on this notion is a system that raises and lowers a weight into a hole in the earth. The depth and diameter would be limited by drilling capabilities, thus the energy capacity would likely be far lower than that of the ocean based variation. Quick bursts of power would be the best mode of operation for such a system. Its advantages would be similar to the above with the addition of location flexibility, and the disadvantages would primarily be these limitations on power and energy.

3.3 Floating Top Platform

With a primary goal of moving critical components to the surface of the water, this design shown in Fig. 3.1.c incorporates a floating top platform which houses the motor/generator, gearbox, and power electronics. Cable comes off of several drums down to counterweight mounted pulleys which then connect to the toroidal shaped buoyant element. The platform must have a far greater buoyancy than the buoyant element for it to remain out of the water. Additionally, the counterweight must exert a high downward force relative to the inverse design.

The main advantage is the ease of maintenance since critical components are out of the water. Another is ease of deployment, so long as the scale allows the entire assembly to be lifted by a ship mounted crane.

A disadvantage to this design is the introduction of waves and elevated sea states to the dynamics of the system. This could potentially be harnessed through a point absorbing wave energy conversion approach, but it then introduces oscillations to mechanical power. Maintaining a secure connection to the undersea cable could also be problematic with the added dynamics of the platform.

3.4 Spider Web Design

As seen in Fig. 3.1.d, the spider web design expands on the floating top platform idea, incorporating multiple buoyant elements under the control of one central floating top platform. An uprated motor/generator could be used by connecting individual cables to a common driveshaft through clutches. Alternately, individual motor/generators could merely share a common floating platform.

A key advantage to this design is the simplified expansion of energy and power capacities. A disadvantage, as in the floating top platform, is the introduction of wave dynamics to the system. However, with a larger top platform comes the possibility of using the slow heaving motion of the platform to force the descent of individual buoyant elements. This may be more manageable than with a smaller platform, which would be susceptible to smaller period waves and rapid heaving. Maintaining a secure connection to the undersea cable could still be problematic as well.

3.5 Multi-Buoy Conveyor

Another approach to the concept is a multi-buoy conveyor system. As seen in Fig. 3.2, numerous smaller sized (1m diameter) buoys are shuttled from an upper staging area to a lower staging area via one way conveyors. The natural sloped roofs in the staging areas force the passive migration of buoys from one offloading point to the next loading point. Power is used to drive buoys down, and power is harnessed from their return up the opposite conveyor.

The intended advantage of this idea is the ability to scale up to massive levels of energy capacity with one common piece of infrastructure and numerous cost effective buoys.

The key disadvantage discovered during modeling is the significant loss of potential energy from the passive buoy migration technique. Another is the complicated mechanical conveyor systems and critical components housed underwater; maintenance could foreseeably become a tremendous cost. Also, undersea currents could potentially dislodge buoys during ascent and descent.

3.6 Common Components

Though many designs exist, it was observed that many still shared the same common components, albeit in different configurations. They are broken into categories in the following

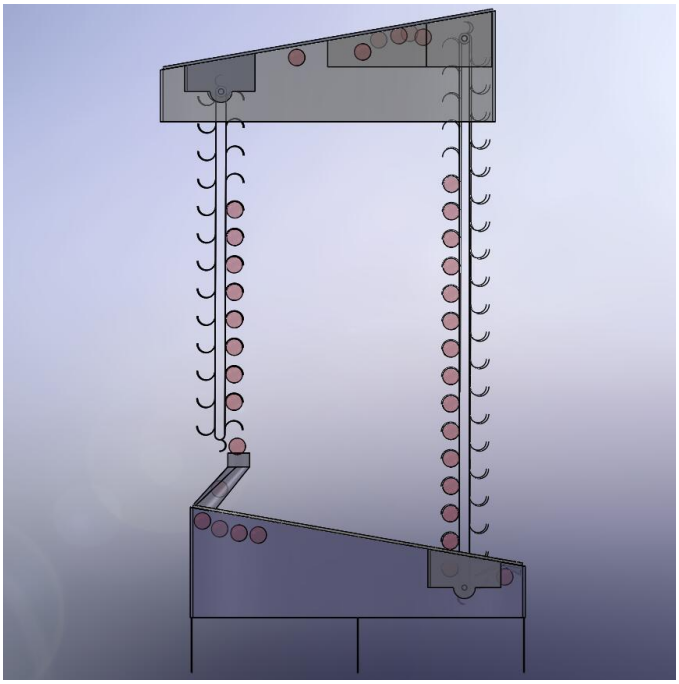

Figure 3.2. A CAD rendering of the multi-buoy conveyor design

subsections and their objectives, constraints, and design options are briefly described. Note that a common objective is to minimize cost.

3.6.1 Buoyant Element

The objective of the buoyant element is to produce the highest constant buoyant force possible when submerged. This objective instantly rules out any sort of balloon or changing volume component, as the volume will decrease with increasing depth. This reduction in buoyant force could potentially reach levels where the system would no longer be able to restore itself. Even in very shallow water, this effect will alter the ability to produce power, though for such systems, it could serve as an approach to reduce costs. Also important is the weight of the element, as it counters the effect of buoyancy and increases the overall system inertia. The trade-off here is the ability to withstand significant pressure, since designs have envisioned depths up to 1000 meters. Approximating the maximum pressure by adding 0.1MPa for every 10 meters of depth results in a maximum pressure differential of 10MPa. To realize such depths will require one or more of the following ideas.

The most likely option is a compressed air reinforced buoyant element. Pressure would be set equivalent to the median operating depth to minimize material strength requirements at minimum and maximum operating depths. This will drastically reduce the weight of structural reinforcement, but with an increase in mass from the compressed air. Calculations have shown substantial weight savings through use of this method.

Another option is mechanical reinforcement through concentric rings, or spokes. This option adds weight, but could result in significantly higher depth ratings.

3.6.2 Load Bearing Cable

The cable serves the critical mission of coupling the buoyant element to the drum. This component must be strong, as lightweight as possible, and as long lasting as possible. Marine grade alloy has been industry standard for decades but suffers from high weight, and a limited lifespan. Additionally, the bending induced when wrapping the cable drum constrains the minimum size of the drum. When the drum diameter is enlarged, the necessary gear ratio increases, reducing the overall efficiency and increasing costs. In the industry, the critical term is the D/d ratio, where D is the drum diameter and d is the cable diameter. A typical D/d value given by an engineer at WireCo is 63 for wire rope.

To meet the above objectives and to reduce the necessary D/d ratio, an alternative synthetic rope made of ultra-high molecular weight polyethylene (trade name Dyneema) is available that carries with it numerous supplementary advantages. Dyneema is 15 times stronger than steel by weight, has a 0.97 specific gravity (meaning it adds to the buoyancy of the system), requires a D/d ratio of only 7.5 - 15, boasts chemical and UV resistance, and is extremely durable [50], [51]. The only notable downfall is its creep tendency under high loads, which could be mitigated through oversizing. A side by side comparison picture of Dyneema with an equivalent strength steel wire rope is shown in Fig. 3.3.

3.6.3 Drum

As the drum serves the crucial role of converting linear to rotary motion, minimizing its diameter is paramount in reducing the necessary gear ratio and motor torque values down the line. As mentioned above, the diameter of the Dyneema is the critical constraint on the size of the drum.

A steel cylinder with rope retaining flanges is a likely candidate for this application. An alternative used in heavy marine lifting applications is a two drum traction winch designed to direct

Figure 3.3. A side-by-side comparison of Dyneema synthetic rope (28mm diameter) with steel wire rope (36mm diameter) [52].

the live load primarily to a load drum [51]. Through wrapping the load drum one or more times, the tension on the storage drum is reduced exponentially which allows for better rope management.

3.6.4 Counterweight

The objective of the counterweight is to balance all buoyant and inertial forces encountered by the system. An optional objective is to remove the need for any supplemental anchoring or mooring methods. The constraints are that it must be transportable, deployable, and able to be permanently left in place.

Concrete is the first and most likely candidate for this task. With low costs per unit volume, and a relatively high density of 2400kg/m^3, a volume slightly larger than the buoy itself would completely handle all forces encountered by the system. Additionally, concrete allows for encapsulation of structural rebar for mounting purposes as well as other re-purposed, dense materials such as old concrete chunks, or waste steel. This benefit can add to the environmental appeal of the system when completing an environmental impact statement.

3.6.5 Gearbox

In order to achieve high torques and low rotational speeds, heavy duty gearing is needed. Typically, efficiency losses grow with increasing gear ratios, so an objective is to minimize the

necessary gear ratio. This is already accomplished by keeping a low D/d ratio, and employing a low speed, high torque motor. After this, keeping the inertia ratio relatively low allows for stable and accurate control of the system.

To determine if commercially made gearboxes exist that can handle the potentially massive torques produced through buoyancy, maximum ratings were researched. Bosch Rexroth produces planetary gearboxes for wind turbines with torque ratings up to 1.26MNm or 2MW generators. Another Italian company, Dinamic Oil, produces planetary gearboxes with torque ratings up to 2MNm.

Another option could be to directly couple the motor shaft to the outer edge of the drum via matched gears. This option would limit the gear ratio and require use of a high torque, low speed motor coupled by significant structural elements. Additionally, it would raise the likelihood of foreign debris blocking the the gears, which would have to be mitigated through sealing or other mechanical means.

3.6.6 Motor/Generator

Motor selection involves many attributes and trade-offs, and is a complex decision. To keep things manageable, a high level decision is approached using only several objectives. While a good round trip efficiency is required, gaining a few extra points over competing technologies does not effect a net present value comparison significantly [26]. Despite this, efficiency is still a major consideration for BEST design due to the multiplied effect of bidirectional power flow. Other objectives are to minimize operating speeds while maximizing torque to reduce the necessary gear ratio.

Historically, DC Motors were the first electric machines used in industry. Coming in both brushed and brushless forms, DC motors are typically characterized by a continuous current flow and operate at variable voltages, making control simple [53]. Generally, DC motors require more maintenance than AC motors, raising their operational costs [54]. With recent advances in AC motor control, DC motors are tending to be replaced with AC motors [51].

AC motors can be either synchronous, as in a permanent magnet synchronous machine, which rotates at a sub-multiple of its supply frequency, or asynchronous, as in an induction motor, which slightly leads or lags its supply frequency [53]. Both can be controlled by a wide variation of schemes. Generally, AC motors are viewed as simple and sturdy “all purpose motors” that require less maintenance than DC motors, making their operational costs low [54].

Capital costs of four quadrant drive systems, which includes the motor, power electronics, and controller, tend to be lower for DC drives than AC due to the power electronics involved [54]. However, in general, the lifespan of AC motors has tended to be longer [54].

In the case of BEST, maximizing the lifespan couples well with AC motors, which are commonly used for electricity generation applications [55] and can fare well in corrosive or wet environments [56].

Between an AC synchronous motor and an AC induction motor, costs tend to favor the latter [57], while operation can be made similar through proper control schemes. Additionally, induction motors avoid the use of rare earth metals required for high performance permanent magnet synchronous machines, which on the other hand tend to have very high efficiencies [58].

A company in Italy, Magnetic S.p.a., manufactures an HTQ series of synchronous motors featuring a high pole count of permanent magnets [59]. This allows for low operating speeds and high torques which perfectly suit the BEST application. A product brochure for these motors can be seen in the appendix.

3.6.7 Regenerative Drive

Inherent in BEST is the need for a regenerative drive, or four quadrant motor controller. Additionally, when coupled to a power grid, a power conversion system is vital for proper integration. To avoid the need for large contact switches, the associated power spikes, general wear and tear, and complicated power engineering challenges, a commercial drive is considered.

Several candidates were found capable of performing the necessary functions and include the Unidrive SP from Emerson Electronics, the Transomik UZ from Kimo, the ACS 800-11 from ABB, the 1130 Line Regenerative Drive from Unico, and the PowerFlex series from Allen-Bradley. For reference, the specifications and features of the Unidrive SP are included in the appendix.

3.6.8 Undersea Transmission Cable

A significant cost will be incurred transporting electricity to and from the shoreline via an undersea transmission cable. The objective is to minimize both this cost and transmission losses while requiring minimal future maintenance.

Two options currently exist: AC submarine cables and high voltage DC (HVDC) submarine cables. Typically, HVDC cables become economical after a significant distance is traversed, because their principle advantage is their reduced losses. AC systems offer simplified power elec-

tronics for stepping voltages up and down, but cannot carry the same capacity as HVDC due to the effective power being calculated from RMS voltage, which is roughly 0.707 times that of an identical DC conductor [60]. Since BEST will always be aimed at being close to shorelines, the advantages of HVDC will likely not be realized, so AC is the most likely candidate.

3.7 Scale

As alluded to above, the calculation of various components at different scales involves multiple dependent variables. To mitigate the complexities of designing a system, a spreadsheet was created to allow several design choices to serve as inputs, and their dependent relationships to be calculated as outputs. Note that multiple convenience based choices can be made as to whether a parameter is an input or an output, and these calculations only provide a basic estimate of system parameters which is useful for designing and planning.

Selected inputs include bidirectional system power flow (P_m), full speed motor angular velocity (ω_m), a target buoy velocity (v_b), cable diameter (d), the D/d ratio, and one way system efficiency (β).

Dependent outputs include motor torque (τ_m), drum diameter (D), drum angular velocity (ω_D), gear ratio (N), net buoyant force (F_{net}), and the radius (r_b) for a spherical buoyant element.

First calculate τ_m using:

$$\tau_m = \frac{P_m}{\omega_m}. \tag{3.7.1}$$

D can be determined using:

$$D = (D/d)\ d. \tag{3.7.2}$$

This then allows the calculation of ω_D using:

$$\omega_D = \frac{v_b}{2\pi D}. \tag{3.7.3}$$

The gear ratio can then be calculated using:

$$N = \frac{\omega_m}{\omega_D}. \tag{3.7.4}$$

Finally, the net buoyant force requirement can be calculated using:

$$F_{net} = \frac{2N\tau_m}{D\beta}. \tag{3.7.5}$$

where F_{net} can be multiplied by a safety factor of two to ensure ample sizing of a counterweight to oppose dynamics and disturbances from currents.

Assuming a spherical shaped buoyant element, F_{net} can be used to calculate the buoy radius r_b using:

$$r_b = \left[\frac{3}{4\pi\rho}\left(\frac{F_{net}}{g} + m_b\right)\right]^{\frac{1}{3}}, \tag{3.7.6}$$

where m_b is calculated using the formula for the mass of a sphere plus the weight of air:

$$m_b = V_b\left(\frac{3}{2}\,P_{gage}\,\frac{\rho_{mat}}{\sigma_{mat}} + \rho_{air}\right), \tag{3.7.7}$$

where V_b is the volume of a sphere, P_{gage} is the gage pressure which is determined by the difference between the maximum operating pressure and buoy pressure, ρ_{mat} and σ_{mat} are density and yield strength for the selected material, respectively, and ρ_{air} is calculated using the ideal gas assumption:

$$\rho_{air} = \frac{P_{gage}}{RT}, \tag{3.7.8}$$

where R is the gas constant for air and T is the air's temperature at the time of compression.

To determine the depth (H) required for a system to store enough energy for one hour of full power:

$$H = v_b\,t, \tag{3.7.9}$$

where t is one hour in this case.

Chapter 4

Dynamic Modeling and Simulation

To increase efficiency of the development process, provide flexibility, and enable simulations of many combinations of system parameters, dynamic modeling has been conducted within MATLAB's SIMULINK® computing environment. Using physical modeling toolboxes such as Simscape™ allows for accurate representation of non-linear systems without the assumptions required for conventional transfer function models.

During the course of research, two models were constructed: the preliminary, which was aimed largely at proving the concept and attaining a baseline for performance and parameters, and the refined, which expanded on the original model to include additional complexities. The former was presented along with concept ideas and a research plan at the Oceans10 Conference in Seattle, WA in 2010 [14]. The latter was presented at the Clean Technology Conference and Expo in Boston, MA in 2011 [61]. Only the refined dynamic model is presented in this thesis as it is inclusive of and more accurate than the preliminary dynamic model.

After successful demonstration of the refined dynamic model, a control methodology was designed with the intent of meeting the basic needs of a grid operator. This single input single output (SISO) method was then adapted into a dual buoy control system, enabling more efficient use of stored energy and a greater degree of flexibility for power commands.

4.1 Refined Dynamic Model

The refined dynamic model represents the simplest embodiment, shown in Fig. 2.1. This was chosen to minimize the model's complexity, allowing baseline parameters to be implemented and proving the basic concept of BEST. Additionally, similar concepts can be modeled with only minor modifications to the simplest embodiment including the addition of pulleys or changing masses.

4.1.1 Buoyant Mechanical System

The main source of force in the system is due to buoyancy acting on the buoyant element. Buoyancy sources from pressure differences above and below a submerged object. The integration of these pressure differences over the surface area yields an upward force on the object. Archimedes principle takes a higher level view by stating that buoyant force is equal to the weight of the fluid displaced by the object multiplied by gravity:

$$F_{buoyant} = m_w\, g = \rho_w\, V\, g, \tag{4.1.1}$$

where m_w is the mass of displaced water which is equal to the product of ρ_w (the density of water) and V (the volume of water displaced by the object), and g is the acceleration due to gravity which equals 9.81m/s^2. Using a spherical buoyant element with a radius (r_b) of 1.32m, the volume displaced by the buoy (V_b) can be calculated using the equation for the volume of a sphere and equals 9.63m^3, making m_{wb} equal to 9634.1kg.

When accounting for the mass of the buoyant element (m_b) and cable (m_c) as well as the mass of water displaced by the cable (m_{wc}), and taking positive values to be upward in direction, the net force equation becomes

$$F_{NET} = (m_{wb} - m_b + m_{wc} - m_c)\, g, \tag{4.1.2}$$

where m_b, m_{wc}, and m_c are calculated in the following paragraphs.

The maximum operating depth is assumed to be 1000m, where water pressure is roughly 10MPa. With compressed air pressure equal to the outside pressure at 500m depth, a pressure differential of 5MPa can be used for P_{gage}. Typical steel is assumed for the structure of the sphere with a yield strength of 600MPa and density of 7850kg/m^3. Finally, 20°C is the assumed average temperature of air in the rigid buoy. From eq. 3.7.8, this results in a density for air of 61.131kg/m^3. Now using eq. 3.7.7, m_b equals 1534.3kg.

Dyneema rope is selected for its superior properties over steel wire rope. A 28mm diameter DynaOne rope has a safe working load of 100kN [52]. The dry mass is 40kg/100m, and it also has a specific gravity of 0.97, making it slightly buoyant. Assuming 500m of rope on average is payed out, and neglecting changes in cable mass, the dry cable mass (m_c) is calculated to be 200kg.

The rope's volume (V_c) is calculated using the cross sectional area of the rope times the average length payed out and equals 0.3079m^3. Now the mass of water displaced by the rope (m_{wc}) can be obtained using

$$m_{wc} = \rho_w V_c, \tag{4.1.3}$$

which results in 307.9kg.

These results allow for the calculation of net buoyant force from eq. 4.1.2, which equals 80.5kN

As seen in Fig. 2.1, this force acts vertically through the DynaOne rope, which is treated as inextensible, before being wound on a drum with a radius (r_D) of 0.14m. which was calculated using eq. 3.7.2 with a D/d ratio of 10. The use of this drum size makes the torque at the drum (τ_D) equal to 11.27kNm. Using this and a nominal torque rating of 1610Nm from the motor described below, the gear ratio (N) of a planetary gearbox is calculated using

$$N = \frac{\tau_D}{\tau_m}, \tag{4.1.4}$$

and equates to 7:1. Increasing the buoy's size and therefore its buoyant force will increase this gear ratio. There is a trade off between the resultant buoy speed with its accompanying hydrodynamic drag and larger, more expensive gearboxes.

For completeness, it must be noted that there is no spring constant associated with increasing the buoy's depth. This is due to water being treated as an incompressible fluid.

4.1.2 Electromechanical System

The gearbox is coupled to a 50.6kW, 20 pole interior permanent magnet synchronous machine (IPMSM) with a nominal torque of 1610Nm, and a nominal speed of 300rpm. These specifications come from from Magnetic S.p.a. for model HTQ 350 L TEWC 3B which can be found in the appendix.

The IPMSM can act as both a motor and generator through the use of a four quadrant motor driver (4QMD). The 4QMD is chosen to provide control through torque regulation which is limited to 3300Nm peak per the motor's specifications. Of key importance is the ability of the 4QMD to operate in quadrants 1 and 2 of a torque-speed plane, that is positive angular velocity and positive torque, as well as negative angular velocity and positive torque, respectively.

The 4QMD is powered by a 6.5Ah, 200V, 21kW Nickel-Metal-Hydride battery that connects through a voltage regulated DC/DC converter (boost type). This adapts the low voltage of the battery (200V) to the DC bus which feeds the 4QMD at a nearly constant voltage of 400V. The use of this configuration allows for the simulation of bi-directional power flow without modeling a grid interconnection point.

4.1.3 Drag Force and Damping Torque

Hydrodynamic Drag

The primary resistance force on the buoyant element is in the form of hydrodynamic drag, which is modeled using

$$F_{drag} = \frac{1}{2}\,\rho_w\,C_d\,A\,\dot{x}^2, \tag{4.1.5}$$

where ρ_w is the density of water, C_d is the coefficient of drag (0.5 for a sphere), and A is the cross sectional area of the spherical buoyant element.

Viscous Friction Damping

The addition of damping forces that account for gearbox losses and bearing friction are modeled as functions of angular velocity using

$$\tau_d \;=\; c_m\,\omega_m + c_g\,\omega_D, \tag{4.1.6}$$

where τ_d is torque due to damping, c_m is the damping coefficient on the motor's side, ω_m is the angular velocity of the motor, c_g is the damping coefficient after the gearbox, and ω_D is angular velocity after the gearbox. On the motor's side, a value of $1\frac{Nm\cdot s}{rad}$ was chosen for c, while $10\frac{Nm\cdot s}{rad}$ was chosen on the torque multiplied side of the gearbox.

4.1.4 Equivalent Inertias

The equivalent inertia (I_{bc}) of the displaced water, buoy, and cable is calculated by multiplying the sum of their respective masses by the square of the drum's radius:

$$I_{bc} = (m_{wb} + m_b + m_{wc} + m_c)\,r_D^2 \tag{4.1.7}$$

This equates to 228.85kg·m^2.

The inertia of the drum (I_D) is calculated using

$$I_D = \frac{1}{2}\,\pi\,\rho_{mat}\,L_D\,(r_D^4 - r_{Di}^4), \tag{4.1.8}$$

where the material is the same steel as used for the buoy, L_D is the length of the drum, and r_{Di} is the inner diameter of the drum. Assuming a 5cm wall thickness, I_D equals 3.9kg·m^2.

The specified inertia of the motor (I_m) is 1.3kg·m^2, and the assumed inertia of the gearbox (I_g) from the motor's frame of reference is similar at 1.2kg·m^2.

4.1.5 Braking Mechanism

In order to both slow and hold the system at rest, a bidirectional friction clutch mechanism is employed from the Simdriveline™ toolbox. One side is anchored to the housing and the other is coupled to the rotation of the motor, prior to the gearbox. With an effective torque radius (r_b) of 0.25m, 4 friction surfaces (f_s), a peak normal force (F_{peak}) of 1600N, and a coefficient of friction (μ) of 1, the brake applies kinetic friction torque (τ_{KF}) according to

$$\tau_{KF} = r_b \, f_s \, F_{peak} \, \mu. \tag{4.1.9}$$

Similarly, static friction torque (τ_{SF}) is slightly higher and is calculated according to

$$\tau_{SF} = 1.1 \, (r_b \, f_s \, F_{peak} \, \mu). \tag{4.1.10}$$

Both brake models, which are now referred to as τ_B, are applied to the system depending on its state and are activated via a proportional gain (G_B) within the simulation.

4.1.6 Combined Representation

Combining the above equations yields the following nonlinear, second order differential equation which is written from the motor's frame of reference:

$$(\frac{I_{bc} + I_D}{N^2} + I_g + I_m) \, \ddot{\theta} + (\frac{\frac{1}{2} \, \rho_w C_d A}{N^2} r_D) \, \dot{\theta^2} + (\frac{c_g}{N^2} + c_m) \, \dot{\theta} = \frac{F_{NET}}{N} \, r_D - \tau_m - \tau_B G_B \tag{4.1.11}$$

These forces and torques can be visualized with the system diagram shown in Fig. 4.1 and the corresponding Simulink block diagram can be seen in Fig. 4.2.

4.1.7 Simulation

The primary goal of conducting a simulation is to demonstrate functionality of three modes of operation: storage, generation, and standby. To achieve this, the buoy starts at a vertical reference position of 0m, which is considered to be fully submerged. A torque reference just above the equilibrium value is issued and the buoy accelerates downward. After ample time has passed, the torque is terminated and the brake engaged. Following a brief resting period, a torque reference just below the equilibrium value is issued, allowing the buoy to rise, though with resistance from the motor. The torque is then eliminated just in time for the buoy to come to rest in its original starting position. This sequence of events is summarized in Table 4.1.

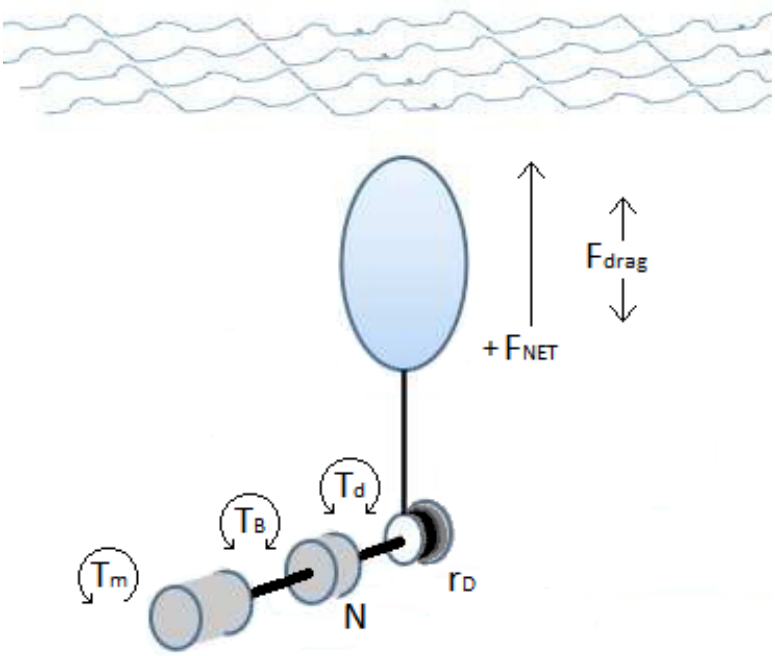

Figure 4.1. A diagram showing all forces and torques on the system.

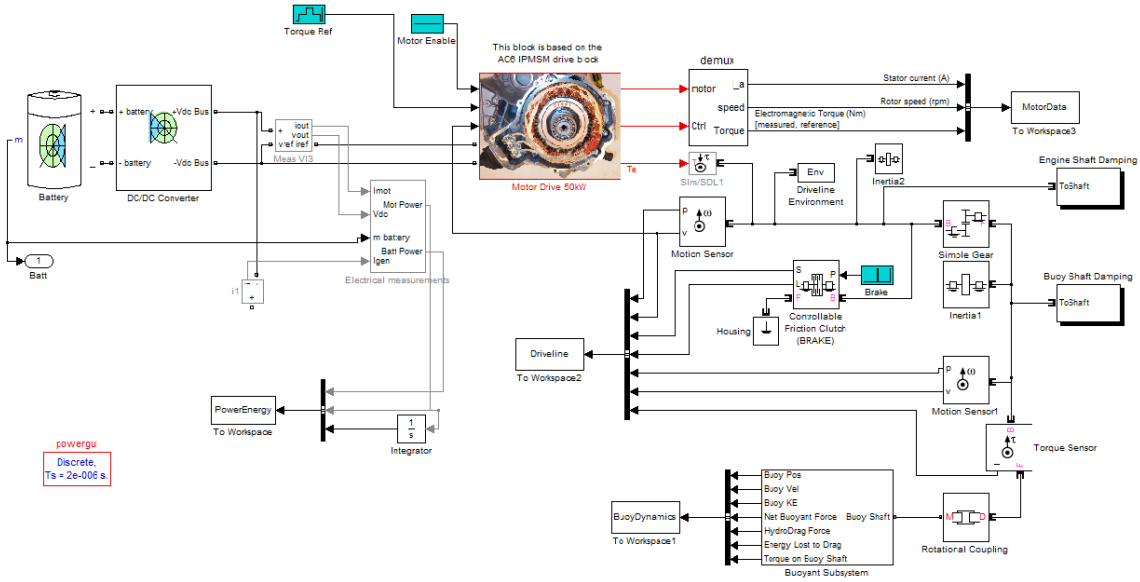

Figure 4.2. A refined dynamic model of BEST. The buoyant subsystem at lower right encompasses the force of buoyancy, hydrodynamic drag, and conversion to rotary motion. This is connected to the motor through a gearbox and includes a braking mechanism. The battery and DC/DC converter are seen at left.

Table 4.1. Timetable of BEST System Control Events

Time(s)	Mode	Event
0	Storage	Apply 1708.70Nm to accelerate the buoy's descent
50	Transition	Eliminate motor torque and decelerate to a stop
50.12	Standby	Apply brake and hold position
60	Generate	Release brake and apply 1496.53Nm to oppose the ascent
103.99	Standby	Decelerate and stop through conventional braking

4.1.8 Results

Electromechanical Performance

Figures 4.3 - 4.6 show the performance of the system in terms of buoyant element position and velocity, as well as motor electrical power and energy, which are explained below.

First, it is important to note from Fig. 4.3 that the buoy does indeed start and finish at the same position. It descends nearly 28.1m in just over 50 seconds, then it ascends the same depth in just under 44 seconds. This difference in time is attributed to the effects of hydrodynamic drag and damping losses. In storage mode, these losses oppose the action of the motor which is working to drive the buoy downwards; in discharge mode, these losses work in tandem with the motor, which is acting to regulate the speed of the buoy.

Figure 4.4 corroborates this result by showing two different steady state velocities being reached for each mode. Storage mode settled into a rate of nearly -0.59m/s while generation mode reached a steady state velocity of nearly 0.67m/s. On the motor's side, angular velocities reached steady states of 29.26 rad/s and -33.41 rad/s for storage and generation modes, respectively. This, combined with the torque output allows for the calculation of mechanical power (P_{m}) using

$$P_{\mathrm{m}} \;=\; \tau_m \, \omega_m, \tag{4.1.12}$$

where τ_m and ω_m are the torque and angular velocity from the motor, respectively.

At steady states, this calculates that the system consumes 50kW during storage mode and produces 50kW during generation mode as shown in Fig. 4.5, which is measured power at the high voltage side of the DC/DC converter. This is no coincidence, as the simulation was setup with matching storage and generation power values resulting from specified motor torque inputs.

Another set of important observations that can be made from Fig. 4.5 regards the system's response, which is defined according to the desired power levels. A 98% response is obtained in

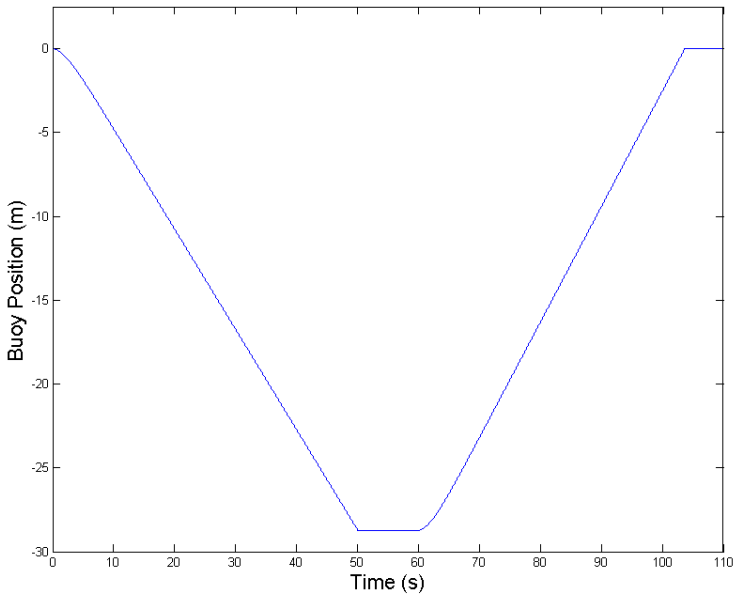

Figure 4.3. Buoyant element position vs. time.

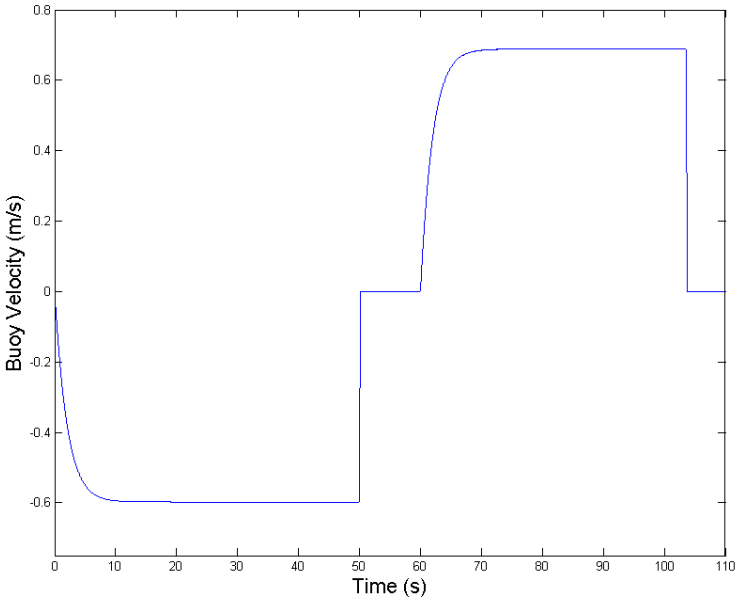

Figure 4.4. Buoyant element velocity vs. time.

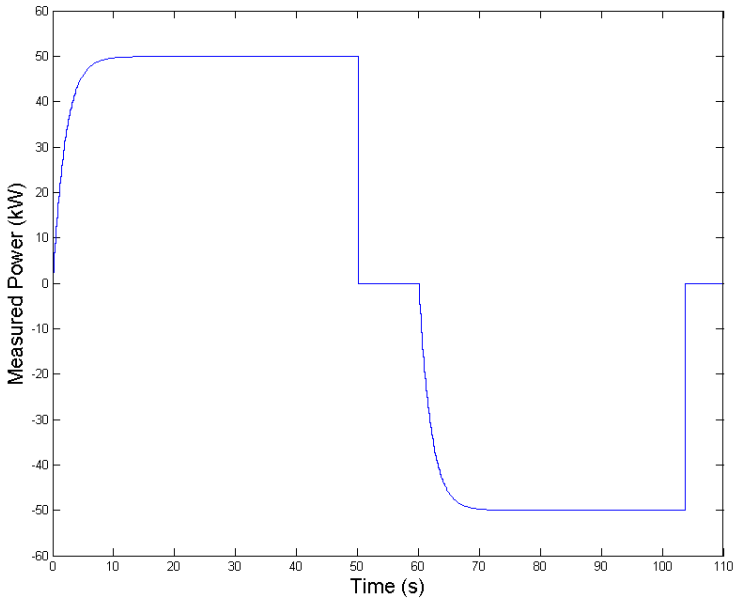

Figure 4.5. Motor power vs. time.

7.9s for storage mode, while the same response is obtained by generation mode in 7.8s. Note that the steady state errors are very low, and there is no overshoot due to the heavy damping in the system. Through torque control, these responses can be greatly improved, which is demonstrated in the following section.

To evaluate the efficiency of the system and mode of operation, the power curve is integrated to give an energy profile versus time as seen in Fig. 4.6. As expected, this graph resembles Fig. 4.3 due to the linear relationship of potential energy to depth. The key difference is that the buoy returns to it's original position, while the energy summation does not equal zero. This is due to efficiency losses from drag and damping and can now be utilized to calculate the overall efficiency of one cycle.

Using a ratio of energy generated over energy stored yields the cycle efficiency (η_m).

$$\eta_m = \frac{E_g}{E_s} \tag{4.1.13}$$

Fig. 4.6 shows 2399.5kJ of energy after storage mode and 303.1kJ of energy after generation mode. Subtracting the final value from the stored energy gives the amount of energy generated as 2096.4kJ. Then using eq. 4.1.13, the round trip efficiency equals 87.4%. This number is a bit high due to the omission of losses within the motor. To include this in an estimate of performance requires the

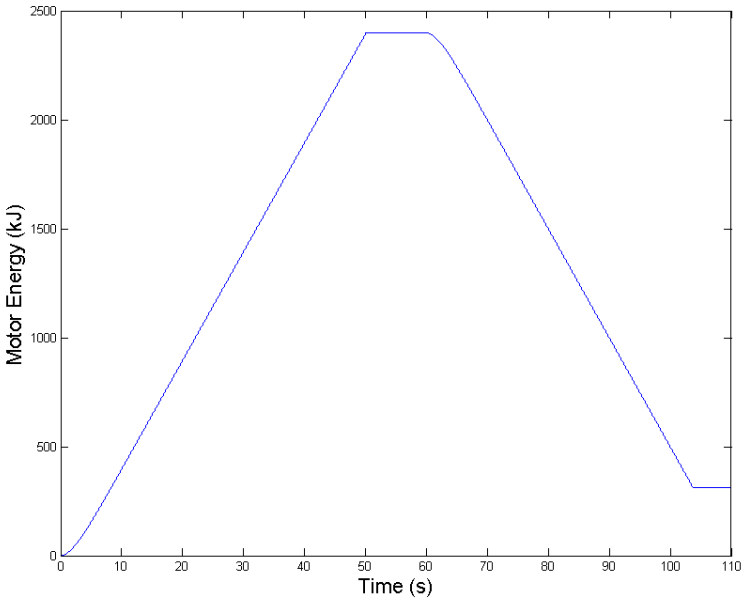

Figure 4.6. Motor energy vs. time

assumption that the motor efficiency value used is good throughout the entire range of operation. 96% is generally considered a good peak efficiency for a motor and is used in the following equation to reestimate the efficiency of the cycle considering both modes of operation.

$$\eta_{est} = (0.96^2)\,\eta_m \tag{4.1.14}$$

This estimate results in a round trip efficiency of 80.5%, which is competitive with existing technologies [18], [36].

Using eq. 3.7.9, the energy capacity of this system can be calculated from the working depth and steady state speed reached during full generation mode. Using the assumption of a 1000m working depth and a speed of 0.67m/s results in a time of 24.95 minutes. Multiplying this by the steady state power generated at that speed gives 20.8kWh of energy capacity.

4.2 Control System Design

In the refined dynamic model, the system was controlled manually using trial and error methods to obtain suitable torque values for desired power inputs and outputs. A feedback torque control loop can be used to improve the response times seen in Figs. 4.4 and 4.5. Additionally, it

enables regenerative braking to take the place of the mechanical brake used to slow the system from generation mode, thus improving the system's efficiency.

4.2.1 Inputs and Outputs

With the goal being to design a SISO feedback controller, and the need of grid operators being the regulation of power, the logical control reference is power P_{ref} and the output is torque τ_m. Angular velocity at the motor (ω_m) is the primary value being fed back, with the measured power (P_{meas}) being used to correct small errors.

4.2.2 Control System Architecture

The control system is organized into three sections: power storage, power generation, and braking. Power storage and generation operate independently of each other and are never producing outputs at the same time. The brake system serves to link the two together for periods when the system is given a zero power reference. As illustrated in Fig. 4.7, a reference power is commanded, rotor speed and power measured are used as feedback, and torque is output to the motor which either produces or consumes electrical power.

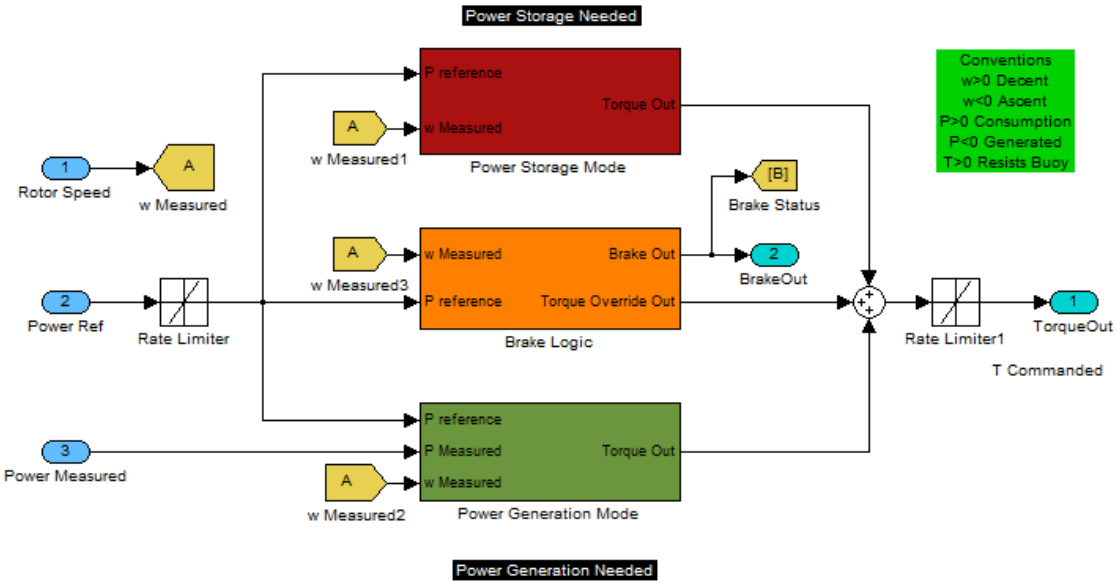

Figure 4.7. A block diagram of the three tier control system

Conventions and Logic

Before proceeding further, it is necessary to first define conventions used for power P, angular velocity of the motor shaft ω_m, and motor torque τ_m. Table 4.2 shows the chosen conventions and relates modes of operation to operational quadrants. Since buoyant force does not change direction and it drives the motor in generation mode, torque is always positive, meaning the motor only operates in quadrants 1 and 2.

	Storage (Quadrant 1)	Generation (Quadrant 2)	Standby (At origin)
P (kW)	> 0	< 0	= 0
ω_m (rad/s)	> 0	< 0	= 0
τ_m (Nm)	> 0	> 0	= 0

Table 4.2. Conventions for signs and units of control terms. Note that Storage mode operates in quadrant 1 and Generation mode operates in quadrant 2 of a torque-speed diagram.

To trigger any branch of the control scheme, several conditions must be met which are shown in Table 4.3. From the operators perspective however, the only concern is the setting of P_{ref}; both ω_m and τ_m are dependent on the controller.

Power Storage Controls

As shown in Table 4.3, when $P_{ref} > 0$ and $\omega_m \geq 0$, the storage branch becomes the active controller of the system.

For a desired reference power, eq. 4.1.12 governs the control of the resultant output power. A proportional-integral (PI) control scheme is employed to correct the error from P_{ref} to P_{meas} with a proportional gain of 10 and an integral gain of 0.5, both derived by trial and error. The PI controller's output is summed with P_{ref} to become the corrected reference power. By dividing this value by the measured rotor speed, an output torque is determined, which is sent to the motor.

Power Generation Controls

As shown in Table 4.3, when $P_{ref} < 0$ and $\omega_m \leq 0$, the generation branch becomes the active controller of the system.

The generation branch is also governed by eq. 4.1.12, however this time, the relationship between τ_m and ω_m plagues the system with instability. To demonstrate, consider when a negative

IF	THEN	Description
$P_{ref} > 0$ AND $\omega_m \geq 0$	Control mode is Storage	Torque is calculated from storage branch
$P_{ref} < 0$ AND $\omega_m \leq 0$	Control mode is Generation	Torque is calculated from generation branch
$P_{ref} = 0$ AND $-0.05 \leq \omega_m \leq 0.05$	Control mode is Standby	Brake engages
$P_{ref} < 0$ AND $\omega_m \geq 0$	Torque output is set to zero	When in storage mode first, then suddenly switched to generation
$P_{ref} > 0$ AND $\omega_m \leq 0$	Torque output is set to maximum	When in generation mode first, then suddenly switched to storage
$P_{ref} = 0$ AND $\omega_m < 0.05$	Torque output is set to maximum	When in generation mode first, then suddenly switched to standby

Table 4.3. Conditions required for activation of controller branches

reference power is first commanded by an operator. The controller switches to the generation branch and, controlling the only output available, maximizes the torque. This achieves the opposite of the desired effect, causing the buoyant element to descend (consume power) rather than ascend (generate power). Conversely, if a system is already generating at a level equal to the reference power, then the operator asks for a lower reference power, the control reduces the torque to the motor, which then allows the buoyant force to increase the buoyant element's negative (ascent) speed, rather than slow it to a stable speed. To correct this issue, the following method is employed which is graphically represented in Simulink as a block diagram in Fig. 4.8.

A PI control scheme is employed to correct the error from P_{ref} to P_{meas} with a proportional gain of 0.06 and an integral gain of 0.05. The PI controller's output is summed with P_{ref} to become the corrected reference power. This is limited by a saturation block to -55kW, then input to a lookup table which uses empirically derived steady state data points from the dynamic system

to calculate an interpolated non-linear function that outputs an estimated torque requirement. The corrected reference power is divided by this value to yield a calculated angular velocity reference. This value is compared with the measured angular velocity to give an error value, which is then multiplied by the recently estimated torque requirement to produce a power error with respect to angular velocity. This error is divided by the calculated angular velocity reference to give a torque error with respect to power and angular velocity which is subtracted from the estimated torque requirement to yield an output torque. Finally, output torque is filtered through another saturation block that prevents abnormal torque commands.

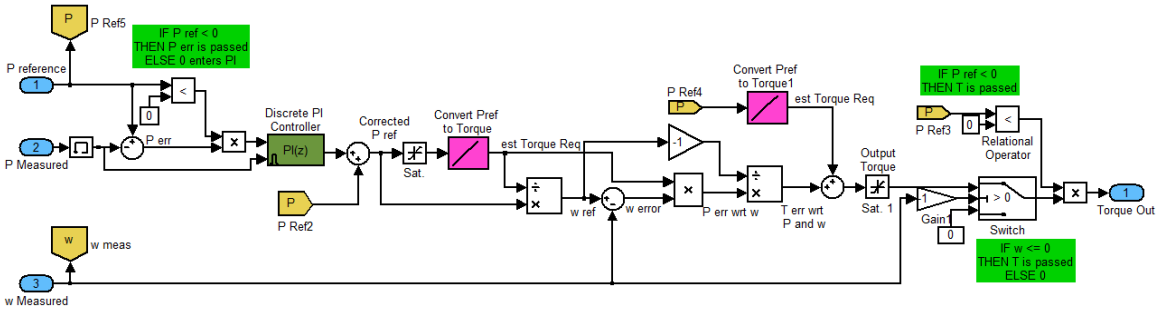

Figure 4.8. A visual representation of the generation branch in Simulink.

Standby Controls

As shown in Table 4.3, when $P_{ref} = 0$ and -0.05 (rad/s) $\leq \omega_m \leq 0.05$ (rad/s), the standby branch becomes the active controller of the system.

To apply braking torque, the standby branch sends a brake gain G_b to the braking mechanism with a value between 0 and 1, with 0 being no brake torque applied and 1 being full brake torque application. Thus, eq. 4.1.9 becomes

$$\tau_{KF} = (r_b \, f_s \, F_{peak} \, \mu) \, G_b. \tag{4.2.1}$$

and eq. 4.1.10 becomes

$$\tau_{SF} = 1.1 \, (r_b \, f_s \, F_{peak} \, \mu) \, G_b. \tag{4.2.2}$$

4.2.3 Results

Dynamic Response

To demonstrate both the dynamic response and control system performance, a sequence of power reference values is sequentially commanded over the course of 100 seconds. In between commanded reference values, ample stoppage time is given to allow the system to return to zero before commanding the next reference value. Figure 4.9 shows the step responses from -50kW to 50kW in 10kW increments.

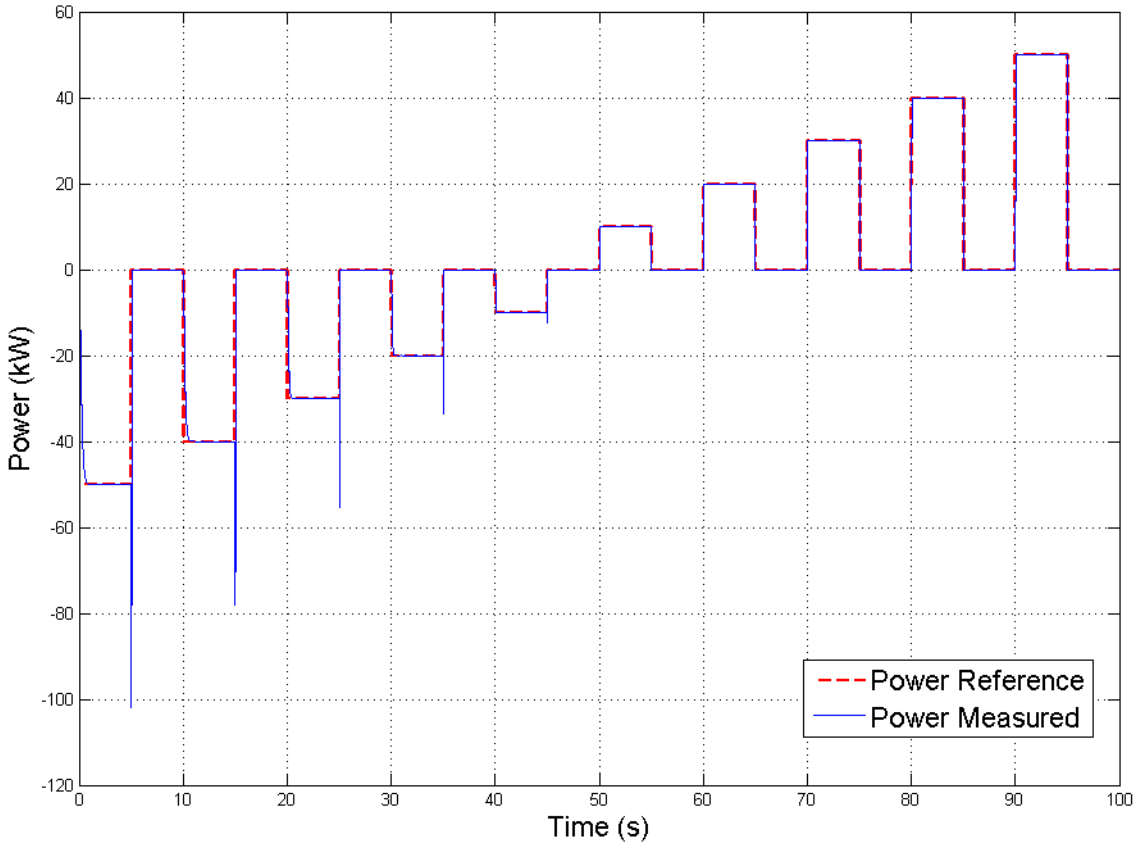

Figure 4.9. A series of BEST power responses vs time. Dashes represent P_{ref}, and solid lines represent P_{meas}.

The most striking observation is the the large negative spikes at the end of each increment in generation mode. In order to slow the buoy from its ascent, some form of opposing force is required. In the previous simulation, the brake was activated to slow the system, however, this dissipates the change in kinetic energy as waste heat. In this simulation, additional motor torque

is applied, thus generating additional electric power. Though this increases the total generated electricity and therefore efficiency of the system, it is problematic since the system response is the opposite of what is commanded. With a potential purpose of this system being to regulate the frequency of the grid, it is important that it closely follows the reference inputs. An alternative approach to mitigate this issue is to transfer the motor's extra regenerative braking power towards the descent of a second buoyant energy storage device, thus eliminating the negative peaks and keeping more energy in the system. This concept is expanded on further in the following section.

Another important observation is that the responses of the system are much faster than the refined dynamic model. Generation mode reaches a 98% response for a -50kW reference in 0.64s with a small steady state error, and storage mode reaches a 98% response for a 50kW reference in 0.07s with no steady state error or overshoot. These response times are under 1/10th and 1/100th the size of the previous simulation for generation and storage modes, respectively.

This time, the response of generation mode is slower than for storage mode, which is related to the controller's instability issue discussed previously. The generation branch controller lets the force of buoyancy accelerate the system while slowly increasing motor torque to oppose it. The referenced power is reached only when both the steady state torque and speed are reached. Conversely, storage mode immediately sets the motor torque to maximum and the system accelerates towards its steady state speed while decreasing the motor torque. Of key importance is that the referenced power is matched before the steady state speed is reached. At this time, the torque begins decreasing while the system's speed slows its rate of increase. Eventually, the steady state speed and torque are reached at a time slightly faster than that of generation mode.

A separate simulation is conducted to more clearly demonstrate this effect through several consecutive changes from 50kW to -50kW, and back to 50kW. Power, torque, and rotor speed are compared along the same time axis and can be seen in Fig. 4.10.

This simulation also verifies the controller's ability to change from full generation to full storage mode and back with minimal steady state errors and response times. From full storage to full generation power took 0.77s for a 98% response with a small steady state error. Full generation to full storage power took 0.21s for a 98% response and again has no steady state error. Also note that the power spike from changing to storage mode from generation mode is just over double the amplitude of the full power value.

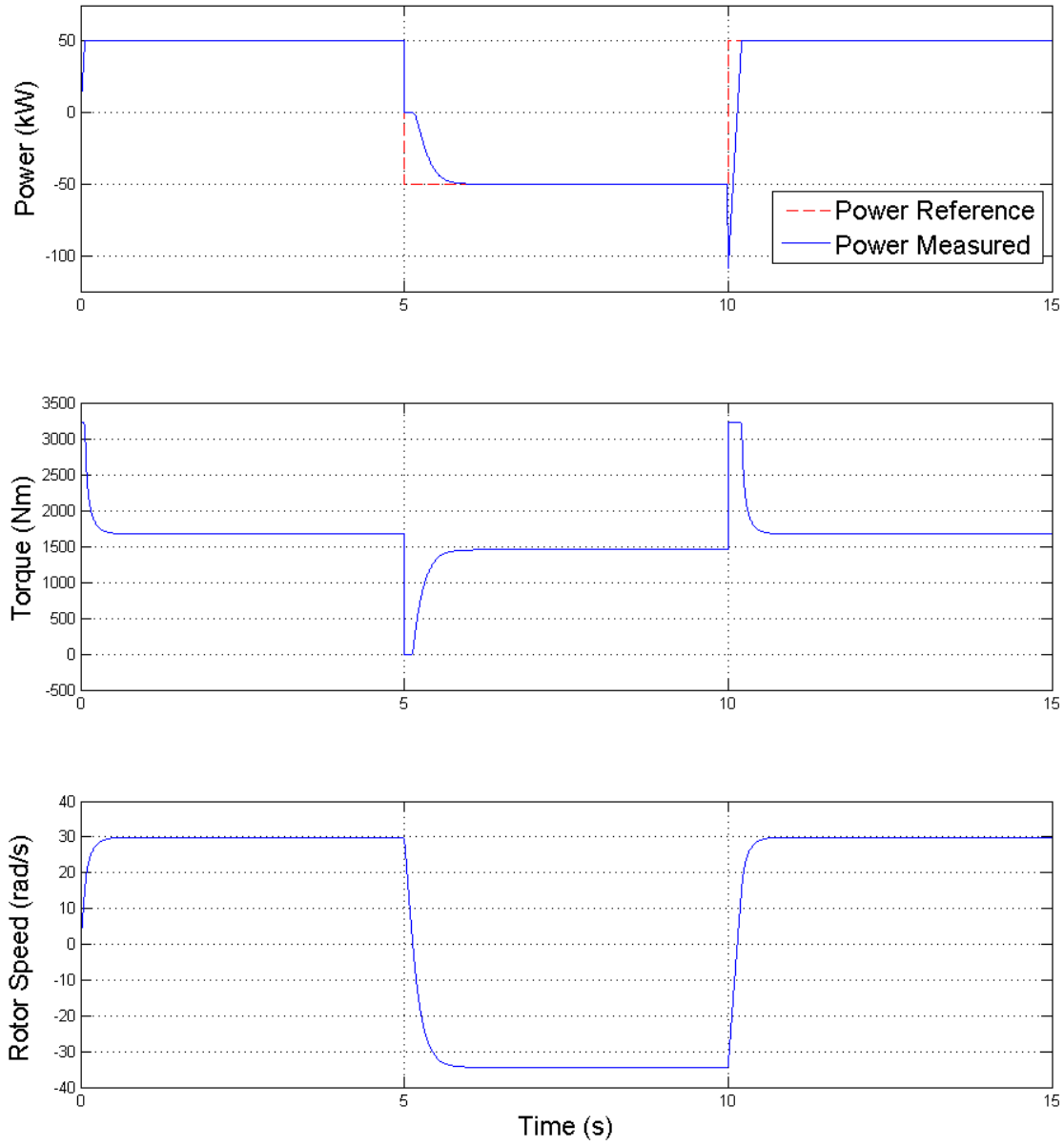

Figure 4.10. Responses of power, torque, and motor speed vs. time for full power storage (0 to 5 seconds), generation (5 to 10 seconds), and storage (10 to 15 seconds) modes of operation.

Combined Representation

Displaying the above findings in a single figure, and using the former scenario with 10kW increments through the entire rated power band yields the 3D plot of power trajectories seen in Fig. 4.11. X, Y, and Z axes represent motor speed, torque, and power, respectively, while time is visualized by the distance between points; large spacing indicates rapid changes while small spacing indicates slow changes.

The long tail on the right side of the graph is representative of the power spike from generation mode deceleration while the clusters of points in the middle represent steady state points for each power level. The lookup tables for the generation mode controller are based on these steady state values.

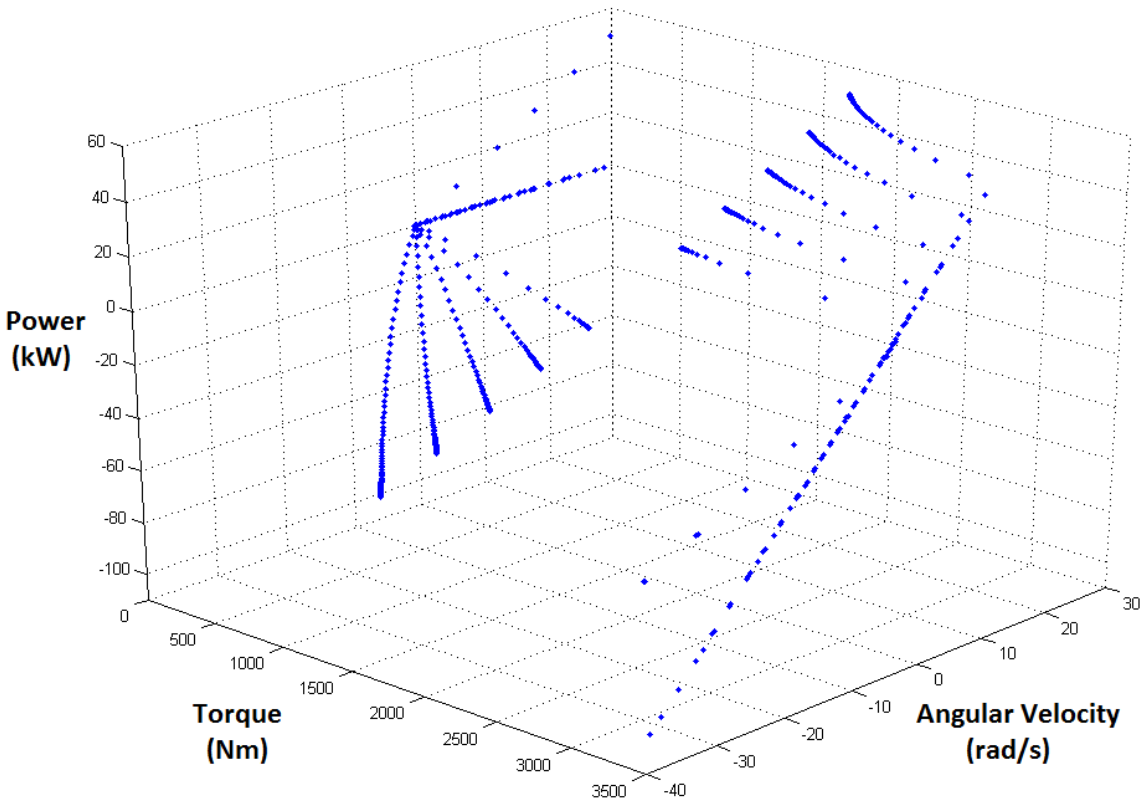

Figure 4.11. A 3D plot showing the relationships between Power, Torque, and Angular Velocity. At left are power trajectories for generation mode at negative 10, 20, 30, 40, and 50kW. At right are power trajectories for storage mode at 10, 20, 30, 40, and 50kW. Data points are taken every 0.01 seconds, therefore the distances between points are representative of elapsed time.

4.3 Dual Buoy Control Model

As mentioned in the preceding section, a significant power spike is created when bringing the system to a stop from generation mode. To absorb this power, the option of introducing an identical second buoy as a slave buoy was explored.

The premise is that a slave buoy can incrementally absorb these bursts of power by transferring it to the motor, thus incrementally driving the slave buoy down. The concept is illustrated in Fig. 4.12.

Over time, the slave buoy will reach a critical depth where it should no longer be used to absorb power, or risk bottoming out. At this time, the roles of primary and slave buoy are switched, and the former slave buoy is cued for the next generation power reference.

Though efficiency gains from this approach vary with the total energy consumed and produced, the amount saved from each stopping event can be quantified through simulation.

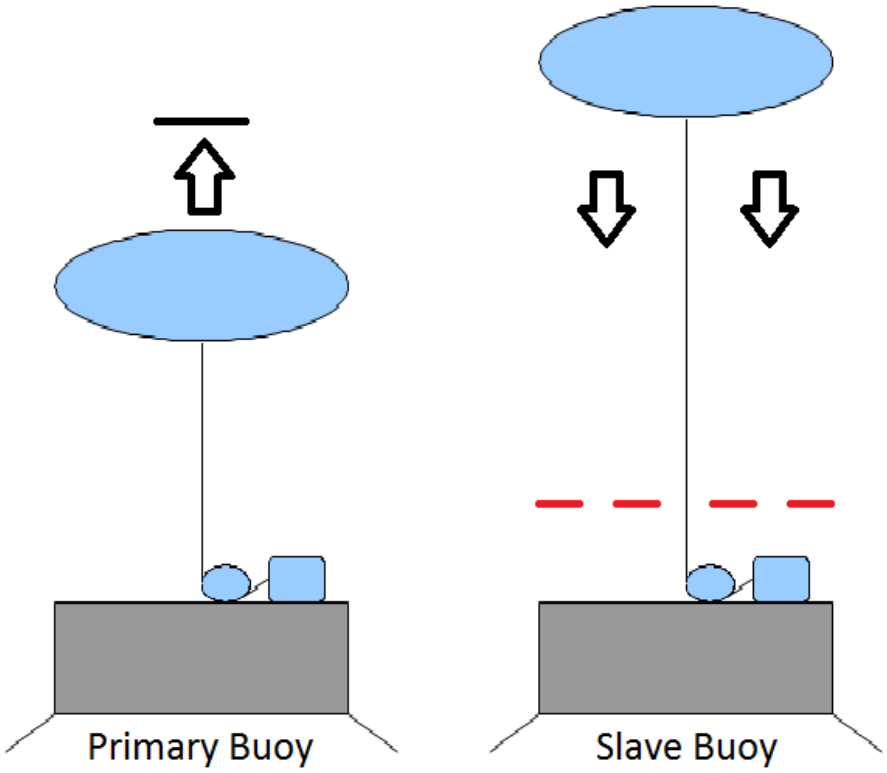

Figure 4.12. An illustration of the dual buoy power transfer technique. As the primary buoy's generation event is halted, the slave buoy receives its excess regenerative braking power, thus gaining additional buoyant potential energy. The red hash lines indicate a switch depth where the slave buoy becomes the new primary buoy and vice versa.

4.3.1 Logic

To establish such a scheme, a series of logic gates are required to determine buoy roles, divide power reference values to appropriate buoys, establish the regenerative braking energy transfer condition, and provide modified power references to the primary and slave buoys. Table 4.4 shows the conditions required by each logic gate and the resulting actions.

To begin, buoy 1 is designated as the primary buoy and buoy 2 as the slave buoy. This is labeled via a status indicator named SlaveTag which can have a value of either 1 or 2, respectively designating which buoy is the slave buoy. To establish which buoy is the active slave buoy, the current depth of the slave buoy is compared with a predetermined depth, Switch$_D$. If the slave buoy exceeds this depth, the primary and slave buoy switch roles at the end of the current regenerative energy transfer.

When SlaveTag equals 1, the slave buoy's reference power (SlvP$_{ref}$) is sent to buoy 1, and the primary buoy's reference power (PrimP$_{ref}$) is sent to buoy 2. Similarly, when SlaveTag equals 2, the slave buoy's reference power is sent to buoy 2, and the primary buoy's reference power is sent to buoy 1.

To determine if the primary buoy is decelerating from a generation event, two conditions must be met: the primary buoy's power reference (PrimP$_{ref}$) must be greater than its measured value (PrimP$_{meas}$) and the primary buoy's angular velocity (ω_P) must be less than zero. When these conditions are satisfied, Regen Energy Xfer equals true.

When Regen Energy Xfer is true, the slave buoy's power reference is set equal to the error between the system's power reference and the primary buoy's measured power. Additionally, the primary buoy's power reference is rate limited to allow ample response time for the slave buoy. When Regen Energy Xfer is false, the slave buoy's power reference is set equal to zero, and the primary buoy's power reference is left unchanged.

4.3.2 Results

A 50 second simulation is conducted with power references switching back and forth between -50kW and 0kW several times. It is assumed that both buoys start at depths suitable for the purposes of testing, though starting positions are referenced at 0m. The switch depth is set at 0.7m and all other model parameters are identical.

Using this methodology successfully removes the visible spike from the system power output. The top graph in Fig. 4.13 shows the measured power at the motor terminal during a

IF	THEN	Description
Slave Buoy = Buoy 1 AND Buoy $1_D <$ Switch$_D$	Buoy 2 = Slave Buoy	Switch slave and primary roles when the slave buoy exceeds the designated switch depth
Slave Buoy = Buoy 2 AND Buoy $2_D <$ Switch$_D$	Buoy 1 = Slave Buoy	Switch slave and primary roles when the slave buoy exceeds the designated switch depth
SlaveTag = 1	SlvP$_{ref}$ = Buoy1P$_{ref}$ AND PrimP$_{ref}$ = Buoy2P$_{ref}$	Send Slave P$_{ref}$ to Buoy 1 Send Primary P$_{ref}$ to Buoy 2
SlaveTag = 2	SlvP$_{ref}$ = Buoy2P$_{ref}$ AND PrimP$_{ref}$ = Buoy1P$_{ref}$	Send Slave P$_{ref}$ to Buoy 2 Send Primary P$_{ref}$ to Buoy 1
PrimP$_{ref} >$ PrimP$_{meas}$ AND $\omega_P < 0$	Regen Energy Xfer = true	The primary buoy is decelerating from generation mode
Regen Energy Xfer = true	SlvP$_{ref}$ = P$_{ref}$ - PrimP$_{meas}$	Slave buoy P$_{ref}$ is equal to the error between P$_{ref}$ and Primary buoy P$_{meas}$
Regen Energy Xfer = true	PrimP$_{ref}$ = P$_{ref}$ (rate ltd.)	Primary buoy P$_{ref}$ is rate limited to allow ample Slave buoy response time
Regen Energy Xfer = false	SlvP$_{ref}$ = 0 PrimP$_{ref}$ = P$_{ref}$	Slave buoy P$_{ref}$ is zero Primary P$_{ref}$ is unchanged

Table 4.4. Logic for dual buoy control methods

deceleration event from generation mode. It is noticed however, that a small overshoot occurs upon the system first reaching zero power and lasts until the measured power from both buoys reaches zero. This could be due to the differences in responses between generation and storage modes, or from a difference in timestep delay methods. The effect is mitigated by limiting the rate of change of the reference power, and produces only 1% steady state error while the buoys are transferring power.

To investigate the power transfer between buoys, power measurements at both buoys are observed. The second and third graphs in Fig 4.13 show these measured power values concurrently, and reveal smooth transferring of regenerative braking power from the primary buoy to the accelerating slave buoy.

By integrating the area under the slave buoy's power curve during a stopping event, the energy added to the system per stopping event is 34.32kJ or 0.00953kWh. Compared with the maximum energy storage capacity of the system calculated in Section 4.1.7, which equals 20.1kWh, this is small at only 0.0473%. Considering that a typical scaled up BEST system is likely to have many modules anyhow, the addition of this control scheme won't foreseeably add significant costs to the system. In fact, it may even reduce the costs of operation both through energy savings and through reduced wear on braking components.

Further effects from this approach can be observed by looking at the depths of both buoys concurrently. The fourth and fifth graphs in Fig. 4.13 show the incremental descent of buoy 2 occurring as buoy 1 comes to rest. It can also be observed from graphs two through five, that after buoy 2 passes the switch depth at 16s, the roles of buoy 1 and 2 are switched, making buoy 1 the new slave buoy. This switching occurs after the deceleration event that caused it has ended.

With the addition of the rate limiter, the peak power reached by the primary buoy decelerating from full speed is reduced to 52.65kW. This is because the regenerative braking power is drawn out over a longer period of time. From this result, it can be concluded that one slave buoy could assist in the deceleration of multiple primary buoys. The time to reach a zero output for the system power will increase as the necessary rate limit for the reference power decreases. Another approach could employ the current ramp rate, but arrange for a cascaded stopping of one primary buoy after another. Again, the time to reach a zero output for the system power will increase, but the possible ratio of primary to slave buoys will also increase. This could extend the system's lifetime through the benefit of shared duties, as well as through the minimization of jerk on the components.

It is important to note that the slave buoy cannot be used to generate power at the same time as primary buoys, as this negates its ability to consume power from them. Its angular velocity

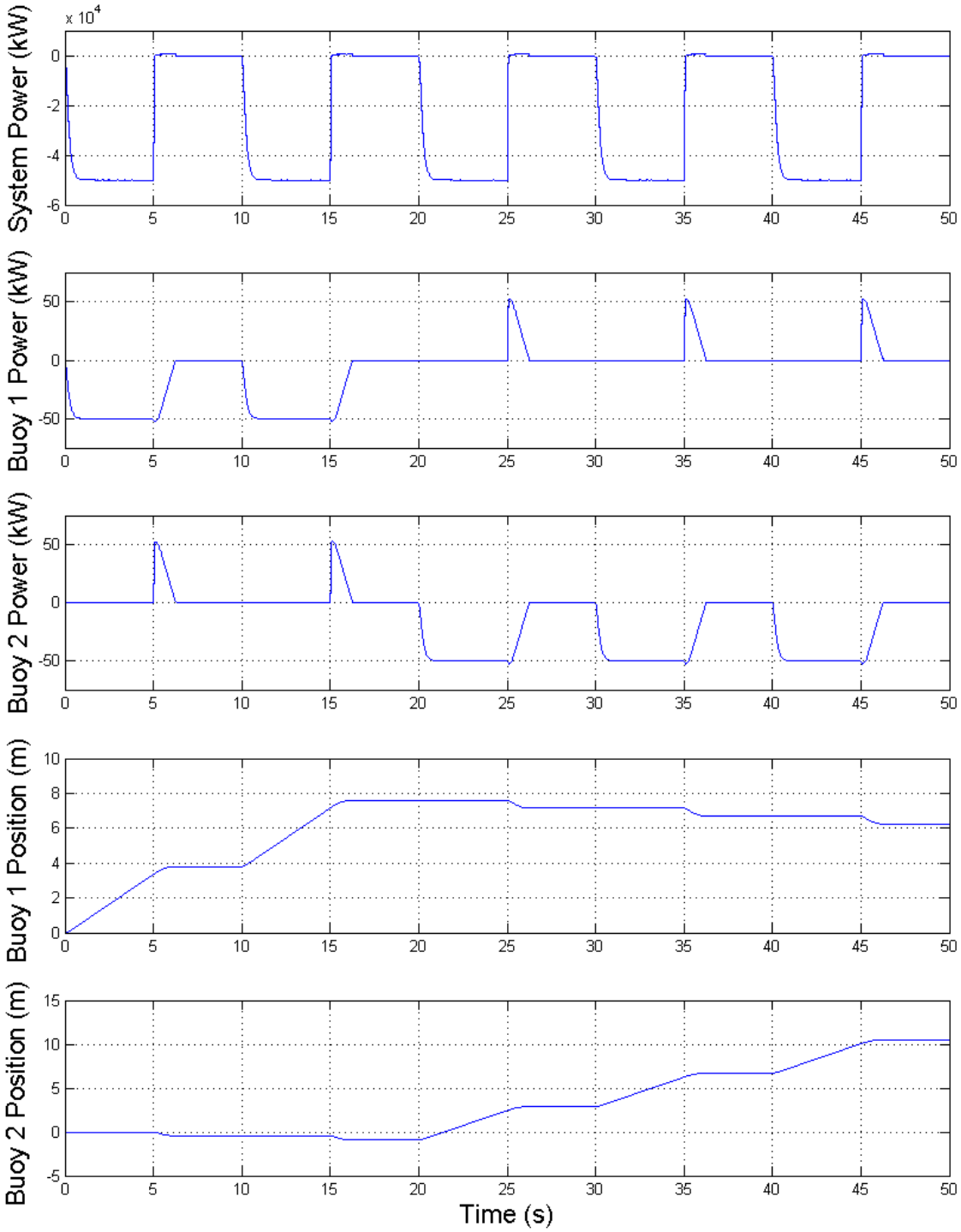

Figure 4.13. Measured data from the dual buoy control simulation. From top to bottom are: measured system power, buoy 1 power, buoy 2 power, buoy 1 position, and buoy 2 position. Note that a position of 0m indicates a starting reference depth only and not actual depths, and buoy 2 reaches its switch depth at 16s.

must be the opposite of the buoys it is being used to stop. However, this condition could always be obviated by reverting back to a braking mechanism.

Chapter 5

Prototype Development

Several scales were considered and explored for the tasks of proving the concept and validating the dynamic model. The former is accomplished at a miniature scale, the results of which are presented first. Several scaled-up options for the latter are then discussed.

5.1 Miniature Scale

A miniature scale approach was undertaken to achieve a basic proof of concept as well as gather empirical efficiency data. Available in the lab was an unknown DC, brushed, Maxon A-max series motor with an attached 19:1 gearbox. From comparison with the specifications of similar motors, this motor was assumed to be capable of 10W or less.

5.1.1 Test Bench Design and Construction

To perform proof of concept tests at this scale, a waterless, weight dropping method was deemed similar enough to the buoyancy based method, and much simpler up front. A test bench was designed to use the Maxon motor and gearbox as the powertrain for storing the gravitational potential energy of the weight, then producing electrical power upon its descent.

A platform houses the motor, driver, and control boards, with Unistrut structural members supporting the load from a string wound on a shaft that drops through a hole. The versatile platform can be used off of a table or the edge of a building for weight based tests, or it can be used off of the edge of a swimming pool for buoyancy based tests. Fig. 5.1 shows the concept as drafted in SolidWorks.

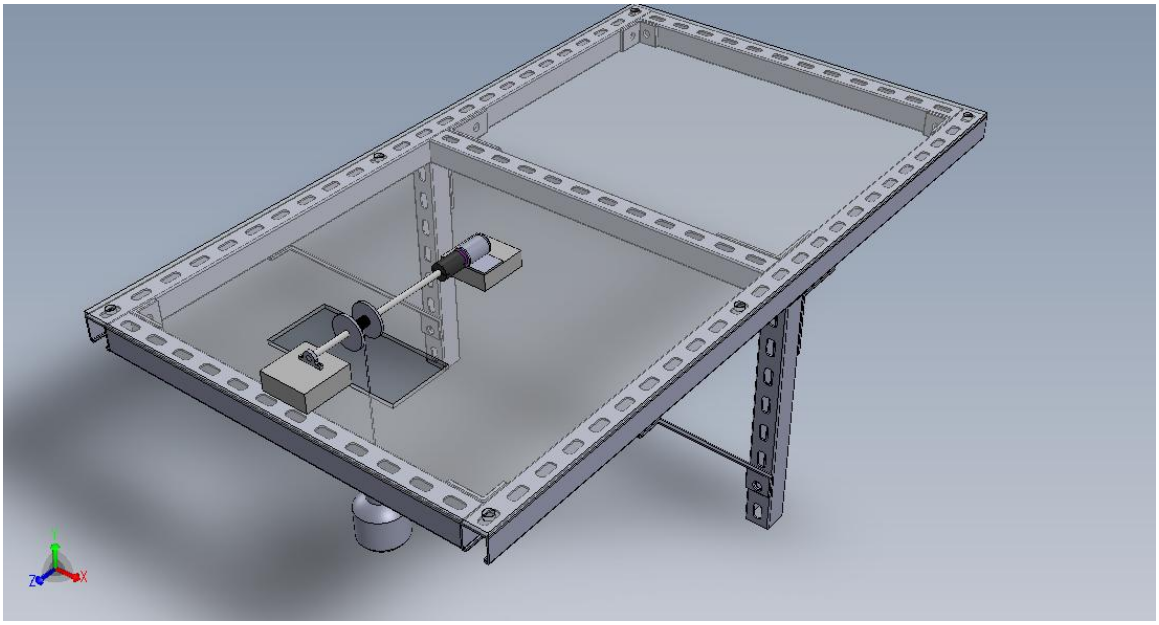

Figure 5.1. The test bench design for weight based prototype testing

5.1.2 Analog Control Setup

To enable control of the bidirectional power flow in the system, a regenerative motor driver is necessary. Though designing and building a switching circuit is possible, a commercial board ensures reliability and safety. Dimension Engineering, a hobby electronics company, sells a line of SyRen regenerative DC brushed motor drivers. The SyRen 10 was selected based on this system's power requirements, which is under 10W. Under the proper mode of operation, 5V analog control signals are used to direct the speed of the motor, while the higher voltages used to drive the motor are isolated to the supply side of the circuit.

5.1.3 Capability of Equipment

Before building the test bench, a mock-up test was performed in the lab to verify the motor's ability to both drive and be driven by the same load. A 2.5lb weight was attached to a string which was wound around a 2cm diameter drum coupled to the motor. The motor was driven by the SyRen motor driver which was powered by a DC power supply set at 9.5V. Using a potentiometer to control the output voltage, the motor was able to successfully pull the load up several feet to a table, then lower it while providing opposing torque. The use of a manual control enabled the use of a National Instruments USB data acquisition device for measuring the supply voltage and the voltage

across a 10ohm resistor, thus providing a current measurement. These values were then multiplied to yield the power, both consumed and generated, which is the basis for the results seen in seen in Fig. 5.2.

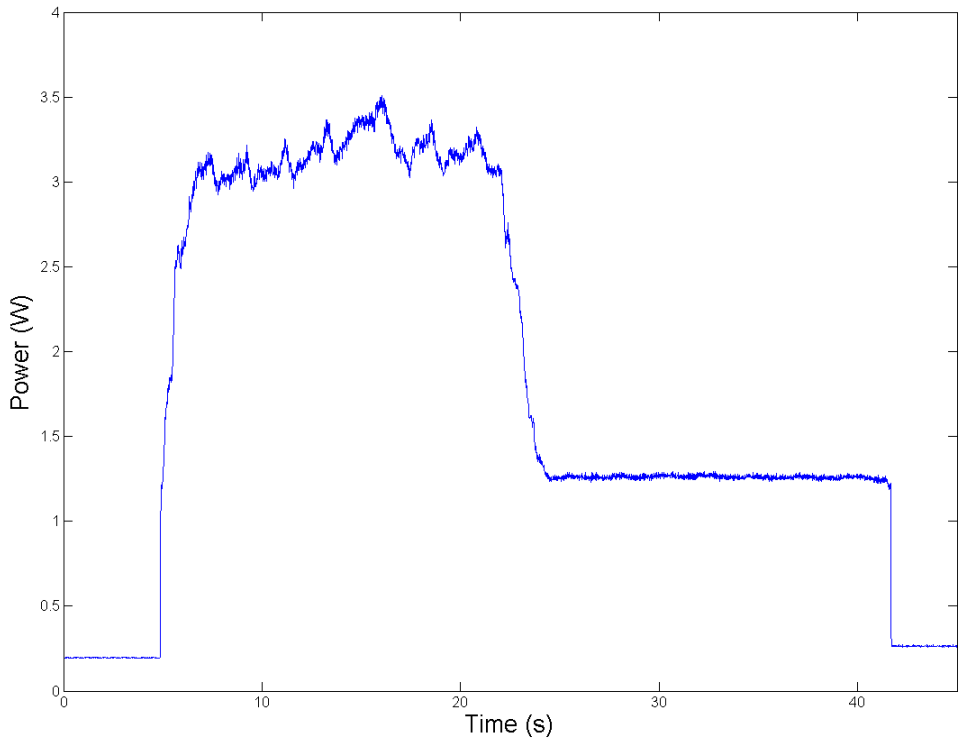

Figure 5.2. Results from the laboratory test using a DC motor and weight. The higher jagged portion of the curve at left represents the motor lifting the weight, while the smooth portion of the curve at right represents the weight driving the motor.

At the left side of Fig. 5.2, the motor uses just over 3W of power to pull the weight up, taking just over 18s to ascend 2ft to the table's edge. Immediately, the voltage applied from the potentiometer is reduced to allow the weight to descend, generating 1.25W for just over 18s. Similar to the simulation, these segments of power stored and power generated can be integrated with respect to time to yield the total energy consumed and produced, respectively. Integrated power losses across the resistor of approximately 0.2W are also subtracted from both of these results to increase the accuracy of the measurement. Energy consumed equals 52J and energy produced equals 20kJ. Then from eq. 4.1.13, the efficiency is 38.5%.

Comparing this result to specifications for similarly sized Maxon motor and gearbox pairs corroborates well. Similar motors had efficiencies near 82% and similar gearboxes had efficiencies near 70%. Multiplying these together, once for each production and consumption, results in a slightly reduced, though rough efficiency estimate of 32.9%.

5.1.4 Drop Test

To make a more accurate assessment of the concept's performance, a drop test was arranged off of the edge of the Atrium in Holmes Hall on the University of Hawaii at Manoa's campus. As seen in Fig. 5.3, the test bench was installed on the third floor, approximately 45ft from ground level using the same 2.5lb weight and motor. This time, a long shaft with a diameter of $5/16^{th}$in was used to accommodate the need for increased string winding; thus the load torque at the shaft was slightly reduced relative to the table test.

Figure 5.3. The drop test setup in the Holmes Hall Atrium.

The same National Instruments USB data acquisition device was used for measurements, as the aim of these tests was only to capture power and efficiency data. The DC power source was set to 9.5V and a laptop running MATLAB was used to log data.

The test began with the weight at ground level where the motor applied torque to start its ascent. As seen in Fig. 5.4, roughly 2W of power was consumed at first, though this amount varies throughout the lift. This was due to the changing diameter of the shaft as string was continuously wound over itself. At just over 2.3 minutes, the string migrated off of itself onto bare shaft, causing the small observed decrease in power. On occasion, it would contact the edge of the test bench hole seen in Fig. 5.3, causing a brief increase in torque before reversing its winding direction. Minus constant resistive losses of 0.2W for the 3 minutes of lifting, the motor is calculated to have consumed 356J.

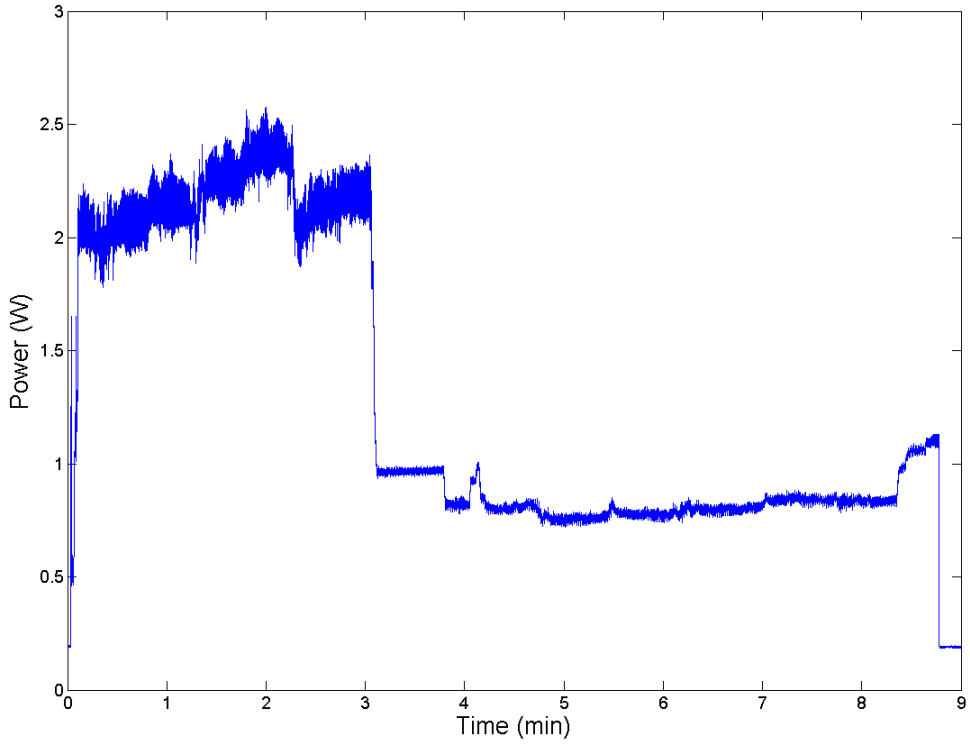

Figure 5.4. Results from the 45ft drop test. The curve from 0 to 3 minutes represents power being consumed as the weight is lifted from ground level. From 3 to almost 9 minutes, the weight descends the same distance while driving the motor and generating power. The small changes in output are largely a result of effects from string winding and the resulting change in effective shaft radius.

Just after 3 minutes elapsed, the weight was stopped and held steady by motor torque, which is seen in Fig. 5.4 as the constant 1W segment. After 0.75 minutes, the weight was allowed to begin descending with a small resistive torque being applied by the motor. Generation mode then proceeded for roughly 5 minutes, experiencing small changes in torque induced by the unwinding string, as well as slight potentiometer adjustments at the beginning and end of the period. At 8.75 minutes, the weight touched down and the power reduced to a level consistent with resistor losses only. Minus these losses, the motor is calculated to have generated 187J.

Using eq. 4.1.13, the efficiency is calculated to be 52.6%, which is higher than the previous test. The most likely reason for this is a reduction in friction within the gearbox caused by heat from the motor reducing the viscosity of its lubricating grease.

With these results, the experiment served its purposes. The concept of storing and discharging gravitational potential energy through a motor under constant load has been proven, and empirical efficiency data exceeding expectations has been collected.

5.2 Small Scale

Initially, it was thought that building the device at a reasonably small scale would provide a balance of cost effectiveness with accurate representation of a full scale system. A 1hp system was targeted largely due to the availability of a descent sized permanent magnet synchronous AC motor and a 49.2:1, 1hp gearbox that could potentially be mated.

The motor was purchased from China at a heavily discounted price due to the fact that the parameters were unknown. This presented the first challenge because system design hinges on the motor's capabilities. As no motor testbed was discovered near the University, stall torque and current could not be measured. Even the test procedure suggested by Assistant Professor Garmire, which was to measure voltage at varying speeds, and currents at varying torques was not possible without a heavy duty test stand and, more importantly, a versatile AC motor driver. To gain a rough estimate of motor performance, the case was examined for indicative markings. A case size of "56" was discovered and checked against NEMA specifications to give an approximate size of 5hp or 3.73kW. The obvious problem is the gearbox's 1hp rating, therefore a larger replacement would be necessary.

For driving and regenerating from the motor, a versatile 4Q motor driver capable of handling this machine as well as other types of AC motors was located from Control Techniques, a subsidiary of Emerson Industrial Automation. The Unidrive SP 2202 was selected with a price of

$1430 and can be coupled with dozens of customizable modules for communicating and controlling through various means.

If Holmes Hall is structurally able to support higher weight drop tests, this scale could prove to be a useful and publicitiy enhancing experiment, especially when tied to the 8kW solar array already installed on the roof. Applications for ramp rate reduction could be tested using a system of this scale while load shifting tests would simply involve the addition of several more units.

5.3 Medium Scale

Since the dynamic models were conducted at the 50kW scale, and the recent ARPA-E funding opportunity announcement [48] is calling for scales of at least 20kW, the option of testing at the 50kW scale was briefly explored.

Most importantly, testing at this scale will involve significant costs. The motor used in simulations from Magnetic S.p.a. (HTQ 350 L TEWC 3B) was quoted to cost roughly $15,250 and a corresponding 4Q AC driver, a Unidrive SP model, for $8,250. Thus the costs from these two components alone is $23,500. A 7:1 gearbox at this scale would easily cost several thousand dollars as well.

This is before even considering the challenges associated with moving to the ocean environment. The 3.64m diameter buoy would need to be custom built and the decision made on which design variation to pursue with all the associated research and detailed design. Additionally, permits from State and Federal agencies as well as the local utility will need to be acquired and potentially an environmental assessment performed.

Such a system would be aiming to drastically further the concept from proof of concept stage directly to the pilot testing stage. In Department of Defense terminology, this would move the concept from a technology readiness level of a 3 to a 7, which is a tremendous and risky jump. A more realistic plan would be to perform relevant small scale testing first before embarking on this scaled up and complicated challenge.

Chapter 6

Cost Comparison Analysis

To determine commercial viability relative to existing commercial systems in a Hawaii context, a cost comparison analysis (CCA) was undertaken. A CCA is a method of comparing the costs of certain projects over a specified period of time. By including time in the comparison, factors such as operational costs, replacement costs, and performance degradation can be analyzed from a net present value (NPV) standpoint.

The energy storage candidates selected were Xtreme Power's DPR battery system, which has been implemented in five Hawaii locations including the Keahawa Wind Farm on Maui as well as the Kahuku Wind Farm on Oahu [62], and conventional pumped hydroelectric energy storage (PHES), due to its tremendous market share in the global energy storage sector. As discussed in Chapter 1, these technologies are not direct competitors with each other, as their capabilities serve different grid needs. Comparing buoyant energy storage technology with them allows for comparison with both sides of the spectrum (fast response, low capacity and slow response, high capacity).

6.1 Assumptions

In order to perform such an analysis, especially when incorporating an early stage technology, several assumptions are required. The system sizes are assumed to be 20MW maximum power output, and 20MWh of capacity. These sizes are relatively near that of the aforementioned wind farm battery storage banks in the Hawaiian Islands. Common assumptions among the three technologies are a 40 year investment period, and a 2% discount rate.

6.2 Cost Estimates

6.2.1 Xtreme Power's DPR

Originally, the CCA was performed using an installed cost of $500 per kWh for Xtreme Power's DPR found online at [62]. This cost per unit energy metric can be misleading with battery technologies and to be accurately compared, requires that the depth of discharge (DOD) be taken into account. Xtreme power has a PowerCell^{TM} Warranty Curve that gives a guaranteed battery lifetime based on its maximum DOD [32]. 80% is assumed since battery life becomes excessively short beyond that. This means that to have an even capacity with BEST and PHES, the battery bank must be upsized to 25MWh. The resulting CCA still favored batteries until a more accurate estimate of installed costs was given publicly by an agent of Xtreme Power at the Clean Technology 2011 Conference and Expo in Boston, MA. $1250/kWh was the given value, which corroborates with Lux Research's price range for advanced lead acid technologies [23]. This value then produced an updated capital cost estimate of $31,250,000.

Annual operations and maintenance (O&M) costs are conservatively estimated at $10 per kW. The DPR is "Designed for a 20 year life with easy PowerCell^{TM} replacement" according to a company published specification sheet [32]. Another 3rd party [62] revealed an estimated cell life of 10 years, which corroborates with Xtreme Power's Warranty Curve: 80% DOD warrants roughly 3600 cycles, with roughly one cycle per day, the system should last 10 years. Combining these two sources and assuming cell replacements will cost 50% of the system cost, the system will be replaced once and the cells twice over the 40 year comparison period.

6.2.2 Conventional Pumped Hydroelectric

Using information from a study of hydroelectric power options in Hawaii completed by the Hawaii Technology Development Venture (HTDV) [63] an estimate of $2500 per kW of PHES is assumed for a hypothetical system. This price reflects the cost of land use and limited options available in Hawaii resulting in a capital cost estimate of $50,000,000.

Annual O&M costs are assumed to be 0.5% of capital costs, with a lifetime of 40 years.

6.2.3 Buoyant Energy Storage Technology

A 1MW modular design was calculated using the equations presented in Section 3.7. Input parameters included a 450rpm, 1MW rated motor from General Electric's Pegasus line, a

target buoy velocity of 0.27m/s, a Dyneema load bearing cable of 32mm diameter, a D/d ratio of 15.64, and a one way system efficiency of 92.5%. Output parameters included a 9m diameter buoy, a gear ratio of 44:1, and a depth requirement of 972m. Such depths can be found within 7 nautical miles of Oahu's South West point near the Campbell Industrial Complex, in proximity to several other power generation facilities and high voltage transmission lines.

The cost estimate for a twenty module array was broken into individual components and installation labor, and a cost per unit assigned to each. Table 6.1 shows the breakdown which produced a capital cost estimate of $23,042,220. To assume a profitable manufacturing and installation process, a profit margin of 15% is added to this cost, resulting in $26,498,553.

Annual O&M costs are assumed to be significantly higher than PHES and batteries due to the nature of the marine environment and the long system lifespan of 40 years, therefore 3% of capital costs is assumed.

6.3 Results

With the above assumptions in place, the net present value (NPV) in each year (n) is calculated using:

$$NPV = -\frac{\textit{Capital Costs + O\&M Costs}}{(1+i)^n} \tag{6.3.1}$$

where i is the discount rate.

After 40 years, BEST has a NPV of $-$\$48,679,900, Xtreme Power's DPR has a NPV of $-$\$79,304,922, and PHES has a NPV of $-$\$56,975,647. The negative sign in front of these values would normally indicate a bad investment, but since benefits are omitted it is expected. The smaller the absolute value, the better in this case. In the Hawaii context and with the above assumptions, BEST appears to be an excellent long term alternative to other leading commercial technologies from an economic standpoint.

As stated earlier, the lifetime of a system plays a large role in its NPV. Evaluating the sensitivity of this factor, along with the other assumptions, would provide a more rigorous and accurate CCA.

To take this comparison another step further, actual benefits from each technology would also need to be evaluated and added into the equation. Monetizing these benefits, however, is a challenging and complex problem. Typically, the expected benefits of a project are very site and use specific. Thus, for a true Cost Benefit Analysis, specific projects will need to be evaluated on a case by case basis.

Capital Equipment	**Cost per unit ($)**	**Units**	**Total Cost ($)**
Buoy	50,000	20	1,000,000
Cable (1km)	100,000	20	2,000,000
Drum	5,000	20	100,000
Motor	165,882	20	3,317,640
Motor Driver & Controls	212,000	20	4,240,000
Gearbox	100,000	20	2,000,000
Counterweight	11,729	20	234,580
Undersea Cable (7 miles)	7,000,000	1	7,000,000
Maintenance Access	5,000	20	100,000
Sensors/Communication	25,000	20	500,000
Total Equipment Cost	**1,674,611**	**20**	**20,492,220**
Capital Labor			
Onshore Construction	25,000	20	500,000
Transportation	50,000	1	50,000
Marine Deployment	50,000	20	1,000,000
Grid Tie-in	500,000	1	500,000
EIS/Permits/Utility Coordination	500,000	1	500,000
Total Labor Cost	**1,125,000**		**2,550,000**
Total Capital Cost			**23,042,220**

Table 6.1. Capital cost estimate for a 20MW, 20MWh BEST system

Chapter 7

Conclusion

7.1 Summary

The challenge of utility scale power intermittency was discussed and energy storage introduced as a method to mitigate its effects. Benefits and commercialized variations were presented before introducing buoyant energy storage technology. Several embodiments were conceptualized with the simplest being selected to move forward to dynamic modeling. A dynamic model was presented that demonstrates the system's performance in terms of efficiency and response times. A control system was then designed and tested to simplify the operation of the system, making it useful for a grid operator. An efficiency and operationally enhancing strategy was then demonstrated that uses a slave buoy to absorb regenerative braking energy from a stopping primary buoy. A miniature prototype was tested to prove the concept and gather performance data. Additional options were then introduced for furthering its development at larger scales. Finally, a cost comparison analysis was conducted to juxtapose the net present value of buoyant energy storage technology with the commercialized pumped hydroelectric and battery energy storage methods.

7.2 Key Results and Implications

The first results of dynamic modeling were the fast response times demonstrated by the system. Using the developed control methodology, generation mode reaches a 98% response in 0.64s and storage mode reaches the same response in 0.07s. Such times allows the system to be used for frequency regulation, a valuable grid ancillary service. Coupled with the ability to scale, BEST should be able to serve this market with larger available energy capacities than battery and flywheel competitors. Scaling will likely reach a point of diminishing returns when compared with

PHES and CAES systems which are largely cost based on power rather than energy, however these systems do not serve the frequency regulation market. This scalability also allows BEST systems to be specifically engineered for individual utility needs. A leading market research firm has indicated that a highly scalable and adjustable system could stand to take a significant share of the growing energy storage market.

Another result of dynamic modeling was an estimate of the system's round trip efficiency. At 80.5%, the performance is competitive with existing battery, flywheel, compressed air, and pumped hydroelectric energy storage systems. With efficiency accounting for only small differences in NPV comparisons by industry experts, this result merely maintains BEST as a potential candidate for utility scale energy storage.

The miniature proof of concept accomplished its primary goal which was to demonstrate the storage of gravitational potential energy and the corresponding discharge using the same load. It also demonstrated round trip performances that exceeded the initial estimates from equipment specifications.

The cost comparison analysis revealed that BEST is cheaper than advanced lead acid battery systems and, in the Hawaii context, pumped hydroelectric energy storage systems. This was based on many assumptions, but nonetheless shows great potential for BEST to approach the cost targets set by the DoE ahead its competitors.

The combination of the above results strongly imply that further development and testing of the buoyant energy storage concept is warranted.

7.3 Future Work

With the results from the miniature scale prototype, more in-depth testing can commence to validate the presented control methodologies, first at the miniature scale, then at the small scale. As the tested system was in air and removed the effects of hydrodynamic drag, water based testing will also be required to test the controllers ability to handle non-linear disturbances. These water based tests will also enable the validation of response times and efficiency estimates.

System optimization can also be conducted to determine a minimal cost sytem. Factors such as working depth and therefore undersea cable length, which has a significant cost, can be evaluated alongside various buoy, motor, and gearbox combinations. Such efforts will be critical to approaching the DoE's cost goal of $100/kWh.

7.4 Funding Opportunities

In early March of 2012, a proposal was co-authored with Whirl Energy in San Francisco for a solicitation from the Hawaii Technology Development Venture (HTDV). The $300k proposal includes graduate research work performed at UHM and capital for building two 2.5kW ocean based systems. If awarded, this work will prove the concept, validate dynamic model results, reveal life cycle effects from the ocean, and uncover manufacturing, assembly, and installation methodologies.

Another solicitation was recently released by the DoE's ARPA-E for grid scale energy storage development [48]. With combined phase awards of up to $3.2 Million, this type of grant would be tremendous for the development of this concept, potentially paving the way for full scale array testing. The proposal is currently being drafted, again in conjunction with Whirl Energy, with the intent of demonstrating response times, round trip efficiency, long cycle life, scalability, and a path to achieving a cost of $100/kWh.

Appendix A

Magnetic HTQ 350 Motor Specifications

motori coppia serie HTQ

HTQ series torque motors

magnetic

generalità | general features

I motori HTQ torque MAGNETIC sono motori sincroni a magneti permanenti destinati all'integrazione diretta nelle macchine industriali. Nati dalle esigenze sempre più spinte dell'automazione sono stati progettati per offrire un prodotto con elevate capacità di coppia a basse velocità e per poter eliminare i tradizionali componenti della catena cinematica, permettendo di aumentare la precisione e il rendimento delle macchine industriali. L'elevato rendimento intrinseco che caratterizza questi motori li rende particolarmente adatti anche ad applicazioni di generazione elettrica, nel settore eolico ed idroelettrico. MAGNETIC, interpretando le esigenze di mercato e affinando l'esperienza in diverse applicazioni ha perfezionato una serie di motori sincroni ad elevato numero di poli che adottano magneti dell'ultima generazione in neodimio-ferro-boro.

MAGNETIC torque motors HTQ series are permanent magnets synchronous motors designed for industrial machines integration. They have been specially engineered to achieve the higher and higher performances required in the automation field by a high torque capability at low speed and by the elimination of the traditional components of the kinematic chain which allows to increase the precision and the efficiency of industrial machines.The high efficiency typical of these motors makes them particularly suitable even for applications of electricity generation in hydroelectric field and from wind turbines. In order to meet the market requirements MAGNETIC, on the ground of its experience of many applications in different fields, has designed a new synchronous motors series with high poles number and equipped with last generation magnets made of neodymium, iron and boron.

principali caratteristiche della serie
main characteristics of the series

> coppia continuativa da 54 Nm a 1750 Nm (versioni personalizzate fino ad oltre 15.000 Nm)
> elevata capacità di coppia a basse velocità
> velocità nominali da 20 RPM a 600 RPM
> dimensioni contenute
> bassa rumorosità
> esecuzione non ventilata IC400 con grado di protezione IP 54
> esecuzione raffreddata a liquido IC3W7 con grado di protezione IP 54
> personalizzazioni meccaniche (sporgenza d'albero, accoppiamento meccanico B3, B5, B35 e B14 ecc…) ed elettriche a seconda delle esigenze
> avvolgimento trifase a stella senza neutro accessibile

> *continuous torque from 54 Nm to 1.750 Nm (up to over 15.000 Nm in customized versions)*
> *high torque at low speed*
> *nominal speed from 20 RPM to 600 RPM*
> *reduced dimensions*
> *low noise*
> *non-ventilated execution to IC400 with degree of protection IP 54*
> *liquid cooled execution to IC3W7, degree of protection IP 54*
> *customized solutions both mechanical (shaft end, mechanical coupling, B3, B5, B35 and B14 etc.) and electrical, according to the requirements*
> *three-phase star winding with no access to neutral*

perchè utilizzare un motore HTQ
why use a HTQ motor

> precisione di movimento
> elevato rendimento con conseguente aumento dell'efficienza per la riduzione degli attriti di sistema
> diminuzione dei tempi e costi di manutenzione dovuti all'eliminazione di pulegge, riduttori e qualsiasi altro organo meccanico che necessiti di una manutenzione periodica
> riduzione della rumorosità per l'eliminazione di componenti meccanici (pulegge, riduttori) e della ventilazione assistita.
> riduzione di ingombri macchina per le dimensioni contenute dei motori stessi e l'eliminazione di componenti meccanici (pulegge, riduttori)
> miglior integrazione del motore con la macchina
> aumento della produttività

> *motion precision*
> *high performance with consequent increase of the efficiency due to the reduction of the system frictions*
> *reduction of time and maintenance costs resulting from the removal of pulleys, gears and any other mechanical part that needs periodic maintenance.*
> *noise reduction by the elimination of mechanical components (pulleys, reducers) and auxiliary ventilation.*
> *reduced overall dimensions of the machine due to the reduced dimensions of the motors and the elimination of mechanical components (pulleys, reducers etc.).*
> *enhanced integration of the motor on the machine*
> *increase of productivity*

L'uso dei motori HTQ torque MAGNETIC consente perciò di ridurre il **TCO (total cost of ownership)**, cioè il costo complessivo di tutte le spese da sostenere durante l'intero ciclo di vita di un bene durevole: acquisto, manutenzione, energia per la gestione e il funzionamento, dismissione.

*The use of MAGNETIC HTQ motors allows to reduce the **TCO (total cost of ownership)**, that is the gross amount including all the expenses incured during the life cycle of the equipment: purchase, maintenance, energy for operation, removal.*

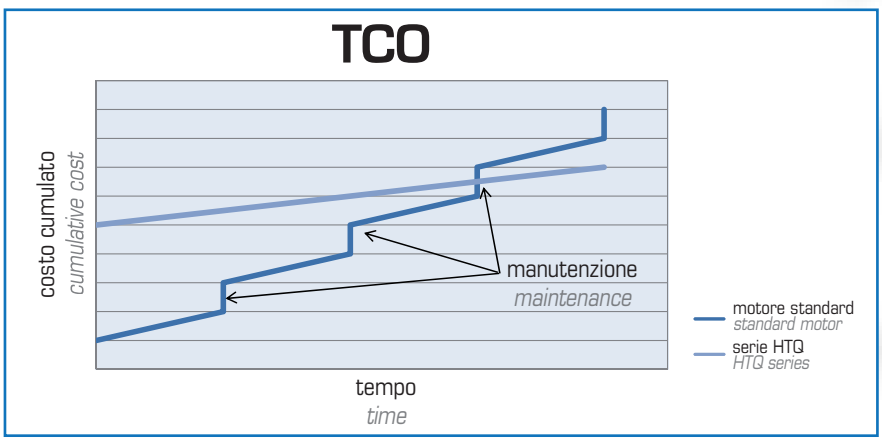

A titolo di esempio, si può considerare un estrusore in cui è necessario programmare la manutenzione del motore e dei componenti meccanici (puleggia, riduttore) con conseguente fermo macchina e mancata produzione; con la tecnologia torque questi tempi vengono ridotti se non annullati.

As an example you can consider an extruder that needs scheduled maintenance of motor and mechanical components (pulley, gearbox) with consequent stop of the machine and production standstill. By means of torque technology this down time is reduced or totally eliminated.

applicazioni | applications

> trafile di filo metallico
> estrusori e macchine per la plastica
> assi di macchine utensili
> argani di sollevamento
> mini e micro generatori eolici e idroelettrici

> *wire extrusion*
> *machines and extruders for plastics*
> *multi axis machine tools*
> *lifting winches*
> *mini and micro wind turbines and hydroelectric systems*

norme di riferimento | standard rules

I motori sincroni della serie HTQ sono costruiti secondo le norme CEI EN 60034-1, conformi alle IEC34-1. Sono pertanto in armonia con le normative dei principali Paesi Europei.

HTQ motors are manufactured in fully accordance with standard CEI EN 60034-1 and they comply with IEC 34-1, therefore in accordance with the rules of the main European countries.

isolamento | insulation

Tutta la serie è dimensionata in classe F, pertanto la massima sovratemperatura ammessa è di 105°C. Ciononostante, per aumentare l'affidabilità della macchina, i materiali isolanti sono per la quasi totalità in classe H (Δt max 125°C, temperatura assoluta max dell'isolante 180°C). L'impregnazione è sempre doppia e realizzata sottovuoto a garanzia della penetrazione della resina. L'avvolgimento è realizzato con fili di rame rivestiti di uno smalto speciale, più resistente ai picchi e alle veloci variazioni di tensione generate dall'inverter. In ogni caso si consiglia di contenere la frequenza del PWM e verificare che non sussistano fenomeni di rifrazione sui cavi che possono generare picchi di tensione ed alti dv/dt.

The whole series is dimensioned in F class, the max. overtemperature allowed is therefore 105°C. Anyway, in order to increase the machine reliability, almost all the insulating materials are in class H (Δt max 125°C, absolute max. foreseen temperature 180°C). The impregnation is always double and made under vacuum to guarantee the resin penetration.The winding is made of copper foreseen with special enamel to resist to the peaks generated by the inverter (high voltage variations, dv/dt). In any case it is advisable to contain the PWM frequency and to check that there is no refraction phenomenon on very long power supply cables (high voltage peaks and dv/dt).

protezione termica | thermal protection

È realizzata con termoprotettore a contatto normalmente chiuso avente le seguenti caratteristiche:

Temperatura di intervento	135 ± 5°C
Tensione massima	48 Vcc, 230 Vca
Max portata dei contatti	6 Acc, 6 Aca (cosφ=0,6)

In alternativa, è possibile prevedere altri tipi di sensori a seguito elencati:
> termistore PTC tipo SNM130ES520
> PT100 tipo 41SRPE06
> KTY84-130

It is realized through a normally closed contact heat protector with the following characteristics:

Operating temperature	*135± 5°C*
Max. oltage	*48 Vdc, 230 Vac*
Capacity of the contacts	*6 Adc, 6 Aac (cosφ=0.6)*

Alternatively it is possible to foresee the following types of sensors:
> *thermistor PTC type SNM130ES520*
> *PT100 type 41SRPE06*
> *KTY84-130*

opzioni | options

> **Raffreddamento**: il motore può essere fornito in versione chiusa non ventilata TENV (IC400 secondo CEI EN60034-6) e con raffreddamento a liquido TEWC (IC3W7 secondo CEI EN60034-6). A richiesta è possibile avere un raffreddamento con ventilazione a mantello che non necessita di un circuito idraulico ma consente di ottenere un buon rapporto dimensioni/coppia.
> **Trasduttore di posizione**: il motore può essere fornito con varie tipologie di encoder a seconda delle esigenze. Il montaggio dell'encoder può essere coassiale, nel caso di motori standard o a semiasse cavo, oppure accoppiato tramite cinghiolo nel caso di motori in versione asse cavo.

> ***Cooling**: the motor can be supplied in closed not ventilated version TENV (IC400 according to CEI EN60034-6) and with liquid-cooling TEWC (IC3W7 according to CEI EN60034-6). On request it is available a cooling system with external ventilation that does not need an hydraulic circuit but allows to achieve a good ratio dimensions/torque.*
> ***Position transducer**: the motor can be supplied with different types of encoder in accordante with customer's requirement.*
The encoder assembling can be coaxial, in case of standard or hollow axle shaft motors or coupled through belt in case of hollow shaft motors.

Encoder Hengstler type S21	***Encoder Hengstler type AD 36***	***Encoder Heidenhain type EQN 1325***
Sinusoidal 2048 ppr 1Vpp signals; Sine/Cosine 1 period absolute waves/rev.; zero pulse; 5VDC	*Absolute multiturn (4096 rev.) position on 31 bits; 8192 ppr 1Vpp signals; BiSS interface; 5VDC*	*Absolute multiturn (4096 rev.) position on 13 bits; sinusoidal 2048 ppr 1Vpp signals; EnDat01; 5VDC*

> **Freno**: a richiesta è disponibile il motore completo di freno di stazionamento o emergenza.
> **Angus**: il motore può essere fornito dell'anello paraolio su richiesta.
> **Collegamenti**: l'esecuzione standard prevede una basetta per la potenza e il connettore per il trasduttore.
A richiesta è possibile avere i cavi liberi con lunghezza 1 m oppure i connettori (sono sempre forniti di parte fissa e volante).
> **Accoppiamento**: il motore può essere fornito con diverse tipologie di sporgenza d'albero a seconda delle esigenze e delle applicazioni:
- albero sporgente (con o senza chiavetta)
- asse cavo con o senza chiusura dello statore
- semi asse cavo (foro cieco)
- albero sporgente con profilo scanalato
- asse cavo con profilo scanalato

Il motore può essere fornito come roto-statore quindi senza cuscinetti e integrabile alla macchina stessa.
Nella versione completa possono essere applicate diverse tipologie di cuscinetti a seconda dell'applicazione:
- sfere - sfere
- sfere - rulli

Nelle applicazioni da estrusore è possibile applicare il cuscinetto rinforzato.
> **Protezioni**: l'esecuzione standard prevede la protezione in IP54 mentre a richiesta è possibile in IP65.
> **Verniciatura**: i motori vengono verniciati con sottofondo epossidico atto a ricevere qualsiasi tipo di smalto di finitura. A richiesta è possibile prevedere cicli di verniciatura speciali.

> ***Brake**: the motor complete with holding/emergency brake is available on request.*
> ***Oil seal**: on request the motor can be supplied with Angus-ring oil.*
> ***Connections**: standard set up involves a terminal board for the power and connector for the transducer.*
On request it is possible to supply free cables 1 m long or connectors (always supplied complete of male and mating).
> ***Coupling**: the motor can be equipped with different types of shaft end according to the request and the application:*
- shaft with or without keyway
- hollow shaft
- blind hole shaft
- shaft with external gear teeth
- hollow shaft with internal gear teeth
The motor can be supplied as rotor-stator, therefore with no bearings and suitable to be integrated to the machine.
In the complete version different types of bearings can be provided according to the application:
- balls - balls
- balls - rollers
In extruder applications it is possible to use reinforced bearings.
> ***Protections**: normally in IP54, on request IP65.*
> ***Painting**: preliminary painting for external surface with epoxy bicomponent primer is foreseen, suitable for any type of finishing enamel. Special paint finishes can be provided on request.*

definizione dei parametri | parameters

I valori riportati nelle tabelle corrispondono alle seguenti definizioni:
> **Coppia di stallo TnO**: coppia continuativa erogabile dal motore a velocità prossima a zero con ΔTmax=105K (Tamb.max=40°C)
> **Coppia massima Tp**: coppia massima di accelerazione erogabile dal motore
> **Velocità massima nmax**: velocità massima con carico pari alla coppia nominale Tn e tensione al motore pari alla massima erogabile dal convertitore (Vca)
> **Area 1**: poiché l'aumentare della velocità determina maggiori perdite nel motore, occorre considerare un declassamento della coppia continuativa (S1 CEI EN 60034-1) in funzione della velocità come riportato sul grafico
> **Area 2**: nella scelta del motore necessita considerare la velocità fino a cui viene richiesta l'erogazione della coppia massima richiesta: la limitazione è dovuta alla tensione massima fornibile dal convertitore

The values indicated on the tables correspond to what follows:
> ***Stall torque TnO**: continuous torque that can be supplied by the motor while running at a speed near zero with ΔTmax=105K (max room T=40°C)*
> ***Max torque Tp**: acceleration torque that can be supplied by the motor*
> ***Max speed nmax**: max speed when the load is equal to the nominal torque Tn and the voltage supplied to the motor is equal to the max voltage that can be delivered by the drive (Vac)*
> ***Area 1**: since an increase in speed results in bigger losses of the motor, it is necessary to derate the continuous torque (S1 IEC34-1) according to the speed as shown in the graph*
> ***Area 2**: when choosing the motor it is necessary to take into account the speed up to which the max torque has to be supplied; this depends on the max voltage which can be delivered by the converter*

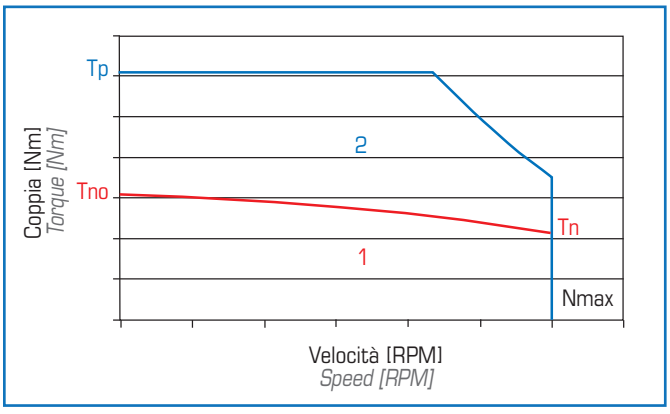

HTQ 120

Vca 3 x 345 Vrms

motore *motor*	codice *code*	Pn W	Tno Nm	Tn Nm	Tp Nm	J kgcm²	Nnom RPM	Nmax@2Tno RPM	Nmax@Tp RPM	Ino Arms	In Arms	Ip Arms	N. poli *No. poles*	W kg
HTQ 120 S TENV	**8A**	270	3,7	3,2	12	17,5	800	1106	698	1,1	1	4	14	2,3
HTQ 120 M TENV	**4A**	310	7,3	6,6	24	27,0	450	498	220	1,1	1	4,1	14	4,1
	6A	410	7,3	6,5	24	27,0	600	671	391	1,3	1,2	5	14	4,1
	8A	520	7,3	6,2	24	27,0	800	884	592	1,7	1,4	6,1	14	4,1
HTQ 120 L TENV	**4A**	440	10,0	9,3	37	36,5	450	470	224	1,3	1,2	5,5	14	6,0
	6A	570	10,0	9,1	37	36,5	600	620	368	1,7	1,5	6,6	14	6,0
	8A	720	10,0	8,6	37	36,5	800	847	577	2,1	1,8	8,3	14	6,0

100455/0 - ROTOR STATOR VERSION (STANDARD)

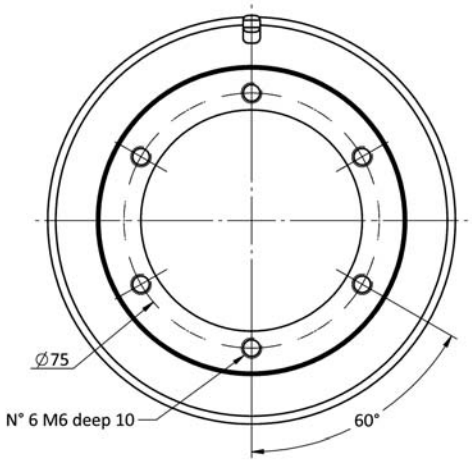

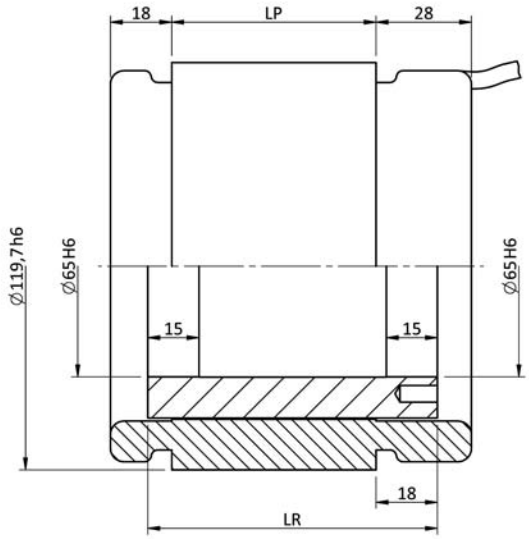

tipo *type*	LP	LR
HTQ 120 S	30	55
HTQ 120 M	60	85
HTQ 120 L	90	115

REQUIRED MATING DIMENSIONS

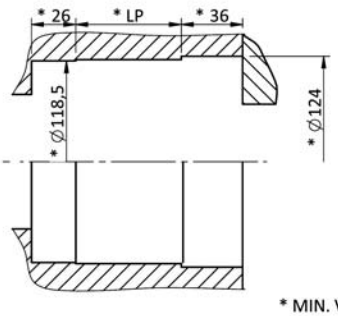

* MIN. VALUE

Il motore HTQ 120 è disponibile oltre nella versione rotostatore (dis.100455/0) anche in versione complete con meccanica identica al ns.BLQ 65/66 (per i disegni fare riferimento al catalogo dei servomotori brushless serie BLQ).

The motor HTQ 120 is available both in rotor + stator kit (frameless, dwg.100455/0) and complete execution with solid shaft. In case of complete execution the dimensions are like our BLQ65/66 (the relative drawings are available on our catalogue of the brushless servomotor BLQ series).

TABELLA COMPARATIVA / ***COMPARATIVE TABLE***

HTQ 120 S	**BLQ 66 K**
HTQ 120 M	**BLQ 66 S**
HTQ 120 L	**BLQ 66 P**

CATALOGO PRELIMINARE:
I dati e le prestazioni sono indicativi e sono soggetti a variazioni e/o modifiche senza preavviso.

PRELIMINARY CATALOGUE:
Data and performances are provided as a guide and can be changed without notice.

HTQ 240

Vca 3 x 345 Vrms

motore *motor*	codice *code*	Pn kW	Tno Nm	Tn Nm	Tp Nm	J kgcm²	Nnom RPM	Nmax@2Tno RPM	Nmax@Tp RPM	Ino Arms	In Arms	Ip Arms	N. poli *No. poles*	W kg
HTQ 240 S TENV	**1A**	0,77	52	49	200	670 (410)	150	150	47	2,8	2,7	11,8	20	43 (22)
	3A	1,49	52	47	200	670 (410)	300	249	125	3,6	3,3	15	20	43 (22)
	4A	2,13	52	45	200	670 (410)	450	403	266	5,2	4,5	21,4	20	43 (22)
	6A	2,65	52	42	200	670 (410)	600	541	388	6,6	5,3	27,2	20	43 (22)
HTQ 240 L TENV	**1A**	1,41	95	90	400	1170 (740)	150	146	47	4,1	3,9	18,6	20	60 (37)
	3A	2,70	95	86	400	1170 (740)	300	278	170	6,6	5,9	29,5	20	60 (37)
	4A	3,62	95	77	400	1170 (740)	450	450	326	9,7	7,9	44,3	20	60 (37)
	6A	4,27	95	68	400	1170 (740)	600	582	432	12	8,6	54,5	20	60 (37)

Tra parentesi, i dati della versione a dis. 100439

Between brackets the data of the version referred to our drwg. 100439

100439/A - BLIND HOLE SHAFT VERSION B5 (OPTION)

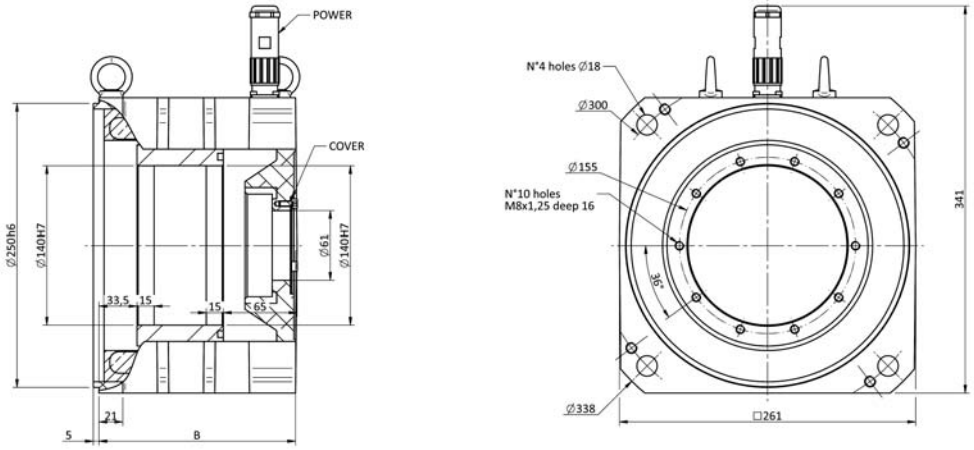

100438/A - SHAFT END VERSION B5 (STANDARD)

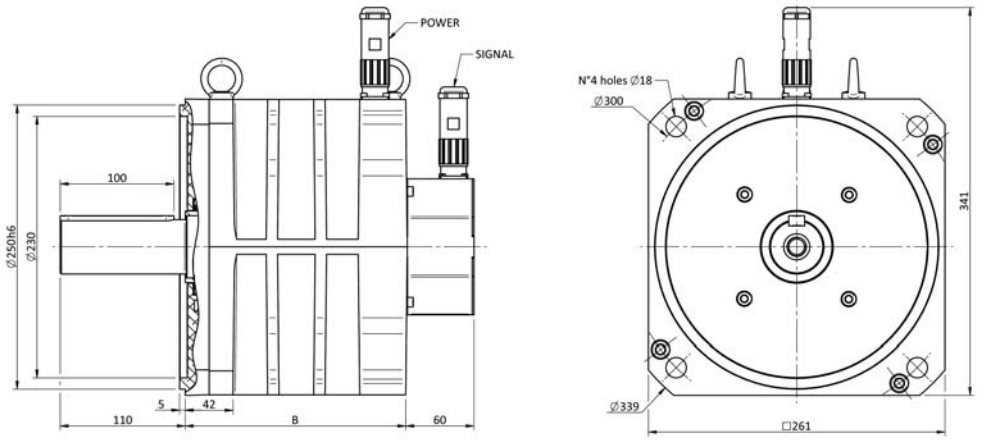

tipo *type*	B 100438/A	B 100439/A
HTQ 240 S	195	174
HTQ 240 L	255	234

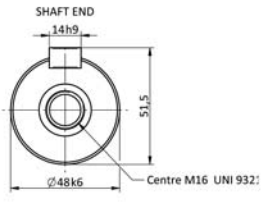

CATALOGO PRELIMINARE:
I dati e le prestazioni sono indicativi e sono soggetti a variazioni e/o modifiche senza preavviso.

PRELIMINARY CATALOGUE:
Data and performances are provided as a guide and can be changed without notice.

HTQ 300

motore *motor*	codice *code*	Pn kW	Tno Nm	Tn Nm	Tp Nm	J kgcm²	Nnom RPM	Nmax@2Tno RPM	Nmax@Tp RPM	Ino Arms	In Arms	Ip Arms	N. poli *No. poles*	W kg
HTQ 300 S TENV	**1A**	2,25	155	143	400	905	150	136	80	7,1	6,8	20,7	22	155
	3A	4,28	155	136	400	905	300	267	172	13,2	11,6	37,1	22	155
	4A	5,79	155	123	400	905	450	397	261	19,3	15,1	53,6	22	155
HTQ 300 M TENV	**1A**	4,09	290	261	800	1588	150	134	81	12,3	11,4	38,1	22	240
	3A	7,36	290	234	800	1588	300	258	165	22,7	18,5	69	22	240
	4A	8,94	290	190	800	1588	450	396	257	34,5	22,5	103,5	22	240
HTQ 300 L TENV	**1A**	5,85	410	372	1200	2271	150	134	82	17,4	15,8	55,7	22	320
	3A	10,00	410	318	1200	2271	300	263	167	32,6	25,2	103,5	22	320
HTQ 300 S TEWC	**1B**	3,72	250	237	400	905	150	136	100	14,2	13,5	25	22	155
	3B	6,84	250	218	400	905	300	279	210	26,3	23,4	46,9	22	155
	4B	9,43	250	200	400	905	450	415	318	39,2	31,3	68,3	22	155
HTQ 300 M TEWC	**1B**	8,62	580	549	800	1588	150	150	121	36,6	34,9	55,6	22	240
	3B	16,32	580	520	800	1588	300	285	233	66,8	59,6	100,1	22	240
	4B	22,08	580	469	800	1588	450	436	357	100,1	80,6	150,2	22	240
HTQ 300 L TEWC	**1B**	12,38	830	788	1200	2271	150	146	115	50,1	47,5	79	22	320
	3B	23,20	830	739	1200	2271	300	291	234	96,7	84,7	150,2	22	320

100423/A - HOLLOW VERSION B14 (OPTION)

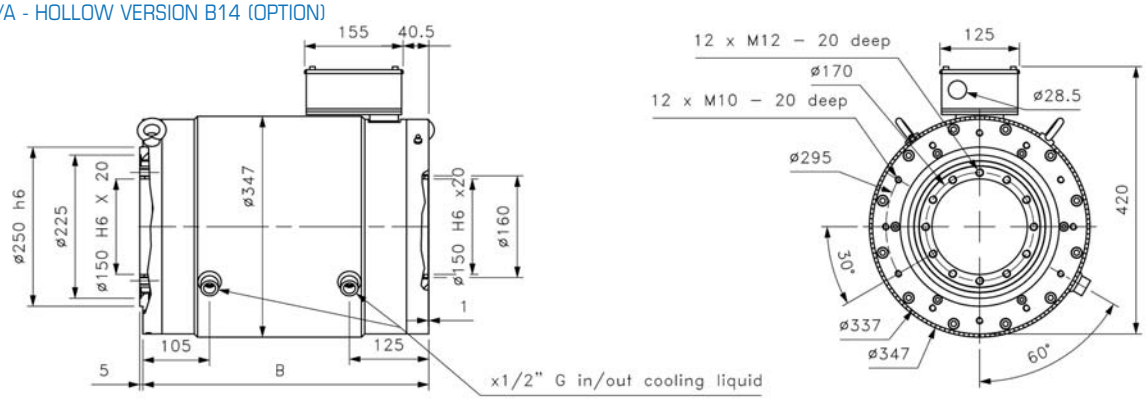

100422/B - SHAFT END VERSION B3 (STANDARD)

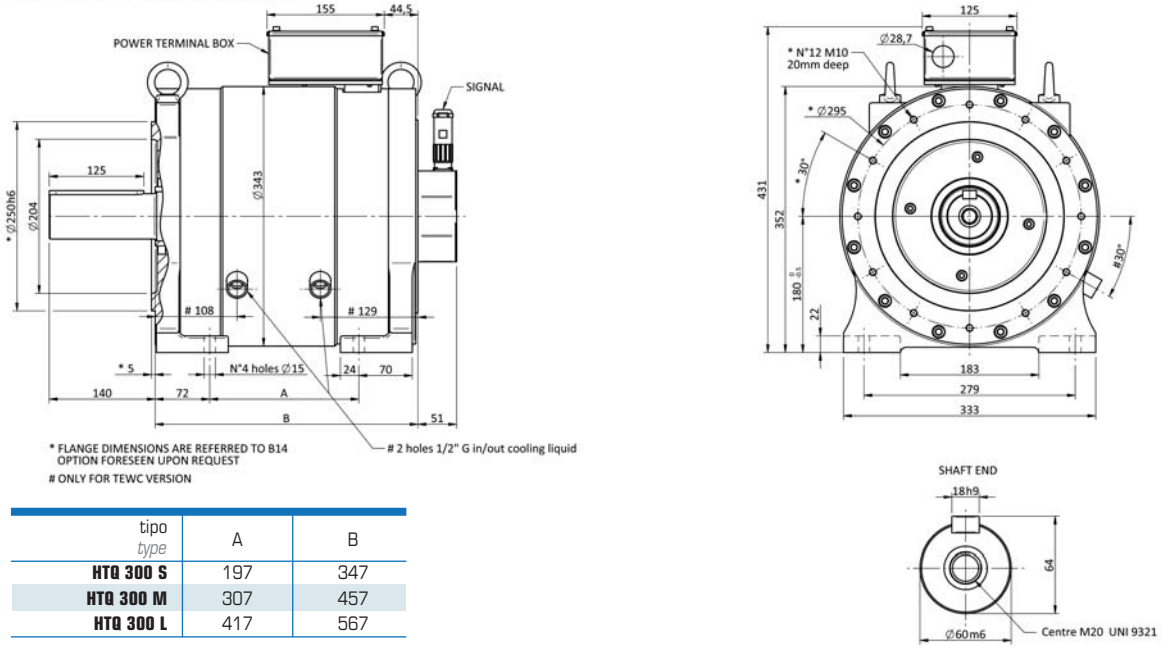

tipo *type*	A	B
HTQ 300 S	197	347
HTQ 300 M	307	457
HTQ 300 L	417	567

CATALOGO PRELIMINARE:
I dati e le prestazioni sono indicativi e sono soggetti a variazioni e/o modifiche senza preavviso.

PRELIMINARY CATALOGUE:
Data and performances are provided as a guide and can be changed without notice.

HTQ 350

motore *motor*	codice *code*	Pn kW	Tno Nm	Tn Nm	Tp Nm	J kgcm²	Nnom RPM	Nmax@2Tno RPM	Nmax@Tp RPM	Ino Arms	In Arms	Ip Arms	N. poli *No. poles*	W kg
HTQ 350 S TENV	**1A**	7,2	520	461	2400	9400	150	142	89	18,2	15,9	88	20	399
	3A	11,3	520	358	2400	9400	300	288	210	33,7	23	163	20	399
	4A	7,8	520	166	2400	9400	450	450	406	59,5	18,6	285	20	399
HTQ 350 M TENV	**1A**	8,4	620	536	2800	11200	150	141	90	21,1	18,2	104	20	452
	3A	12,6	620	401	2800	11200	300	282	206	38,6	25	190	20	452
HTQ 350 L TENV	**1A**	9,5	700	604	3300	13010	150	150	98	25,2	21,5	127	20	504
	3A	13,8	700	439	3300	13010	300	293	215	45,5	28,2	228	20	504
HTQ 350 S TEWC	**1B**	18,1	1190	1149	2400	9400	150	150	115	48,4	46,6	104	20	399
	3B	34,1	1190	1086	2400	9400	300	300	253	88,6	80,8	191	20	399
	4B	47,9	1190	1016	2400	9400	450	450	404	134,2	113,3	287	20	399
HTQ 350 M TEWC	**1B**	22,2	1450	1410	2800	11200	150	150	121	60,5	58,3	127	20	452
	3B	42,6	1450	1354	2800	11200	300	300	256	110,4	100,7	229	20	452
HTQ 350 L TEWC	**1B**	26,5	1750	1686	3300	13010	150	148	117	69,7	67,1	143	20	504
	3B	50,6	1750	1610	3300	13010	300	300	279	140,5	128,3	287	20	504

100440/A - SHAFT END VERSION B3 (STANDARD)

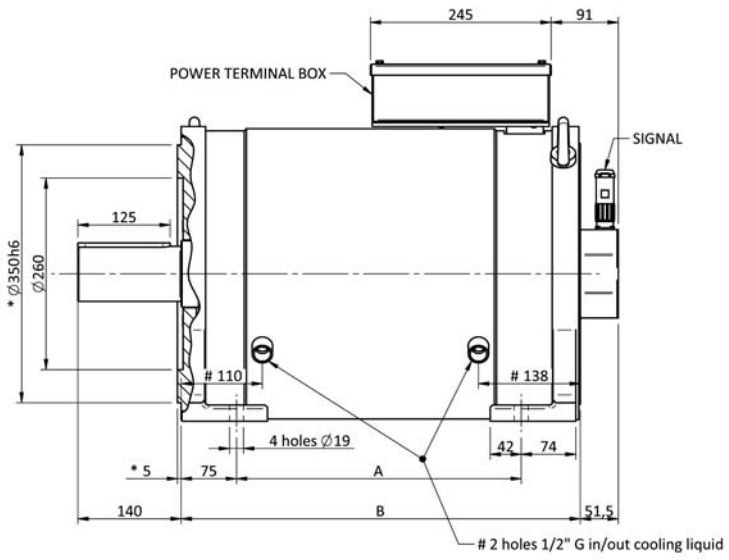

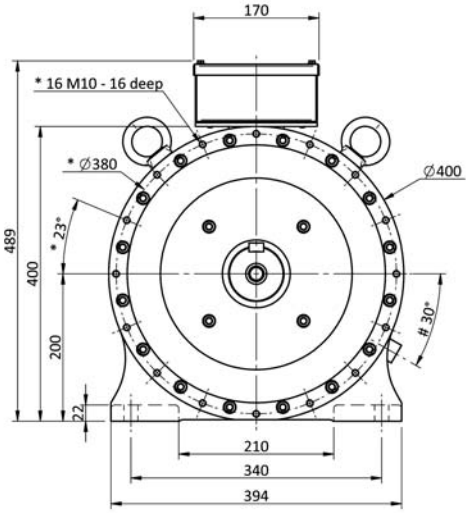

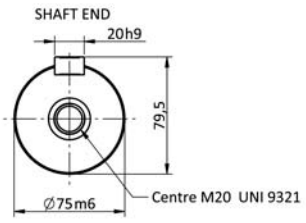

* FLANGE DIMENSIONS ARE REFERRED TO B14
OPTION FORESEEN UPON REQUEST

DIMENSIONS ONLY FOR TEWC VERSION

tipo *type*	A	B
HTQ 350 S	386	541
HTQ 350 M	446	601
HTQ 350 L	506	661

CATALOGO PRELIMINARE:
I dati e le prestazioni sono indicativi e sono soggetti a variazioni e/o modifiche senza preavviso.

PRELIMINARY CATALOGUE:
Data and performances are provided as a guide and can be changed without notice.

HTQ 565

Vca 3 x 345 Vrms

motore *motor*	codice *code*	Pn kW	Tno Nm	Tn Nm	Tp Nm	J kgm²	Nnom RPM	Nmax@2Tno RPM	Nmax@Tp RPM	Ino Arms	In Arms	Ip Arms	N. poli *No. poles*	W kg
	1B	56	3800	3500	6800	6,06	150	122	88	185	170	350	42	910
HTQ 565 S TEWC	**3B**	100	3800	3200	6800	6,06	300	222	161	335	275	640	42	910
	4B	123	3800	2600	6800	6,06	450	313	228	471	315	890	42	910
	1B	87	6000	5500	10000	8,93	150	126	92	302,4	280	560	42	1280
HTQ 565 M TEWC	**3B**	154	6000	4900	10000	8,93	300	228	168	535	440	990	42	1280
	4B	190	6000	4000	10000	8,93	450	345	254	806	540	1500	42	1280
	1B	117	8000	7400	13000	11,8	150	126	93	400	380	750	42	1650
HTQ 565 L TEWC	**3B**	210	8000	6700	13000	11,8	300	257	191	820	680	1500	42	1650

100444/0 - SHAFT END VERSION B3 (STANDARD)

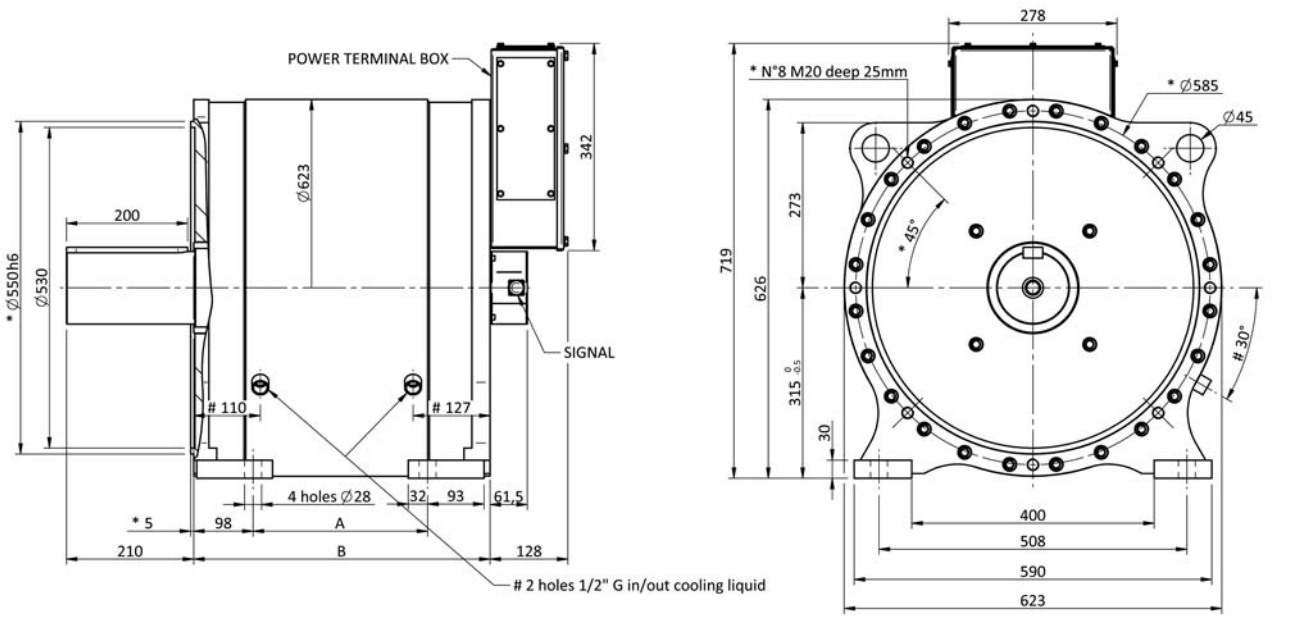

* FLANGE DIMENSIONS ARE REFERRED TO B14 OPTION FORESEEN UPON REQUEST

ONLY FOR TEWC VERSION

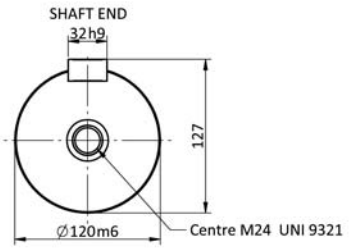

tipo *type*	A	B
HTQ 565 S	288	489
HTQ 565 M	413	614
HTQ 565 L	538	739

CATALOGO PRELIMINARE:
I dati e le prestazioni sono indicativi e sono soggetti a variazioni e/o modifiche senza preavviso.

PRELIMINARY CATALOGUE:
Data and performances are provided as a guide and can be changed without notice.

MAGNETIC PRODUCT RANGE

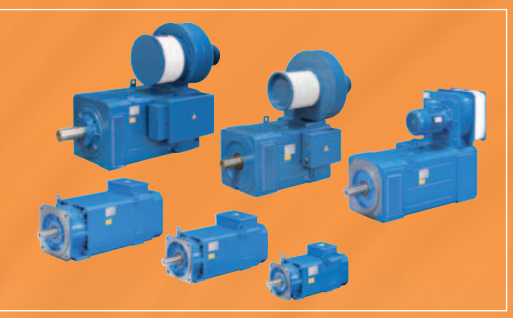

ASYNCHRONOUS VECTORIAL
SERVOMOTORS

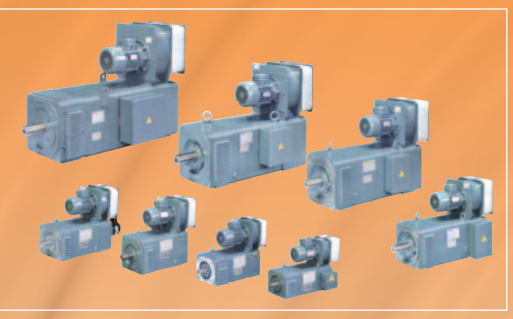

D.C. MOTORS

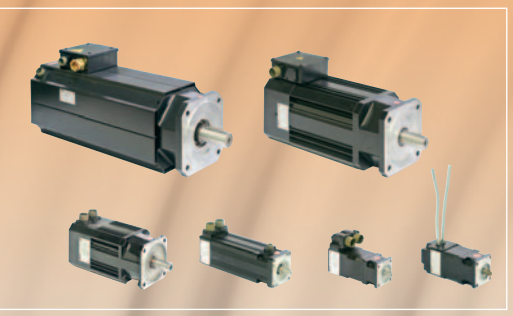

BRUSHLESS SERVOMOTORS

D.C. SERVOMOTORS,
TACHOGENERATORS
AND CENTRIFUGAL RELAYS

MAGNETIC S.p.A.
via del Lavoro, 7
I-36054 Montebello Vicentino (VI)
tel. +39 0444 649399
fax +39 0444 440495
www.magnetic.it
info@magnetic.it

I00257/B - 11/2010

Appendix B

Unidrive SP Universal AC Drive

EMERSON
Industrial Automation

Unidrive SP

Universal AC Drive Solutions Platform

0.37kW to 1.9MW
200V / 400V / 575V / 690V

CONTROL TECHNIQUES
www.controltechniques.com

EMERSON
Industrial Automation

The Ultimate Intelligent AC Drive

Performance and flexibility allows you to do something new, creating opportunities to innovate, find better ways to control your application, increase speeds, improve processes and reduce the footprint of your system. Unidrive SP, Control Techniques' high-performance intelligent drive family allows you to achieve this. The ultimate AC drive.

One range, any power

Unidrive SP is a complete drive automation range that covers the power spectrum from 0.37kW to 1.9MW. All drives share the same flexible control interface regardless of the power rating. Drives are packaged in three formats, Panel Mount, Free Standing and Modular.

Panel Mount – Standard drive modules
0.37kW to 132kW
Unidrive SP Panel Mount drives are standard AC input, AC output modules for installation within a control panel. The modules are easy to install and commission and can be applied in a wide range of applications.

NEW – Unidrive SP Size Zero is a new member of the Panel Mount range. It reduces the drive size by 60% for motors from 0.37kW to 1.5kW. The new model has the same parameter set, universal motor control and user interface as the rest of the Unidrive SP range.

Free Standing – Ready to run
90kW to 675kW
Unidrive SP Free Standing offers a fully engineered drive that is supplied within a standard sized cabinet. Free Standing can be ordered to include all of the power input equipment needed to allow immediate connection to the motor and to the power supply.

Unidrive SP Modular – Power system flexibility
45kW to 1.9MW
Unidrive SP Modular offers maximum power system design flexibility. Drive modules can be connected together in a variety of ways to create common DC bus systems, active input systems for returning excess energy to the power supply and parallel drives for high power motors. All drive modules are compact for easy handling.

N1652

2 YEAR Digital Drive Warranty

Certificate No. EMS 54446 003

Certificate No. Q 05176 003

c UL us
E171230

Unidrive SP features

Smartcard for parameter, PLC and Motion program storage

Drive identification marker rail

Optional Keypad, available as high brightness LED or multi-language LCD with plain text

Modbus communications port for PC programming and device interfacing

Terminal Cover*

Sturdy cable management system providing an earthing point for shielded control and power cables

* Features and their locations vary on some drive sizes

Terminal Cover for DC Bus, Low Voltage Power Supply and Onboard EMC filter

Power On / Drive Status LED

Aluminium Heatsink, drive can be mounted on a flat surface, or through panel mounted so that the heat is dissipated outside the enclosure*

3 Option Modules for communications, I/O, additional feedback devices and automation/motion controllers*

Control connections with removable terminals

Power connections with removable terminals*

Universal Encoder Port supporting Incremental, SinCos, SSI, EnDAT and HIPERFACE encoder types

Panel Mount - Page 20

High performance AC & Servo Drive for standard power applications

Free Standing - Page 18

Fully engineered AC drive cabinet for higher power standard applications

Modular - Page 19

Modular high power performance AC Drive for higher power custom applications

Voltage (V)	Power		
	Panel Mount	Free Standing	Modular
200 - 240 1Ph	0.37 - 1.5 kW	-	-
200 - 240 3Ph	0.37 - 45 kW	-	45 - 950 kW
380 - 480 3Ph	0.37 - 132 kW	90 - 675 kW	90 - 1900 kW
500 - 575 3Ph	2 - 150 HP	125 - 700 HP	125 - 1750 HP
500 - 690 3Ph	15 - 132 kW	90 - 660 kW	90 - 1800 kW

Any motor, any encoder

Unidrive SP provides high-performance motor control for induction motors, asynchronous servo and synchronous servo motors. The control mode is simply selected using the drive keypad.

- **Servo** – Precision, dynamic control supporting a wide range of rotary and linear motors
- **Closed Loop Vector** – Ultimate precision control of induction motors offering full motor torque at zero speed
- **RFC Mode (Rotor Flux Control)** – Superior dynamic performance and stability without a feedback device
- **Open Loop Vector** – Good open loop motor performance with minimum configuration
- **Open loop V/f Control** – A simple control algorithm that is ideal for parallel motors
- **Regenerative** – Active front end control mode for harmonic elimination and regeneration

Unidrive includes the hardware required to connect to virtually any feedback encoder type, allowing the designer to select the most appropriate technology for the application:

- **Incremental** - Offers a good balance of cost and performance
- **SinCos** - Provides increased position resolution for precision and low speed applications
- **SSI** - Provides absolute position feedback
- **EnDat & HIPERFACE** - These encoders transfer position data using a high speed communications network, often combined with SinCos technology

EtherCAT

Add the extra features you need

Click-in option modules allow you to customise the drive to suit your needs. Over 25 different options are available including Fieldbus, Ethernet, I/O, extra feedback devices and automation controllers.

Intelligently Driven

Unidrive SP allows the drive system designer to embed automation and motion control within the drive, this eliminates communication delays that reduce performance while CTNet, a high performance drive-to-drive network links the different parts of the system.

Reliability and Innovation

Unidrive SP is designed using a well proven development process that prioritises innovation and reliability. This process has resulted in Control Techniques having a market leading reputation for both product performance and quality.

Global Support

Control Techniques' 54 Drive Centres located in 31 countries ensure that service, support and expertise are just around the corner, all around the world. Our engineers are passionate about drives and are able to offer the level of service that you need, from advice on an application problem to providing a complete drive solution design.

Unidrive SP electrical and mechanical integration

Unidrive SP enables system designers to reduce costs. Standard features such as Safe Torque Off and back-up power supply inputs reduce cabinet size by eliminating external components. Integration options enable the system designer to simplify control and maximise performance.

Simple safety integration

Unidrive SP Safe Torque Off input (formerly referred to as Secure Disable) allows the drive output to be disabled so that the drive cannot generate torque. The reliability is far superior to having a contactor connected to the drive output and requires no extra space, has no moving parts and incurs no extra costs.

- Certified by BGIA and TUV
- Allows the drive to become part of the machine safety system
- Reduces user cost in machine safety designs that must comply with EN954-1 category 3 and EN81-1 for elevators
- Eliminates one or more power contactors
- Eliminates feedback checking arrangement
- Drive can be powered continuously

Safe Torque Off can form part of an EN954-1 Category 4 system by adding control circuitry. Contact your local Drive Centre or Distributor.

For more information please refer to the Guide to the Unidrive SP Safe Torque Off Function, **order code 0175-0317.** Also available for download from www.controltechniques.com

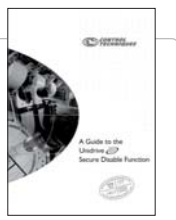

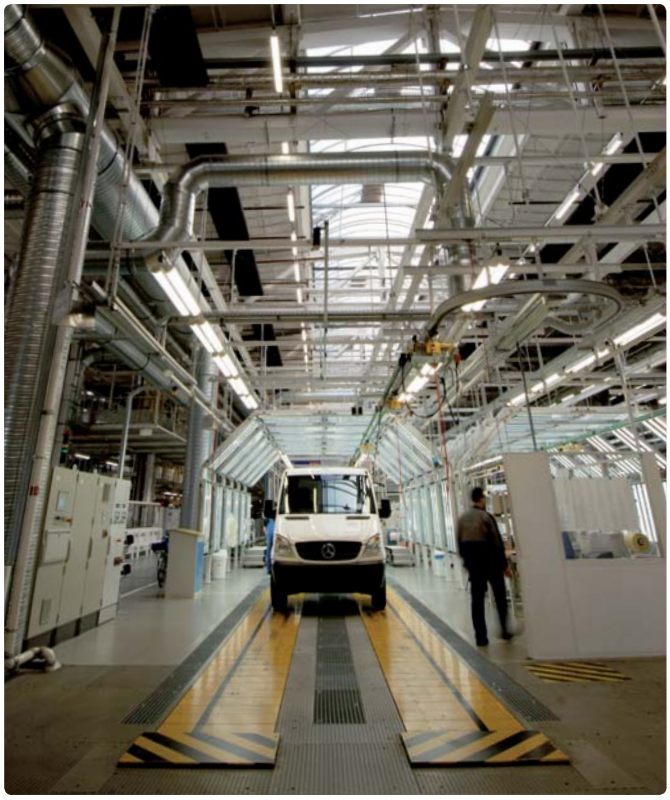

Back-up power supply inputs for continuous operation

24VDC input - control
24Vdc supply allows the control circuits of Unidrive SP to remain active when the AC supply is removed. This enables Fieldbus modules, application modules and encoders to continue to operate.

48-96VDC input - power
Allows the drive power output to control the motor, often used for emergency back-up situations such as for moving elevators to an exit during a power supply failure.

Easy compliance with global EMC standards

Unidrive SP features a built-in filter allowing the drive to comply with EN 61800-3. The filter can be easily removed if required such as when sensitive earth leakage protection is installed. External EMC Filters are available for compliance with EN 6100-6-4.

Integrated brake resistors

Unidrive SP frame sizes 0 to 2 feature an optional heatsink mounted brake resistor. This arrangement simplifies installation, requires no additional space and is self fusing with additional overload protection offered by the drive.

More compact drive systems

Unidrive SP Panel Mount sizes 1 – 6 and Unidrive SP Modular drives can be through panel-mounted to allow heat to be dissipated externally. This reduces the temperature rise inside the control panel. An IP54 mounting kit is included as standard and IP54 versions of the heatsink fan are available as an option. This mounting method allows smaller cabinet dimensions and reduces the need for ventilation.

Unidrive SP Active Input solution for improved energy efficiency

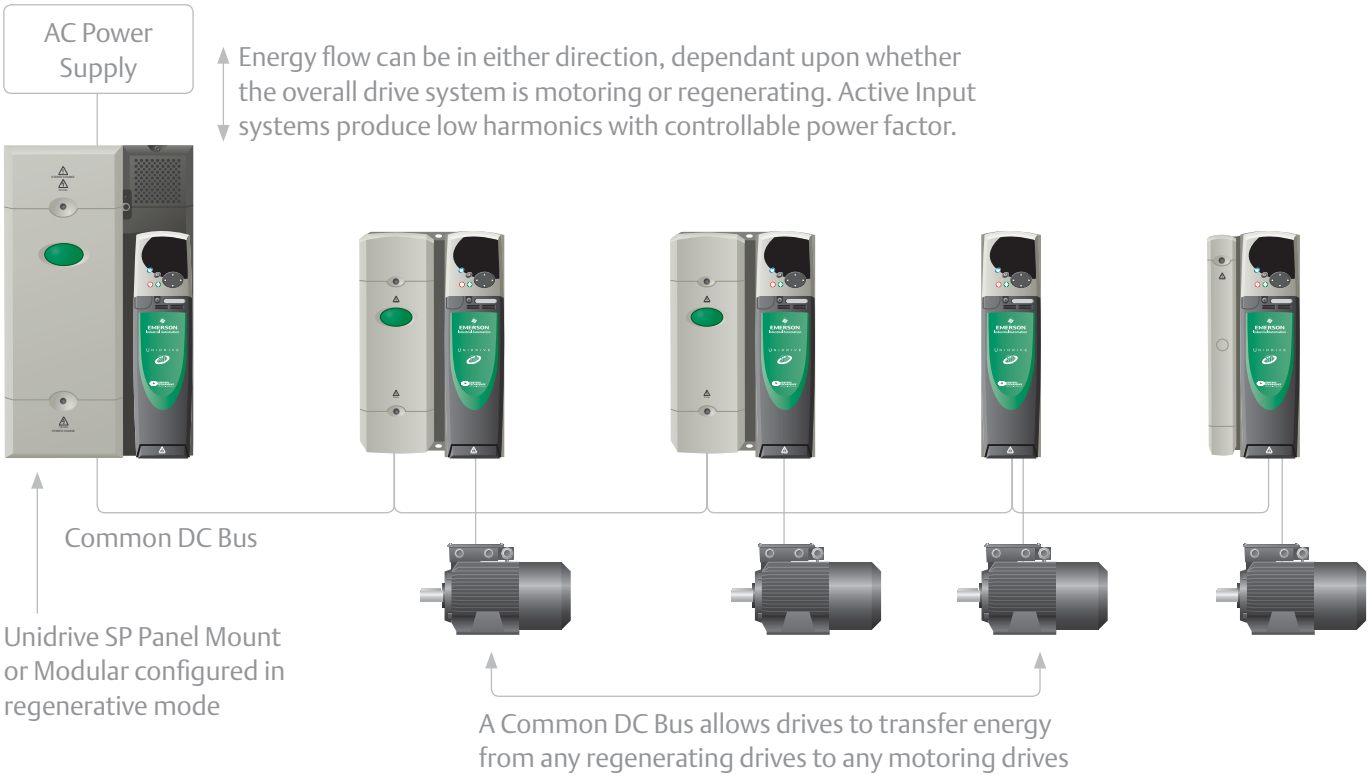

Energy saving and harmonic reduction

In most applications variable speed drives reduce energy consumption by matching the motor speed to the required load.

In applications where there is a significant amount of stored mechanical energy, the drive must be able to dissipate the energy to control the motor speed. This presents a further opportunity to reduce energy consumption by returning the excess energy to a shared DC bus or to the AC supply.

DC bus and active input systems can be configured using either Unidrive SP Modular or Panel Mount drives. DC bus systems reduce running costs by circulating energy between braking and motoring drives. Active input systems return excess braking energy to the mains supply. Benefits include:

- Energy saving
- Sinusoidal input current (low harmonic content)
- Unity or controllable input power factor

Unidrive SP setup, configuration and monitoring

Unidrive SP is quick and easy to set-up. The drives may be configured using a removable keypad, Smartcard or the supplied commissioning software that guides the user through the configuration process.

User Interface Options

Unidrive SP benefits from a number of keypad choices to meet your application needs.

Keypad Options	Details
No Keypad	The drive is supplied as standard with no keypad. This is ideal for high volume applications or where you wish to prevent access to drive settings
SM – Keypad	Hot pluggable, high-brightness LED display
SM – Keypad Plus	Multi-lingual, hot pluggable, backlit LCD display. The display can be customised to provide application specific text
SP0 – Keypad	Hot Pluggable LED for the ultra compact Size 0

SM-Keypad

SM-Keypad Plus

SP0-Keypad

Software and Smartcard Tools for rapid commissioning

Control Techniques software suite makes it easier to access the drive's full feature set. It allows you to optimize the drive tuning, back-up the configuration and set-up a communications network. The software tools can connect using Ethernet, Serial, USB or Control Techniques drive-to-drive network, CTNet.

CTSoft

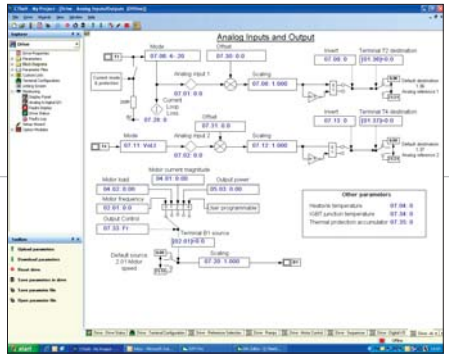

CTSoft is a drive configuration tool for commissioning, optimising and monitoring Control Techniques drives. It allows you to:

- Use the configuration wizards to commission your drive
- Read, save and load drive configuration settings
- Manage the drive's Smartcard data
- Visualise and modify the configuration with live animated diagrams

CTScope

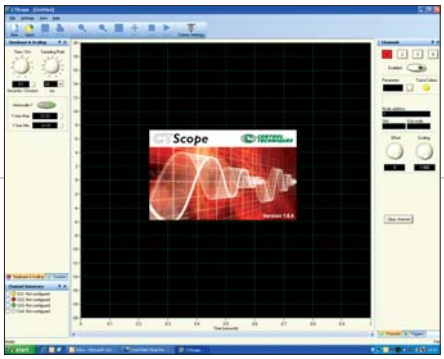

CTScope is a full featured software oscilloscope for viewing and analysing changing values within the drive. The time base can be set to give high speed capture for tuning or for longer term trends. The user interface is based on a traditional oscilloscope, making it familiar and friendly to all engineers across the globe.

Try it, download the full version of CTSoft and CTScope software from www.controltechniques.com

FREE Software

CTOPCServer

CTOPCServer is an OPC compliant server which allows PCs to communicate with Control Techniques drives. The server supports communication using Ethernet, CTNet, RS485 and USB. OPC is a standard interface on SCADA packages and is widely supported within Microsoft products. The server is supplied free of charge and may be downloaded from www.controltechniques.com.

Try it, download the full version of CTOPCServer from www.controltechniques.com

FREE Software

Smartcard

The Smartcard is a memory device that is supplied with every Unidrive SP, it can be used to back-up parameter sets and PLC programs and copy them from one drive to another.

- Parameter and program storage
- Simplify drive maintenance and commissioning
- Quick set-up for sequential build of machines
- Machine upgrades can be stored on a Smartcard and sent to the customer for installation

Easy performance tuning

Auto-tune features accessible through CTSoft or the keypad help you to get the best performance by measuring the motor and machine attributes and automatically optimising control parameters.

EMERSON
Industrial Automation

Unidrive SP - Unparalleled integration flexibility

Control Mode

Open loop motor

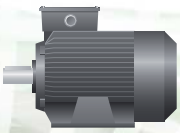

Closed loop motor

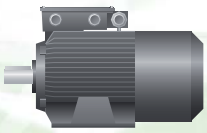

Servo motor

Linear motor

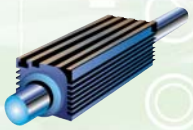

Regenerative Active Front End

Drive Programming and Operator Interface

Options | Standard

Operator Interface

LCD Keypad

LED Keypad

Smartcard

Input/Output

Standard | Options

5 Analogue I/O
7 Digital I/O
1 Safe Torque Off

SM I/O 32

SM I/O Plus

SM I/O Lite

SM I/O Timer

SM I/O 120V

SM PELV

REMOTE I/O

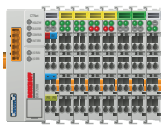

Centralised PLC/Motion Control

Motion Controller

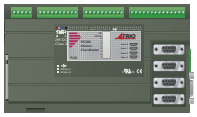

PLC

PC

DC Back up Power Supply

48 - 96V Power

24V Control

Standard

Options

Applications with PLC or Motion functionality

On Board PLC

Easy to use onboard ladder logic PLC at zero cost, ideal for simple applications requiring extra drive functionality

Configured using SyPTLite software

SM Applications Lite

Powerful automation controller using a dedicated microprocessor giving full drive parameter access

Configured using SyPTLite or SyPTPro software

SM Applications Plus

Powerful automation controller with drive to drive networking and full motion capability

Configured using SyPTPro software

SM EZMotion

Motion made easy with intuitive step-by-step configuration

Configured using PowerTools Pro software

Communications

Standard

Options

Modbus RTU

SM EtherCAT

SM LonWorks

SM Profibus DP

SM Interbus

SM CAN

SM DeviceNet

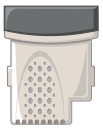

SM Ethernet

SM CANopen

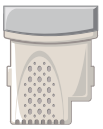

SM SERCOS

Feedback

Standard

Options

Incremental
SinCos high resolution
SSI Absolute
EnDat & HIPERFACE
Communications

SM Universal Encoder Plus

Accepts or replicates all standard feedback types, Input and output

SM Encoder Plus

Incremental input

SM Resolver

Resolver input
Incremental output

SM Encoder Output Plus

Incremental Encoder Output, Input and output

Unidrive SP drive intelligence and system integration

Intelligent drives offer more compact, higher-performance and lower cost solutions in machinery automation applications. Over the past 20 years Control Techniques has pioneered the embedding of programmable automation, motion and communications features within drives.

SyPTLite and on board automation

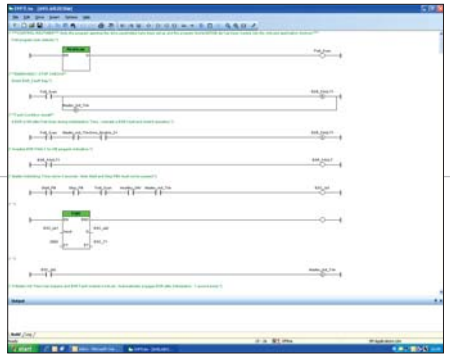

Unidrive SP has an inbuilt programmable controller. It is configured using SyPTLite, an easy-to-use ladder logic program editor, suitable for replacing relay logic or a micro PLC for simple drive control applications.

The software is supplied free of charge. For evaluation, download the full version from www.syptlite.com.

FREE Software

SyPTPro automation development environment

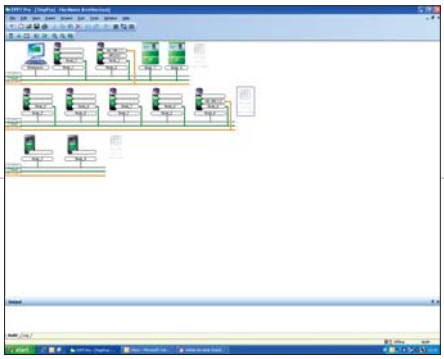

SyPTPro is a full featured automation development environment that can be used for developing tailored solutions for single or multiple drive applications. The programming environment fully supports three industry standard languages: Function Block, Ladder and Structured Text. Motion control is configured using the new PLCopen motion language, supporting multiple axes.

CTNet, a high-speed, deterministic drive-to-drive network links the drives, SCADA and I/O together to form an intelligent networked system, with SyPTPro managing both the programming and communications.

For evaluation, download a demonstration version from www.controltechniques.com.

FREE Software

High Performance Automation

All of Control Techniques automation option modules contain a high performance microprocessor, leaving the drive's own processor to give you the best possible motor performance.

SM-EZ Motion

The SM-EZ Motion option module and PowerTools Pro software provides a user friendly environment for motion programming. The EZ-Motion approach is ideal for applications that are low volume and low engineering time.

- Simple drag & drop programming allows you to create programs "out of the box" without having to write a single line of code
- Programming completed in 5-steps, the software guides you through drive configuration, I/O configurations and programming steps
- Intuitive Windows environment with simple data entry
  - "Fill-in-the-Blank" values
  - "Point and Click" Radio Buttons
  - "Scrolling" menu selections
  - "Drag and Drop" parameters

The module has four digital inputs and two digital outputs for high-speed I/O operations.

SM-Applications Lite

The SM-Applications Lite module is designed to provide programmable control for standalone drive applications or when the drive is connected to a centralised controller via I/O or Fieldbus. SM-Applications Lite may be programmed using ladder logic with SyPTLite or can make use of the full automation and motion capabilities contained within SyPTPro.

- Easy Powerful Configuration – SM-Applications Lite can be used to tackle automation problems from simple start/stop sequencing with a single drive to more complex machine and motion control applications
- Real Time Control –The SM-Applications Lite module gives you real-time access to all of the drives parameters plus access to data from I/O and other drives. The module uses a high speed multi-tasking operating system with task update times as low as 250µs. Tasks are synchronised to the drives own control loops to give you the best possible performance for drive control and motion

EMERSON
Industrial Automation

Unidrive SP machine communications flexibility

PC for programming and monitoring using CTSoft, CTScope, SyPT or OPC. Connect using Serial, Ethernet, USB or CTNet

Fieldbus or Ethernet connection to main controller using a wide range of communications option modules

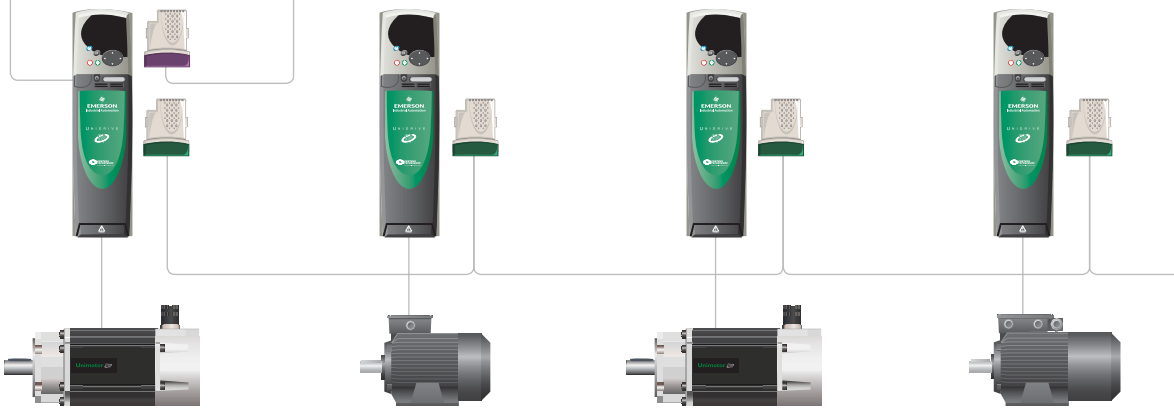

SM-Applications Plus

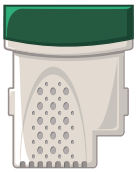

SM-Applications Plus offers all of the features of the SM-Applications Lite module but with additional communications and high speed I/O. SM-Applications Plus is programmed using SyPTPro system programming tool.

- Inputs/Outputs – The module has two digital inputs and two digital outputs for high-speed I/O operations such as position capture and actuator firing
- High speed serial port - The module features a serial communications port supporting standard protocols such as Modbus for connection to external devices such as operator interface panels
- Drive-to-drive communications - SM-Applications Plus option modules include a high speed drive-to-drive network called CTNet, this network is optimised for intelligent drive systems offering flexible peer to peer communications. The bus has the capability to connect to remote I/O, operator panels, Mentor DC drives and PCs using an OPC server

Ethernet connection for remote access, wireless connectivity and asset management

Operator interface connected using serial, Fieldbus or Ethernet

Network connected Remote I/O

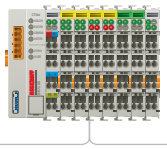

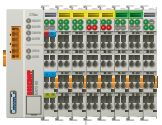

CT Net is a high performance network designed for machine integration. It allows connection to PCs, operator interfaces, I/O and other Control Techniques drives

Fieldbus Communications

Option modules for all common Industrial Ethernet, Fieldbus networks such as Ethernet/IP and Profibus and Servo networks such as SERCOS and EtherCAT are available. We continually develop new modules as new technologies emerge.

'Black box'

SM-Applications and CTNet allow machine designers to design a 'black box' into which customers are able to interface using their preferred Fieldbus or Ethernet interface. This solution improves the machine performance, simplifies the problem of being able to meet customer specifications for different Fieldbus communications and helps to protect your intellectual property.

	Onboard PLC	SM-Applications Lite	SM-Applications Plus
Intellectual property protection	✔	✔	✔
SyPTLite Programming	✔	✔	
SyPTPro Programming		✔	✔
Multi-tasking environment		✔	✔
Motion control capabilities		✔	✔
CTNet drive-to-drive network			✔
Serial port			✔
High Speed I/O			✔

Unidrive SP Free Standing 90kW – 675kW

Higher power performance AC drive

The Unidrive SP Free Standing drive range offers the same advanced feature set as the panel mount drives but in a convenient pre-engineered package.

The drive cabinets can be factory configured so that they are delivered ready to be connected directly to your supply, this eliminates the need for drive panel building saving you time and money whilst also allowing you to focus on your application.

The drive cabinets offer industry leading power / size ratios and are ordered using simple order codes.

Applications

The Unidrive SP Free Standing drives are suitable for higher power applications in both commercial and industrial installations. Typical applications include:

- Energy saving with higher power fans and pumps
- Metal production and processing
- Conveying and handling of bulk materials
- Pulp and paper processing
- Marine applications

Benefits

The Unidrive SP Free Standing drives enjoy the same advantages as our Panel Mounting drives with the following additional benefits:

- Standard AC in / AC out pre-engineered cabinet solution reduces design time, lowers project risk and allows you to focus on getting the application engineering right
- Simple order codes allow you to specify a factory fitted power input scheme for your Free Standing drive. This means your drive is delivered ready to be connected reducing your engineering effort and installation time. The optional power input items include an MCCB, Contactor, EMC Filter and E-Stop
- Empty cabinets and accessories are available to allow you to integrate your own power input scheme or control equipment alongside the drive
- Industry standard form factor and colour allow the cabinets to integrate with new and existing cabinets
- Available with and without braking transistors to optimise costs for your application
- IP21 and optional IP23 enclosures available
- Compact cabinet reduces the space requirement, especially important in retrofit applications: 350kW = 400mm wide & 675kW = 800mm wide

For more information please refer to the Unidrive SP Free Standing brochure, **order code 0175-0346.** Also available for download from www.controltechniques.com

Unidrive SP Modular 45kW – 1.9MW

Modular high power performance AC drive

The Unidrive SP Modular Drives Range offers the same advanced feature set as the panel mount drives but with additional power system flexibility. Drive modules may be arranged to provide a common DC bus system with or without an active input (regenerative, 4 quadrant operation). Very high current motors may be controlled using a multi-drive modular arrangement.

Applications

The Unidrive SPM drives are suitable for applications in both commercial and industrial applications where power scheme flexibility and regenerative energy saving provides an operational advantage. Typical applications include:

- Automotive testing such as car, engine and gearbox dynamometers
- Web control and winding
- Conveying and processing of bulk materials
- Pulp and paper processing
- Marine applications
- Energy saving with high power fans and pumps
- Metal production and processing
- Large cranes
- Renewable energy systems such as photovoltaics

Benefits

Unidrive SP Modular drives enjoy the same advantages as the Panel Mounting drives but with the additional benefits of power system flexibility:

- Higher power motors are controlled using Unidrive SPM modules connected in parallel. This is an economic and compact solution that simplifies installation and improves serviceability
- Reduce running costs using a DC bus system to recycle energy between simultaneously braking and motoring drives such as in a winder / unwinder configuration
- Eliminate harmonics using an active front end
- Minimise harmonics with 12, 18 and 24 pulse operation to allow you to meet and exceed stringent supply regulations
- Modular approach can provide system redundancy, for example if a drive module was non operational in a multi-module installation it may still be possible to operate the application with the remaining modules
- Ultra compact modules allow high power systems to be constructed in non standard enclosures e.g. it is possible to implement a drive system of between 45kW to 1900kW in an enclosure no taller than 1m
- Operation with global power supplies 200V, 400V, 575V and 690V

Modular building blocks

The Unidrive SPM range comprises key modules that can be combined elegantly to achieve your design criteria with maximum economy.

SPMA	AC IN / AC OUT Drive Module
SPMD	DC IN / AC OUT Drive Module
SPMC	AC IN / DC OUT Rectifier
SM Control Master	Master control module for use with SPMA/D
SM Control Slave	Slave control module for use with SPMA/D

For more information and more configuration examples please refer to the Unidrive SPM brochure, **order code 0175-0345.** Also available for download from www.controltechniques.com

EMERSON
Industrial Automation

Unidrive SP Panel Mounted 0.37kW – 132kW
200V 1ph / 200V 3ph / 400V / 575V / 690V

High Performance AC & Servo Drive

Unidrive SP Panel Mount is a high performance drive module for system integration and stand alone applications.

Applications

Due to the inherent performance and flexibility of Unidrive SP, potential areas for its application are limitless, the drives' intelligence and dynamic response allow it to be applied in the most demanding applications.

Typical applications include:

- High speed machines
- Crane and hoist
- Lift and elevator controls
- Pulp and paper machines
- Metal production and processing
- Materials handling systems
- Marine applications
- Printing
- Textile machines
- Converting
- Energy saving with fans and pumps
- Plastics and rubber extrusion machines

Benefits

- Onboard programmable intelligence and generous connectivity allows the removal of external programmable logic controllers and motion controllers, reducing costs and the cabinet size. Unidrive SP features 5 analogue I/O and 7 digital I/O as standard
- Drive option module slots future proof your investment, it also means you only fit the functionality you need, reducing costs and removing complexity. Unidrive SP Sizes 1 to 6 benefit from three option slots with the ultra compact Size 0 featuring two slots
- Available option modules include advanced automation controllers, world-standard fieldbus connectivity options and a comprehensive range of digital and analogue I/O interfaces and feedback devices
- Optional Internal Brake Resistors for Unidrive SP Sizes 0, 1 and 2 reduce your space requirement
- The built in EMC filter is suitable for most applications and can be easily removed where required. Optional external footprint EMC Filters are available where more rigourous standards must be met
- Safe Torque Off, as standard, reduces system costs in machine safety designs
- IP54 through panel mount capability allows convenient heat dissipation and reduces cabinet size
- Operation with global power supplies 200V, 400V, 575V and 690V

Unidrive SP Panel Mount Ratings and Specifications

200-240VAC +/- 10% Single Phase (kW@220V) (HP@230V)

		Normal Duty			Heavy Duty		
Frame Size	Modules	Max Cont Current (A)	Typical Motor Output Power (kW)	(HP)	Max Cont Current (A)	Typical Motor Output Power (kW)	(HP)
0	SP0201	-	-	-	2.2	0.37	0.5
	SP0202	-	-	-	3.1	0.55	0.75
	SP0203	-	-	-	4	0.75	1
	SP0204	-	-	-	5.7	1.1	1.5
	SP0205	-	-	-	7.5	1.5	2

200-240VAC +/- 10% (kW@220V) (HP@230V)

		Normal Duty			Heavy Duty		
Frame Size	Modules	Max Cont Current (A)	Typical Motor Output Power (kW)	(HP)	Max Cont Current (A)	Typical Motor Output Power (kW)	(HP)
0	SP0201	-	-	-	2.2	0.37	0.5
	SP0202	-	-	-	3.1	0.55	0.75
	SP0203	-	-	-	4	0.75	1
	SP0204	-	-	-	5.7	1.1	1.5
	SP0205	-	-	-	7.5	1.5	2
1	SP1201	5.2	1.1	1.5	4.3	0.75	1
	SP1202	6.8	1.5	2	5.8	1.1	1.5
	SP1203	9.6	2.2	3	7.5	1.5	2
	SP1204	11	3	3	10.6	2.2	3
2	SP2201	15.5	4	5	12.6	3	3
	SP2202	22	5.5	7.5	17	4	5
	SP2203	28	7.5	10	25	5.5	7.5
3	SP3201	42	11	15	31	7.5	10
	SP3202	54	15	20	42	11	15
4	SP4201	68	18.5	25	56	15	20
	SP4202	80	22	30	68	18.5	25
	SP4203	104	30	40	80	22	30
5	SP5201	130	37	50	105	30	40
	SP5202	154	45	60	130	37	50

380-480VAC +/- 10% (kW@400V) (HP@460V)

		Normal Duty			Heavy Duty		
Frame Size	Modules	Max Cont Current (A)	Typical Motor Output Power (kW)	(HP)	Max Cont Current (A)	Typical Motor Output Power (kW)	(HP)
0	SP0401	-	-	-	1.3	0.37	0.5
	SP0402	-	-	-	1.7	0.55	0.75
	SP0403	-	-	-	2.1	0.75	1
	SP0404	-	-	-	3	1.1	1.5
	SP0405	-	-	-	4.2	1.5	2
1	SP1401	2.8	1.1	1.5	2.1	0.75	1
	SP1402	3.8	1.5	2	3	1.1	1.5
	SP1403	5	2.2	3	4.2	1.5	3
	SP1404	6.9	3	5	5.8	2.2	3
	SP1405	8.8	4	5	7.6	3	5
	SP1406	11	5.5	7.5	9.5	4	5
2	SP2401	15.3	7.5	10	13	5.5	7.5
	SP2402	21	11	15	16.5	7.5	10
	SP2403	29	15	20	25	11	20
	SP2404	29	15	20	29	15	20
3	SP3401	35	18.5	25	32	15	25
	SP3402	43	22	30	40	18.5	30
	SP3403	56	30	40	46	22	40
4	SP4401	68	37	50	60	30	50
	SP4402	83	45	60	74	37	60
	SP4403	104	55	75	96	45	75
5	SP5401	138	75	100	124	55	100
	SP5402	168	90	125	156	75	125
6	SP6401	205	110	150	180	90	150
	SP6402	236	132	200	210	110	150

500-575VAC +/- 10% (kW@575V) (HP@575V)

Frame Size	Modules	Normal Duty			Heavy Duty		
		Max Cont Current (A)	Typical Motor Output Power (kW)	(HP)	Max Cont Current (A)	Typical Motor Output Power (kW)	(HP)
3	SP3501	5.4	3	3	4.1	2.2	2
	SP3502	6.1	4	5	5.4	3	3
	SP3503	8.4	5.5	7.5	6.1	4	5
	SP3504	11	7.5	10	9.5	5.5	7.5
	SP3505	16	11	15	12	7.5	10
	SP3506	22	15	20	18	11	15
	SP3507	27	18.5	25	22	15	20
4	SP4603*	36	22	30	27	18.5	25
	SP4604*	43	30	40	36	22	30
	SP4605*	52	37	50	43	30	40
	SP4606*	62	45	60	52	37	50
5	SP5601*	84	55	75	63	45	60
	SP5602*	99	75	100	85	55	75
6	SP6601*	125	90	125	100	75	100
	SP6602*	144	110	150	125	90	125

500-690VAC +/- 10% (kW@690V) (HP@690V)

Frame Size	Modules	Normal Duty			Heavy Duty		
		Max Cont Current (A)	Typical Motor Output Power (kW)	(HP)	Max Cont Current (A)	Typical Motor Output Power (kW)	(HP)
4	SP4601	22	18.5	25	19	15	20
	SP4602	27	22	30	22	18.5	25
	SP4603	36	30	40	27	22	30
	SP4604	43	37	50	36	30	40
	SP4605	52	45	60	43	37	50
	SP4606	62	55	75	52	45	60
5	SP5601	84	75	100	63	55	75
	SP5602	99	90	125	85	75	100
6	SP6601	125	110	150	100	90	125
	SP6602	144	132	175	125	110	150

Notes: Select model on actual motor full load current. *The same model can be used on a 575V or a 690V supply, and has two different output ratings. For example: At Normal Duty, SP4603 is suitable for a 22kW output motor on a 575V supply and a 30kW output motor on a 690V supply. Can be used on IT supplies - all voltages, Grounded delta supplies - all voltages except 690V

Normal Duty Suitable for most applications, current overload of 110% for 165 seconds is available. Where motor rated current is less than the drive rated continuous current, higher overloads are achieved.

Heavy Duty Suitable for demanding applications, current overload of 175% for 40 seconds is available for frame size 0 - 5 in closed loop, 150% for 60 seconds in open loop. For frame size 6 current overload of 150% for 60 seconds is available in closed loop and 129% for 97 seconds in open loop. Where the motor rated current is less than the drive rated continuous current higher overloads (200% or greater) are achieved.

Environmental Safety and Electrical Conformance

- IP20/Nema 1 rating, IP54 (NEMA 12) through panel mount
- Ambient temperature -15 to +40°C, 50°C with derating
- Humidity 95% maximum (non condensing) at 40°C
- Altitude: 0 to 3000m, derate 1% per 100m between 1000m and 3000m
- Vibration: Tested in accordance with IEC 60068-2-34
- Mechanical Shock Tested in accordance with IEC 60068-2-27
- Storage temperature -40°C to 50°C
- Electromagnetic Immunity complies with EN 61800-3 and EN 61000-6-2
- With on board EMC filter, complies with EN 61800-3 (2nd environment)
- EN 61000-6-3 and EN 61000-6-4 with optional footprint EMC filter
- IEC 61000-3-4 Supply conditions
- IEC 60146-1-1 Supply conditions
- IEC 61800-5-1 (Power Drive Systems)
- IEC 61131-2 I/O
- EN 60529 Ingress protection
- EN 50178 / IEC 62103 Electrical safety
- Safe Torque Off (formally secure disable), independently assessed by BGIA to EN 954-1 cat 3
- EN 81-1 assessed by TÜV
- EN 61000-6-2, EN 61000-6-4 EMC, UL508C, UL840

Dimensions and Options

For Unidrive SP Free Standing and Unidrive SP Modular drive dimensions and ratings please refer to the relevant brochures.

SP0
Weight:
2.1kg (4.6lbs)

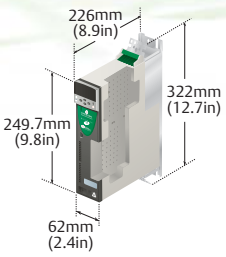

SP1
Weight: 5kg (11lbs)
SP1405 / SP1406:
5.8kg (13lbs)

SP2
Weight:
7kg (15.5lbs)

SP3
Weight:
15kg (33lbs)

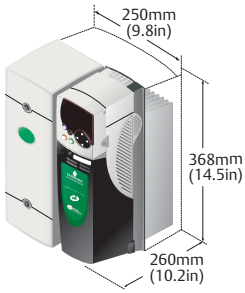

SP4
Weight:
30kg
(66lbs)

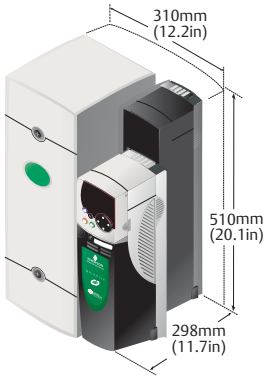

SP5
Weight:
55kg (121lbs)

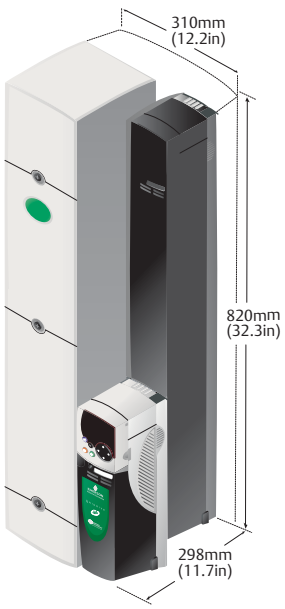

SP6
Weight:
75kg
(165.3lbs)

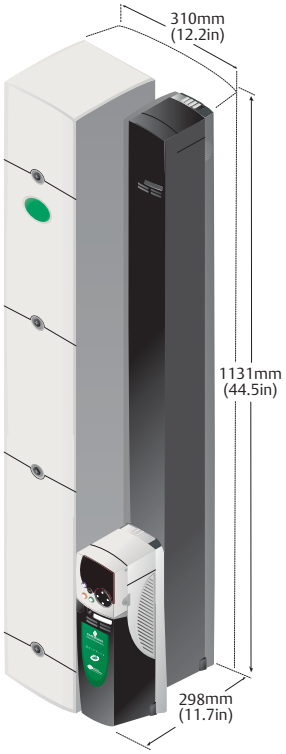

Options

Keypads

Order Code	Details
SM – Keypad	Low cost, hot pluggable, LED display
SM – Keypad Plus	Multi-lingual, hot pluggable, backlit LCD display. The display can be customised to provide application specific text.
SP0 – Keypad	Hot Pluggable LED for the compact Size 0

Braking Resistors

Braking Resistor	Order Code
SP0 Braking Resistor	1299-0001
SP1 Braking Resistor	1220-2756-01
SP2 Braking Resistor	1220-2758-01

EMC Filters

Unidrive SP built-in EMC filter complies with EN 61800-3, External EMC Filters are required for compliance with EN 61000-6-4.

Drive	Order Code	Drive	Order Code
SP0201 to SP0205 (1ph)	4200-6000	SP2401 to SP2404	4200-6210
SP0201 to SP0205	4200-6001	SP3401 to SP3403	4200-6305
SP0401 to SP0405	4200-6002	SP4401 to SP4403	4200-6406
SP1201 to SP1202	4200-6118	SP4601 to SP4606	4200-6408
SP1203 to SP1204	4200-6119	SP5401 to SP5402	4200-6503
SP2201 to SP2203	4200-6210	SP3501 to SP3507	4200-6309
SP3201 to SP3202	4200-6307	SP5601 to SP5602	4200-6504
SP4201 to SP4203	4200-6406	SP6401 to SP6402	4200-6603
SP1401 to SP1404	4200-6118	SP6601 to SP6602	4200-6604
SP1405 to SP1406	4200-6119		

DRIVING THE WORLD...

Control Techniques Drive & Application Centres

AUSTRALIA
Melbourne Application Centre
T: +613 973 81777
info.au@controltechniques.com

Sydney Drive Centre
T: +61 2 9838 7222
info.au@controltechniques.com

AUSTRIA
Linz Drive Centre
T: +43 7229 789480
info.at@controltechniques.com

BELGIUM
Brussels Drive Centre
T: +32 1574 0700
info.be@controltechniques.com

BRAZIL
Emerson do Brazil Ltda
T: +5511 3618 6569
info.br@controltechniques.com

CANADA
Toronto Drive Centre
T: +1 905 201 4699
info.ca@controltechniques.com

Calgary Drive Centre
T: +1 403 253 8738
info.ca@controltechniques.com

CHINA
Shanghai Drive Centre
T: +86 21 5426 0668
info.cn@controltechniques.com

Beijing Application Centre
T: +86 10 856 31122 ext 820
info.cn@controltechniques.com

CZECH REPUBLIC
Brno Drive Centre
T: +420 541 192111
info.cz@controltechniques.com

DENMARK
Copenhagen Drive Centre
T: +45 4369 6100
info.dk@controltechniques.com

FRANCE*
Angoulême Drive Centre
T: +33 5 4564 5454
info.fr@controltechniques.com

GERMANY
Bonn Drive Centre
T: +49 2242 8770
info.de@controltechniques.com

Chemnitz Drive Centre
T: +49 3722 52030
info.de@controltechniques.com

Darmstadt Drive Centre
T: +49 6251 17700
info.de@controltechniques.com

GREECE*
Athens Application Centre
T: +0030 210 57 86086/088
info.gr@controltechniques.com

HOLLAND
Rotterdam Drive Centre
T: +31 184 420555
info.nl@controltechniques.com

HONG KONG
Hong Kong Application Centre
T: +852 2979 5271
info.hk@controltechniques.com

INDIA
Chennai Drive Centre
T: +91 44 2496 1123/
2496 1130/2496 1083
info.in@controltechniques.com

Pune Application Centre
T: +91 20 2612 7956/2612 8415
info.in@controltechniques.com

Kolkata Application Centre
T: +91 33 2357 5302/2357 5306
info.in@controltechniques.com

New Delhi Application Centre
T: +91 11 2 576 4782/2 581 3166
info.in@controltechniques.com

IRELAND
Dublin Drive Centre
T: +353 45 448200
info.ie@controltechniques.com

ITALY
Milan Drive Centre
T: +39 02575 751
info.it@controltechniques.com

Reggio Emilia Application Centre
T: +39 02575 751
info.it@controltechniques.com

Vicenza Drive Centre
T: +39 0444 933400
info.it@controltechniques.com

KOREA
Seoul Application Centre
T: +82 2 3483 1605
info.kr@controltechniques.com

MALAYSIA
Kuala Lumpur Drive Centre
T: +603 5634 9776
info.my@controltechniques.com

REPUBLIC OF SOUTH AFRICA
Johannesburg Drive Centre
T: +27 11 462 1740
info.za@controltechniques.com

Cape Town Application Centre
T: +27 21 556 0245
info.za@controltechniques.com

RUSSIA
Moscow Application Centre
T: +7 495 981 9811
info.ru@controltechniques.com

SINGAPORE
Singapore Drive Centre
T: +65 6468 8979
info.sg@controltechniques.com

SLOVAKIA
EMERSON A.S
T: +421 32 7700 369
info.sk@controltechniques.com

SPAIN
Barcelona Drive Centre
T: +34 93 680 1661
info.es@controltechniques.com

Bilbao Application Centre
T: +34 94 620 3646
info.es@controltechniques.com

Valencia Drive Centre
T: +34 96 154 2900
info.es@controltechniques.com

SWEDEN*
Stockholm Application Centre
T: +468 554 241 00
info.se@controltechniques.com

SWITZERLAND
Lausanne Application Centre
T: +41 21 637 7070
info.ch@controltechniques.com

Zurich Drive Centre
T: +41 56 201 4242
info.ch@controltechniques.com

TAIWAN
Taipei Application Centre
T: +886 22325 9555
info.tw@controltechniques.com

THAILAND
Bangkok Drive Centre
T: +66 2580 7644
info.th@controltechniques.com

TURKEY
Istanbul Drive Centre
T: +90 216 4182420
info.tr@controltechniques.com

UAE*
Dubai Application Centre
T: +971 4 883 8650
info.ae@controltechniques.com

UNITED KINGDOM
Telford Drive Centre
T: +44 1952 213700
info.gb@controltechniques.com

USA
California Drive Centre
T: +1 562 943 0300
info.us@controltechniques.com

Charlotte Application Centre
T: +1 704 393 3366
info.us@controltechniques.com

Chicago Application Centre
T: +1 630 752 9090
info.us@controltechniques.com

Cleveland Drive Centre
T: +1 440 717 0123
info.us@controltechniques.com

Florida Drive Centre
T: +1 239 693 7200
info.us@controltechniques.com

Latin America Sales Office
T: +1 305 818 8897
info.us@controltechniques.com

Minneapolis US Headquarters
T: +1 952 995 8000
info.us@controltechniques.com

Oregon Drive Centre
T: +1 503 266 2094
info.us@controltechniques.com

Providence Drive Centre
T: +1 401 541 7277
info.us@controltechniques.com

Utah Drive Centre
T: +1 801 566 5521
info.us@controltechniques.com

Control Techniques Distributors

ARGENTINA
Euro Techniques SA
T: +54 11 4331 7820
eurotech@eurotechsa.com.ar

BAHRAIN
Iftikhar Electrical Est.
T: +973 271 116
ieepower@batelco.com.bh

BULGARIA
BLS - Automation Ltd
T: +359 32 968 007
info@blsautomation.com

CENTRAL AMERICA
Mercado Industrial Inc.
T: +1 305 854 9515
rsaybe@mercadoindustrialinc.com

CHILE
Ingeniería Y Desarrollo Tecnológico S.A
T: +56 2741 9624
idt@idt.cl

COLOMBIA
Sistronic LTDA
T: +57 2 555 60 00
sistronic@telesat.com.co

CROATIA
Koncar – MES d.d.
T: +385 1 366 7273
nabava@koncar-mes.hr

CYPRUS
Acme Industrial Electronic Services Ltd
T: +3572 5 332181
acme@cytanet.com.cy

EGYPT
Samiram
T: +202 7360849/
+202 7603877
samiramz@samiram.com

FINLAND
SKS Control
T: +358 20764 6639
control@sks.fi

HUNGARY
Control-VH Kft
T: +361 431 1160
info@controlvh.hu

ICELAND
Samey ehf
T: +354 510 5200
samey@samey.is

INDONESIA
Pt Apikon Indonesia
T: +65 6468 8979
info.my@controltechniques.com

Pt Yua Esa Sempurna Sejahtera
T: +65 6468 8979
info.my@controltechniques.com

ISRAEL
Dor Drives Systems Ltd
T: +972 3900 7595
info@dor1.co.il

KENYA
Kassam & Bros Co. Ltd
T: +254 2 556 418
kassambros@africaonline.co.ke

KUWAIT
Saleh Jamal & Company WLL
T: +965 483 2358
sjceng@almullagroup.com

LATVIA
EMT
T: +371 760 2026
janis@emt.lv

LEBANON
Black Box Automation & Control
T: +961 1 443773
info@blackboxcontrol.com

LITHUANIA
Elinta UAB
T: +370 37 351 987
sigitas@elinta.lt

MALTA
Mekanika Limited
T: +35621 442 039
mfrancica@gasan.com

MEXICO
MELCSA
T: +52 55 5561 1312
melcsamx@iserve.net.mx
SERVITECK, S.A de C.V
T: +52 55 5398 9591
servitek@data.net.mx

MOROCCO
Leroy Somer Maroc
T: +212 22 354948
lsmaroc@wanadoopro.ma

NEW ZEALAND
Advanced Motor Control. Ph.
T: +64 (0) 274 363 067
info.au@controltechniques.com

PHILIPPINES
Control Techniques Singapore Ltd
T: +65 6468 8979
info.my@controltechniques.com

POLAND
APATOR CONTROL Sp. z o.o
T: +48 56 6191 207
drives@apator.torun.pl

PORTUGAL
Harker Sumner S.A
T: +351 22 947 8090
drives.automation@harker.pt

PUERTO RICO
Powermotion
T: +1 787 843 3648
dennis@powermotionpr.com

QATAR
AFI Sitna Technologies
T: +974 468 4442
jp33@qatar.net.qa

ROMANIA
Dor Drives International
T: +40 21 337 3465
dordrive@zappmobile.ro

SAUDI ARABIA
A. Abunayyan Electric Corp.
T: +9661 477 9111
aec-salesmarketing@abunayyangroup.com

SERBIA & MONTENEGRO
Master Inzenjering d.o.o
T: +381 24 551 605
master@eunet.yu

SLOVENIA
PS Logatec
T: +386 1 750 8510
ps-log@ps-log.si

TUNISIA
SIA Ben Djemaa & CIE
T: +216 1 332 923
bendjemaa@planet.tn

URUGUAY
Secoin S.A
T: +5982 2093815
secoin@adinet.com.uy

VENEZUELA
Digimex Sistemas C.A.
T: +58 243 551 1634

VIETNAM
N.Duc Thinh
T: +84 8 9490633
infotech@nducthinh.com.vn

* Operated by sister company

P.N. 0175-0339 11/07

Bibliography

[1] US Energy Information Administration. "State Energy Profiles - Hawaii". http://www.eia.gov/state/state-energy-profiles.cfm?sid=HI, November 2009. Accessed July 2010.

[2] US Energy Information Administration. "Average Retail Price of Electricity to Ultimate Customers by End-Use Sector, by State". *Electric Power Monthly*, July:p.114, 2011. http://www.eia.gov/cneaf/electricity/epm/table5_6_b.html, Accessed July 2011.

[3] Global Energy Concepts, LLC. "A Catalog of Potential Sites for Renewable Energy in Hawaii". Technical report, Produced for the State of Hawaii Department of Land and Natural Resources and the Department of Business, Economic Development, and Tourism, December 2006.

[4] "RPS Policies Summary". Technical report, Database of State Incentives for Renewables & Efficiency, http://www.dsireusa.org/summarymaps/index.cfm?ee=1&RE=1, June 2011.

[5] State of Hawaii Department of Business, Economic Development, and Tourism. "Energy Agreement Among the State of Hawaii, Division of Consumer Affairs, and the Hawaiian Electric Companies". http://hawaii.gov/dbedt/info/energy/agreement/, October 2008. Accessed July, 2011.

[6] "HCEI Hawaiian Electric Companies' Energy Agreement Update - Year Two". Technical report, Hawaiian Electric Company, http://www.heco.com/vcmcontent/StaticFiles/pdf/HCEI_2YearUpdate.pdf, January 2011.

[7] "Grid-Scale Rampable Dispatchable Storage". Technical Report DE-FOA-0000290, US Advanced Research Projects Agency - Energy, https://arpa-e-foa.energy.gov, March 2010.

[8] Mark Matsuura. "Island Breezes". *IEEE Power & Energy Magazine*, 7(6):59–64, November 2009.

[9] C. Bloyd, K. Johnson, J. Torres, and J. Hernandez. "APEC Workshop on Renewable Energy Grid Integration Systems - Workshop Summary". Technical report, APEC Energy Working Group, http://www.sandia.gov/regis/REGIS-finalreport.pdf, March 2009.

[10] Electricity Storage Association. "Power Quality, Power Supply". http://www.electricitystorage.org/ESA/applications, May 2009. Accessed July, 2010.

[11] The Hawaiian Electric Company. "Reliability". http://www.heco.com - Renewable Energy, Issues and Challenges, Reliability. Accessed July, 2010.

[12] Hawaii Natural Energy Institute. "Oahu Wind Integration Study - Final Report". Technical report, University of Hawaii, Feb 2011.

[13] The Hawaiian Electric Company. "Curtailment". http://www.heco.com - Renewable Energy, Issues and Challenges, Curtailment. Accessed July, 2010.

[14] T. Thornbrue and R. Ghorbani. An Introduction to Large Scale Buoyant Energy Storage Technology. In *OCEANS 2010 Conference*, September 2010.

[15] The Hawaiian Electric Company. "Energy Storage". http://www.heco.com - Renewable Energy, Issues and Challenges, Energy Storage. Accessed July, 2010.

[16] R.B. Schainker. Executive overview: Energy storage options for a sustainable future. In *IEEE Power Engineering Society General Meeting*, volume 2, pages 2309–2314, June 2004.

[17] Hawaii Renewable Energy Development Venture. "Technology Assessment - Grid Energy Storage Systems". http://www.hawaiirenewable.com, December 2009. Accessed July, 2010.

[18] Jim Eyer and Garth Corey. "Energy Storage for the Electricity Grid: Benefits and Market Potential Assessment Guide". Technical Report SAND2010-0815, Sandia National Laboratories, Feb 2010.

[19] "Smart Grid System Report". Technical report, U.S. Department of Energy, July 2009.

[20] "A Systems View of the Modern Grid". Technical report, National Energy Technology Laboratory, January 2007.

[21] Joe Miller. "Energy Central series on the Seven Principal Characteristics of the Modern Grid". Technical Report Article 2 of 7, NETL MGS Team and Horizon Energy Group, April 2008.

[22] Federal Energy Regulatory Commission. "Frequency Regulation Compensation in the Organized Wholesale Power Markets - Docket Nos. RM11-7-000 and AD10-11-000". http://www.ferc.gov/whats-new/comm-meet/2011/021711/E-4.pdf, February 2011. Accessed August 2011.

[23] John Kluza and Jacob E. Grose and Yakov Berenshteyn and Michael Holman and Lux Research, Inc. "Grid Storage: Show Me the Money". http://www.luxresearchinc.com/coverage-areas/smart-grid-and-grid-storage/84-lux-researchgridstorageshowmethemoney.html, March 2010. Accessed June 2011.

[24] BCC Research LLC. "Utility-scale Electricity Storage Technologies: Global Markets(EGY056B)". http://www.bccresearch.com/pressroom/report/code/EGY056B, January 2011. Accessed August 2011.

[25] Pike Research. "Global Energy Storage Capacity to Multiply 100-fold by 2021". http://www.pikeresearch.com/newsroom/global-energy-storage-capacity-to-multiply-100-fold-by-2021, November 2011. Accessed March 2012.

[26] Lux Research, Inc. "Grid Storage: Connecting the Dots in a Fragmented Market". http://info.luxresearchinc.com/lux-research-grid-storage-tracker-webinar/, December 2011. Accessed March 2012.

[27] D. T. Bradshaw. "Pumped Hydroelectric Storage (PHS) and Compressed Air Energy Storage (CAES)". In *Proc. IEEE PES Meeting on Energy Storage*, 2000.

[28] Godfrey Boyle. *Renewable Energy*, volume 2nd edition. Oxford University Press, 2003. ISBN10: 0199261784.

[29] Dan Rastler. “New Demand for Energy Storage”. *Electric Perspectives*, pages 30–47, September/October 2008.

[30] Sandia National Laboratories. “Untitled”. http://www.sandia.gov/media/NewsRel/NR2001/images/jpg/minebw.jpg, 2001. Accessed July 2010.

[31] Electricity Storage Association. “Batteries - Technology Description”. http://www.electricitystorage.org/ESA/applications, 2010. Accessed July, 2011.

[32] Xtreme Power Corporation. “DPR 15-100C Spec Sheet”. http://www.xtremepower.com/xp-technology/dpr-sizes.php, 2011. Accessed July 2011.

[33] Babak Fahimi, Alexis Kwasinski, Ali Davoudi, Robert S. Balog, and Morgan Kiani. “Charge It!”. *IEEE Power & Energy Magazine*, 9(4):54–64, July/August 2011.

[34] Xtreme Power Corporation. “Recent Articles”. http://www.xtremepower.com/news/recent-articles.php, 2011. Accessed August 2011.

[35] Pew Center on Global Climate Change. “Electric Energy Storage - Climate Tech Book”. http://www.pewclimate.org/docUploads/Energy-Storage-Fact-Sheet.pdf, 2009. Accessed July, 2011.

[36] Basem Alamri and Abdussalam Alamri. “Technical Review of Energy Storage Technologies when Integrated with Intermittent Renewable Energy”. In *Sustainable Power Generation and Supply 2009, Int’l Conference on*, pages 1–5. SUPERGEN ’09, April 2009.

[37] P. Fairley. “Flywheels Keep the Grid in Tune”. *IEEE Spectrum*, 48(7):16–18, July 2011.

[38] Beacon Power Corporation. “Annual Report 2010”. http://investors.beaconpower.com/annuals.cfm, June 6, 2010. Accessed July 2011.

[39] D. Castelvecchi. “Spinning into Control”. *Science News*, 171(20):312–313, May 2007.

[40] M. L. Lazarewicz and A. Rojas. “Grid Frequency Regulation by Recycling Electrical Energy in Flywheels”. In *IEEE Power Engineering Society General Meeting*, volume 2, pages 2038–2042, Denver, CO, June 2004. IEEE.

[41] Beacon Power Corporation. “Photo Gallery”. http://beaconpower.com/company/201107-gallery.asp, June 2011. Accessed July 2011.

[42] Chris Witty, GlobeNewswire. "Beacon Power Flywheel Plant in Stephentown Reaches Full 20 MW Capacity". http://phx.corporate-ir.net/phoenix.zhtml?c=123367&p=irol-newsArticle&ID=1576441&highlight=, June 21, 2011. News Release. Accessed July 2011.

[43] S.P. Sukhatme and J.K. Nayak. *Solar Energy: Principles of Thermal Collection and Storage*, volume 3e. Tata McGraw-Hill, New York, 2008.

[44] Lisa Sena-Henderson, Tom Mancini, Sandia National Laboratories. "Advantages of Using Molten Salt". http://www.webcitation.org/60AE7heEZ, January 2006. Accessed March 2012.

[45] M.M. El-Wakil. *Powerplant Technology*, volume 1e. McGraw-Hill, New York, 2002.

[46] "Gemasolar Thermosolar Plant". http://en.wikipedia.org/wiki/Gemasolar, March 2012. Accessed March 2012.

[47] National Geographic. "Gemasolar, Non-Stop Energy". http://www.nationalgeographic.com.es/2011/10/25/gemasolar_energia_non_stop.html, October 2011. Accessed April 2012.

[48] Energy Storage SBIR/STTR FOA. Technical Report DE-FOA-0000674, US Advanced Research Projects Agency - Energy, https://arpa-e-foa.energy.gov, 2012.

[49] Robert A. Huggins. *Energy Storage*. SpringerLink, New York, 2010.

[50] Dyneema. "Dyneema®, the world's strongest fiber ™". http://www.dyneema.com/en_US/public/dyneema/page/about/Material.htm#Material-content, 2012. Accessed March 2012.

[51] John F. Bash. *Handbook of Oceanographic Winch, Wire and Cable Technology*, volume 3e. National Science Foundation, 1999.

[52] Updraft Advanced Lifting Technologies. "Dynaone HS vs. Steel Wire Rope". http://www.updraft.eu/hebeschlingen-technische-daten-en.html. Accessed March 2012.

[53] Abishek. "Difference Between DC and AC Motors". http://www.differencebetween.net/technology/difference-between-dc-and-ac-motors/, July 2011. Accessed March 2012.

[54] ABB Automation Products GmbH. "DC or AC Drives? A guide for users of variable-speed drives (VSDs)". http://www05.abb.com/global/scot/scot239.nsf/veritydisplay/046e0b4cdc2fe50ac1257466003a8443/$file/3adw000059.pdf. Accessed March 2012.

[55] Paul C. Krause, Oleg Wasynczuk, and Scott D. Sudhoff. *Analysis of Electric Machinery and Drive Systems*, volume 2e. Wiley-IEEE Press, 2002.

[56] Ted Stearns. "Replacing your DC motors? Think AC". http://www.reliableplant.com/Read/7052/dc-motors-ac. Accessed March 2012.

[57] Wikipedia. "Electric Motor". http://en.wikipedia.org/wiki/Electric_motor#Torque_capability_of_motor_types. Accessed March 2012.

[58] Calogero Cavallaro and et. al. Efficiency enhancement of permanent-magnet synchronous motor drives by online loss minimization approaches. *IEEE Transactions on Industrial Electronics*, 52(4):1153 – 1160, August 2005.

[59] Magnetic S.p.a. "HTQ series torque motors". http://www.magneticspa.it/products/htq-series-torque-motors~1.html, April 2012. Accessed April 2012.

[60] Wikipedia. "High-Voltage Direct Current". http://en.wikipedia.org/wiki/High-voltage_direct_current, April 2012. Accessed April 2012.

[61] T. Thornbrue and R. Ghorbani. Dynamic Model Refinement for Buoyant Energy Storage Technology. In *Clean Technology 2011 Conference and Expo*, June 2011.

[62] Paul Dvorak. "Wind Power Engineering & Development". http://www.windpowerengineering.com/tag/xtreme-power/, 2011. Accessed March 2012.

[63] Hawaii Renewable Energy Development Venture Technology Assessment. "Small Pumped Hydro Storage". http://www.hawaiirenewable.com/wp-content/uploads/2009/12/5.-Small-Pumped-Hydro.pdf, December 2009. Accessed March 2012.